Cape Peninsula
University of Technology

HIGH VOLTAGE DIRECT CURRENT STRATEGY SOLVING POWER DELIVERY SHORTAGES TO LOCALIZED AREA OF NATIONAL GRID

by

Johan Smith

Thesis submitted in fulfilment of the requirements for the degree

Master of Technology: Electrical Engineering

in the Faculty of Engineering

at the Cape Peninsula University of Technology

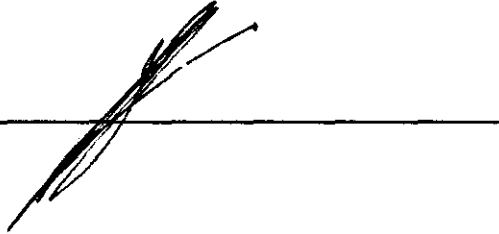**Supervisor: Professor G. Atkinson-Hope**

Cape Town

June 2009

DECLARATION

I, Johan Smith, declare that the contents of this thesis represent my own unaided work, and that the thesis has not previously been submitted for academic examination towards any qualification. Furthermore, it represents my own opinions and not necessarily those of the Cape Peninsula University of Technology.

Signed _____

Date 17/11/2009

ABSTRACT

The industrial and population growth of a nation can cause power delivery problems to localized areas of a national grid through their increased demand for electrical energy. One reason for these power shortages is the insufficient current carrying capacity of existing high voltage alternating current, (HVAC), transmission lines supplying the area. High voltage direct current (HVDC) transmission lines are a possible solution as they provide better power delivery than HVAC lines.

New or upgraded HVAC lines, or HVDC lines or combinations of HVAC and HVDC lines are possible solutions to improve power delivery. This research investigates the various line possibilities using theory and cutting edge frequency and time domain software tools. The challenge is how to approach this problem. What methodology or structure should be used? Thus one of the contributions of this work is the development of a strategy (flow chart), for solving power delivery problems to localized areas of a national grid through individual or combinations (e.g. parallel operation) of HVAC and/or HVDC transmission lines. The main contribution is the evaluation of a HVDC system as a solution to overcoming power delivery shortages to a localized area of a national grid.

Three different software packages (two industrial and one academic) namely, PSCAD/EMTDC (time domain), DIgSILENT PowerFactory (frequency domain) and MathCAD software are evaluated for their capability to perform the simulation studies necessary to prove the possible solutions given in the developed flow chart. The PSCAD/EMTDC software package is evaluated for integrated HVAC/HVDC load flow analyses, DIgSILENT for individual and parallel combinations of HVAC lines and MathCAD to prove hand calculations to software results.

Five case studies are conducted. The first case study demonstrates a healthy system with no delivery shortcomings, the second case study portrays the delivery shortcoming due to increased localized area demand, and the remaining three case studies explore possible solutions to solve the problem. The first possible solution is to construct an identical HVAC line in parallel to the existing line. The advantage of the HVAC parallel system is that when a problem arises on one of the lines the remaining line can still supply some of the power to the localized area. The upside of this system is that the construction of a new transmission line can lead to high cost and new land for right of a way (ROW) is necessary. The second possible solution is to replace the overloaded HVAC transmission line with a HVDC transmission system. The advantage of such a system is the increase of power delivery, but harmonic problems need to be addressed when using such a system.

The final solution investigated is an integrated system (HVDC in parallel with HVAC) this configuration has the scope to deliver increased power with the advantage of some contingency when the HVDC or HVAC line is out of commission. All the software that was utilized to perform the necessary simulation studies has proven to be efficient in obtaining the desired results.

The simulation studies conducted shows the strengths and weaknesses of the industrial grade software packages and this contribution will help future researchers on this topic by saving them time and effort. The case studies give insights into the engineering considerations that should be taken into account when assessing a certain transmission line solution to increase the power delivery to a localized area of a national grid.

The three case studies conducted as possible solutions, namely, two HVAC lines in parallel (Case study 3), HVAC line replaced with a HVDC line (Case study 4), and an integrated HVAC/HVDC system (Case study 5) were found to be effective to solve the problem.

Where cost and right of way of lines is not a constraint and contingency is of utmost importance, then it is found and recommended that an Integrated HVAC/HVDC network should be used as it provides the best of the three to increase power delivery.

ACKNOWLEDGEMENTS

I wish to express my gratitude to all of the following:

- My Heavenly Father and Saviour for His spiritual guidance during this project.
- Professor Gary Atkinson-Hope my supervisor, for his encouragement, his guidance and expert advice during the duration of this project.
- Mr Willem Stemmet for his help with various problems during the project.
- To the people, who are closest to me: My parents for their support, encouragement and for the opportunity to better my academic qualification, Karen for her loving support and everybody else that contributed to this project.

TABLE OF CONTENTS

CHAPTER FOUR: HVDC THEORY

CHAPTER FIVE: SOFTWARE TOOLS

CHAPTER SIX: DEVELOPMENT OF A STRATEGY

CHAPTER SEVEN: NETWORK DESCRIPTION

CHAPTER EIGHT: CASE STUDY SCENARIOS AND RESULTS

CHAPTER NINE: ANALYSIS OF RESULTS

CHAPTER TEN: CONCLUSIONS

REFERENCES

APPENDICES

LIST OF FIGURES

LIST OF TABLES

LIST OF SYMBOLS

R is the resistance

L is inductance

C is capacitance

R_{dc} is the DC resistance

R_{ac} is the AC resistance

L_a is inductance per- phase,

r is the radius of the conductor

r' is a fictitious conductor radius

D is the distance between conductors

GMR is the Geometric Mean Radius

D_{eq} is the geometric mean

D_{SL} is the equivalent GMR

d is the distance between the conductors in the bundle

X_L is the inductive reactance

X_{LT} is the total inductive reactance

ε is the absolute permittivity of the conductor used

q_a is the charge in the a phase

V_{an} is the phase to neutral voltage

f is the frequency

C_{an} is the per phase capacitance

C_T is the total capacitance

X_C is the capacitive reactance

X_{CT} is the total capacitive reactance

R_T is the total resistance

l is the length of the transmission line

Z is the impedance

G is the conductance

B is the susceptance

Y is the admittance

Z_T is the total impedance

θ_z is the impedance angle

θ_Y is the admittance angle

B_L is the inductive susceptance

B_C is the capacitive susceptance

Z_C is the characteristic

V_S is the sending-end L-N voltage (V)

V_R is the receiving-end L-N voltage (V)

I_S is the sending-end current (A)

I_R is the receiving-end current (A)

δ is the angle between V_S and V_R

$V_{(x)}$ is the voltage at position x of the line

$I_{(x)}$ is the current at position x of the line

Q is the reactive power

P is the real power

S is the apparent (complex) power

P_R is the receiving end real power

P_S is the sending end real power

Q_R is the receiving end reactive power

Q_S is the sending end reactive power

I^* is the complex conjugate of I.

V_m is the peak AC voltage

γ is the extinction angle gamma

μ is the overlap angle

V_{d6prec} is the six-pulse DC voltage produced by the rectifier

$V_{d6precavg}$ is the average six-pulse DC voltage produced by the rectifier

$I_{d12precavg}$ is the twelve-pulse DC current that is produced by the rectifier

$I_{d12pinvavg}$ is the average twelve-pulse DC current produced by the inverter

$V_{d12pinvavg}$ is the average twelve-pulse DC voltage produced by the inverter

X_{com} is the commutation transformers reactance in pu

α is the converter firing angle

p is the pulse number of the converter

kpu is the static voltage dependency constant (real power)

kqu is the static voltage dependency constant (reactive power)

CHAPTER ONE
INTRODUCTION

1.1   Background

A national grid supplies localized areas in a country. These areas are usually supplied by high voltage alternating current (HVAC) overhead transmission lines. Due to industrial and population growth and lack of generation capacity on the grid and/or in the localized area, such areas can experience power delivery shortages leading to controlled outages (contingency). One of the main factors that can cause this problem is the lack of current carrying capacity of the existing HVAC lines supplying the localized areas as they have reached their thermal limits due to this increased demand. When their limit is exceeded, lines are tripped, causing an outage and shortages are experienced (Padiyar, 1990:3).

Even if generation capacity is increased, the problem is still not solved because of lack of transmission line capacity. Different line solutions exist to solve this problem, one being the construction of more HVAC overhead lines to supply the area, or replacing the existing transmission lines with overhead lines that can transfer more power to the localized area on the assumption that there is adequate generation capacity.

When constructing new overhead lines the obtaining of land for the path and erection of the transmission towers is a problem. This land is mostly privately owned and is referred to as the "Right Of Way" or ROW. Thus, where it is possible, existing ROW should be optimized to its fullest potential (Koshcheev, 2003:7), (Padiyar, 1990:3). One way to optimize existing ROW is to replace its HVAC lines with HVDC lines.

There is thus a need to explore the application of HVDC lines as a possible solution to power delivery problems.

1.2   Shortcomings

From the literature review conducted, it was found that much is written on HVAC and HVDC lines but very little of the research work published focuses on case specific studies on integrated HVAC/HVDC systems, especially not power delivery to a localized area of a national grid. However it is also found that there is a lack of software evaluation of their application for such studies. This can be attributed to the lack of cost effective industrial grade software tools capable of conducting such studies, available to researchers.

There is however one time domain software packages, PSCAD/EMTDC and one frequency domain package, DIgSILENT available with capability for such studies. These tools are also able to conduct steady-state frequency domain studies.

There is also no publications on a methodology on how to go about finding a possible solution for alleviating power shortages, and the consequences that goes along with their applications.

1.3 Need for research

There is thus a need for the development of a strategy in the form of a flow chart to guide engineers in their approach (methodology) to decide on a solution to increase the power delivery to a localized area of a national grid. All possible line solutions need to be proven, and their pros and cons need to be highlighted. There is also a need to evaluate potential software packages and to conduct case specific industrial grade studies involving HVAC and HVDC transmission lines and to make recommendations.

1.4 Research boundaries

Even though a number of options exist (e.g. construction of new generators in the localized area, load management, etc.), for increasing power delivery to a localized area, the focus of this work will be solely on transmission line solutions. Harmonics are briefly explained and mentioned as HVDC systems typically include filters. Studies will thus focus on fundamental frequency. The software used (PSCAD/EMTDC) can produce steady-state results but certain steps should be taken to obtain these results. An angular stability limit of +/-35° will be used as a constraint for the HVAC transmission lines. Only a twelve-pulse mono-polar HVDC configuration will be considered in this work.

1.5 Main contributions of the thesis

A strategy in the form of a flow chart is developed to propose a method for finding a solution to a power delivery shortage to a localized area of a national grid due to the lack of thermal capacity of overhead HVAC transmission lines. Case specific studies involving individual and combinations of HVAC and HVDC lines are conducted to demonstrate their effectiveness as solutions to the problem encountered.

Two different software packages, PSCAD/EMTDC (time domain) and DIgSILENT (frequency domain) are evaluated for their capability to conduct steady-state analysis, even though the one, PSCAD/EMTDC, is a time domain simulation tool.

Devices from the PSCAD/EMTDC toolbox were assessed and methods implemented so that steady-state results could be obtained despite that this package is not specifically geared to generate steady-state specific results like DIgSILENT. This was necessary so that results from the two industrial grade software tools could be evaluated especially for their capability to conduct integrated HVAC/HVDC system studies. Hand calculations using a MathCAD program is also developed for comparison of HVAC studies to DIgSILENT results so as to establish a benchmark and obtain confidence in software results. Five case specific studies where conducted using these software tools and hand calculations (MathCAD) making this work unique.

1.6   Outline of the thesis

In Chapter two the historic background of HVDC and HVAC transmission is reviewed. This is followed by the advantages and disadvantages of utilising HVDC systems. The main considerations are given when planning a transmission line (economics, technical performance and reliability), and each of these are discussed. Still in Chapter two the current research in the field of HVDC is given.

Chapter three covers the HVAC theory necessary for conducting the HVAC case studies. Different transmission line models are discussed (short, medium and long) as well as methods to calculate power flow in a HVAC network. The operating point is also discussed in Chapter three.

The necessary HVDC theory is given in Chapter four. In this chapter the operation of a mono-polar HVDC link is discussed in detail. The roll of all the different components is highlighted and all the relevant control angles are explained. Harmonic analysis is covered in terms of harmonic cancellation and it is shown how transformer topologies can cancel out harmonics. The last section in Chapter four covers the basic HVDC control systems.

In Chapter five all the software tools that is used is shown with the considerations that should be taken into account when using them. A table is given which compares the different software packages used.

The developed strategy (flow chart) is given and explained in Chapter six.

Following Chapter six, all the network models used are given in Chapter seven. In this chapter all the relevant parameters are given to be able to model the different networks.

The case studies conducted are explained in Chapter eight and all the results obtained are given.

This is followed by the analysis of results which is given in Chapter nine and finally conclusions and recommendations are made in Chapter ten.

CHAPTER TWO
LITERATURE REVIEW

2.1 Historic background of HVDC

The first practical application of electricity was direct current and one of the first economically working transmission systems was built by Tomas A. Edison in 1882. The system was built in Pearl Street, New York. It supplied direct current at 110 V to an area of about 1.6 km in radius (Kimbark, 1971:1-2). The biggest problem encountered at that time, with DC was changing the voltage levels. With the invention of the transformer and the induction generator in the 1890's, led to AC transmission systems. The transformer made it possible to create different voltage levels. The first transmission of three-phase alternating current took place in 1891. This was a 25 kV transmission line, approximately 175 km long and was built between Lauffen and Frankfurt. It was soon accepted as the only feasible solution for generation, distribution and transmission of electrical energy (Arrillaga, 1988:2).

Increasing demand for electricity has led to the erection of power stations. In many cases power stations are situated at distances far from load centres. This led to a search for efficient power transmission systems resulting in increased voltage levels. As AC transmission systems at that time were found to be less efficient because the power delivered was reduced by reactive power losses. This led to the development of the first commercially viable HVDC system (Padiyar, 1990:1).

This was a 100 kV, 20 MW DC link between the Swedish mainland and the island of Gotland. These early HVDC transmission systems were found to be unreliable due to the fact that the converters consisted of mercury arc valves, which created back fire during the conversion process which resulted in the destruction of the valves.

In the middle of the 20th century thyristor valves were developed, which solved these "mercury arc valve" problems. With these problems eliminated, HVDC no longer struggled with reliability issues (Kimbark, 1971:3).

The popularity of HVDC increased more and more and systems are being introduced globally in the modern time. Figure 2.1 shows the growth in HVDC transmission schemes since 1954 up to 2008 (Arrillaga, 1988:9).

HVDC transmission schemes constructed
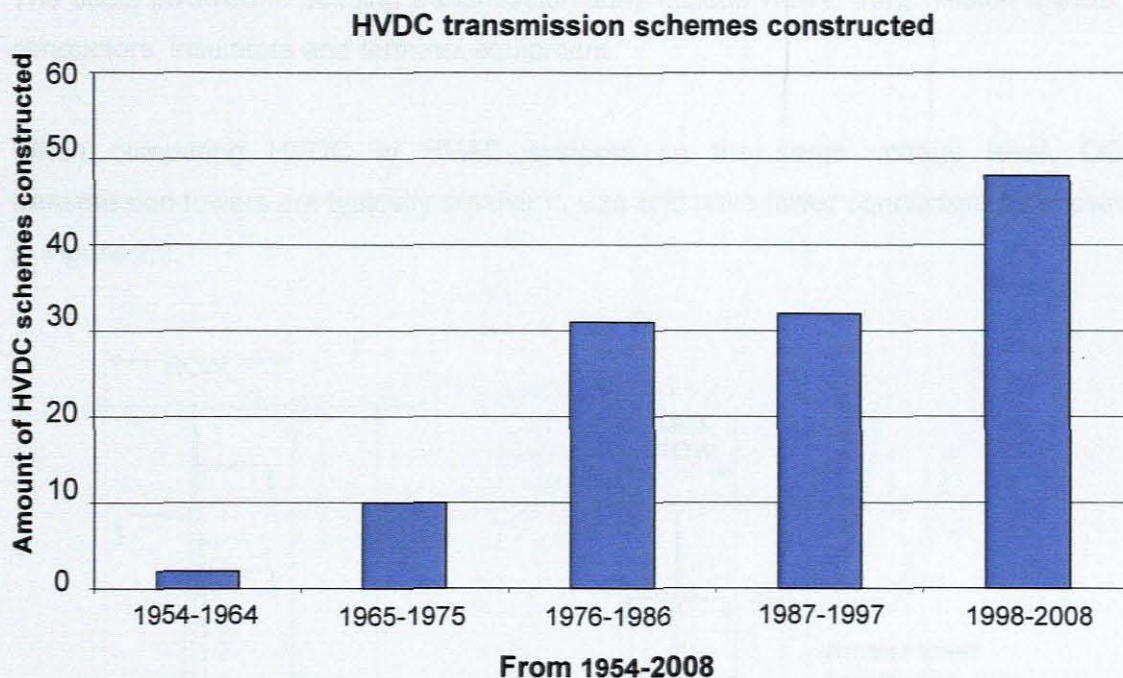
Figure 2.1: Growth in HVDC popularity through the years.

From this it can be seen that the number of HVDC transmission lines more than doubled in 1976 to 1986 and 1987 to 1997 period over the period of 1965 to 1975. The interest increased even further as 48 systems where built in 1998 to 2008 compared to 32 previously. This shows that HVDC is becoming a preferred alternative to HVAC transmission lines for bulk power transfer. However HVDC systems has advantages and disadvantages when compared to HVAC transmission systems.

2.2 Advantages of HVDC over HVAC transmission lines

When planning a transmission system usually three factors are considered, namely:

- Economics of transmission systems
- Technical performance
- Reliability

There are several more considerations, (e.g. ROW, tower constructions, conductors used, reactive compensation etc.), but they fall under the main headings given above (Padiyar, 1990:2).

6

2.2.1 Economics of transmission systems

Transmission lines are sometimes constructed on land owned by private people. Servitudes are negotiated and the width is usually defined as the right of way (ROW). The costs involved in building transmission lines include ROW, transmission towers, conductors, insulators and terminal equipment.

When comparing HVDC to HVAC systems on the same voltage level, DC transmission towers are typically smaller in size and have fewer conductors as shown in Figure 2.2.
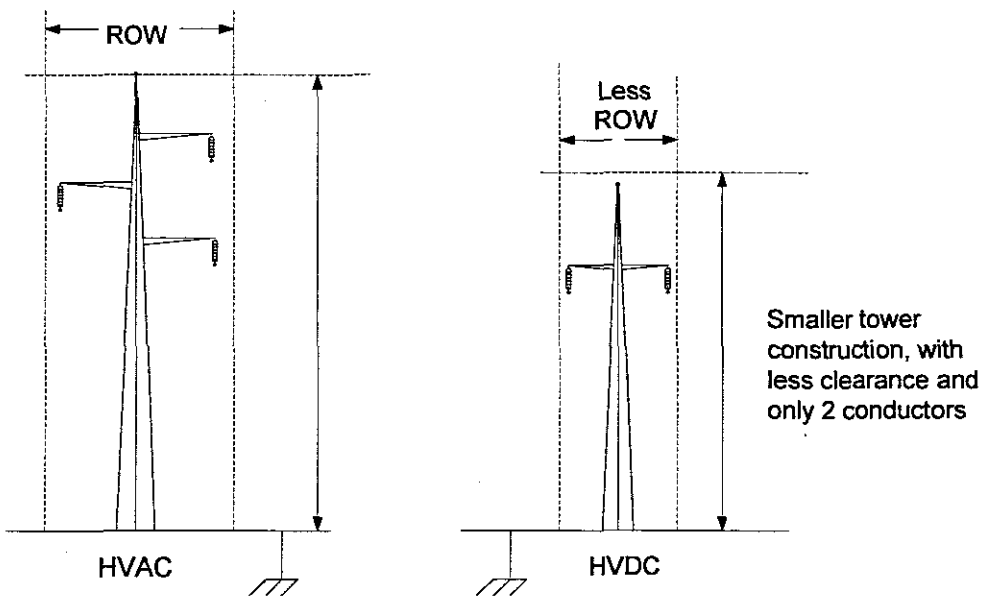
Figure 2.2: HVAC towers compared to HVDC towers

In modern days the visual effect of transmission towers is as important. From Figure 2.2 it can be seen that HVDC towers have less of a visual impact than those of the HVAC towers (Koshcheev, 2003:2).

When comparing the ROW of an 800 kV HVAC transmission line transporting 2000 MW to a 500 kV HVDC transmission line transporting 3000 MW, it was found that the HVDC uses 33 % less ROW (Weimers, 2003).

If 10.000 MW needs to be transmitted across transmission lines and 800 kV HVAC is compared to 750 kV HVDC it is clear from Figure 2.3 that there is a big difference between HVAC and HVDC in terms of number of towers utilized.

HVDC uses less tower constructions, therefore less ROW is used.

HVAC 800 kV

HVDC 750 kV
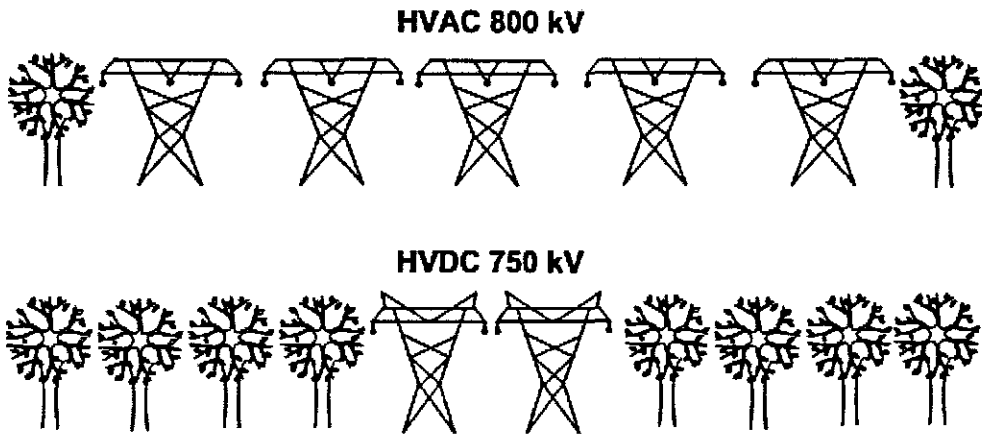
Figure 2.3: Difference in ROW between HVAC and HVDC

Thus a great advantage is obtained in regard to the size of land used when utilizing HVDC transmission lines (Weimers, 2003).

2.2.2 Technical performance

The power losses on a DC line compared to an AC line are reduced due to 3 factors. The first factor is the use of fewer conductors, with HVDC only two conductors are necessary (where earth return is not used), where HVAC needs three. This means that for the same current carrying capacity of the conductors used the HVDC scheme will have 67 % of the I^2R losses to that of AC lines. Where R is the resistance of the line and I is the current through the transmission line (Padiyar, 1990:2). Secondly, the absence of skin effect with DC application is also beneficial in reducing power losses marginally. The third factor which contributes to reducing the losses is the reduction in corona compared to that of AC lines (Padiyar, 1990:2).

DC also has an advantage over AC transmission as the power delivered is controllable by means of converter control. Converter control gives control over the amount of power that is being transmitted (Padiyar, 1990:3).

HVAC lines often require reactive power compensation to regulate voltage. Shunt capacitors are usually used for compensation. With HVDC transmission no reactive power compensation is necessary for the transmission line, making HVDC more suitable for long distance power transfer (Padiyar, 1990:4).

The power transfer in AC lines is dependent on the angular displacement between the voltages at both ends of the line. For a given power level, the angle increases with distance.

The maximum power that can be sent over a line is limited by the consideration of steady-state and transient stability. With converter control the stability in HVDC systems can be enhanced (Arrillaga, 1988:1).

2.2.3 Reliability

By replacing mercy-arc valves with thyristor valves, HVDC systems have become much more reliable, increasing their popularity.

2.3 Disadvantages of HVDC over HVAC transmission lines

HVDC schemes have certain drawbacks which should be taken into account when considering the application of such a system. The first is cost. HVDC uses expensive terminal equipment (converter stations, both rectifier and inverter). When utilizing HVDC for bulk power transmission, a break-even distance between HVAC and HVDC has been determined at approximately 800 km for overhead lines as shown in Figure 2.4 (Padiyar, 1990:2).

d*=break-even distance
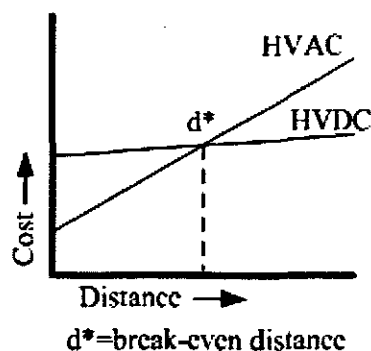
Figure 2.4: Break-even distance

As converter technology advances this break-even distance becomes less. In 2005 it was already less than 600 km (Power, 2005).

The second disadvantage of HVDC is the complexity of tapping off power along a transmission line. Multi-terminal HVDC schemes have been used in the past but they are not cost effective and HVAC are still much more flexible when it comes to tapping off power along a transmission path (Kimbark, 1971:3).

Another disadvantage concerning HVDC systems is the generation of harmonics due to the non-linear operation of converters. They inject harmonic currents into associated HVAC systems that cause distorted voltage and/or current waveforms.

An example of a three phase set of waveforms is shown in Figure 2.5. Harmonic filters and specific transformer connections need to be implemented to eliminate these harmonics produced by a converter station (Padiyar, 1990:5).
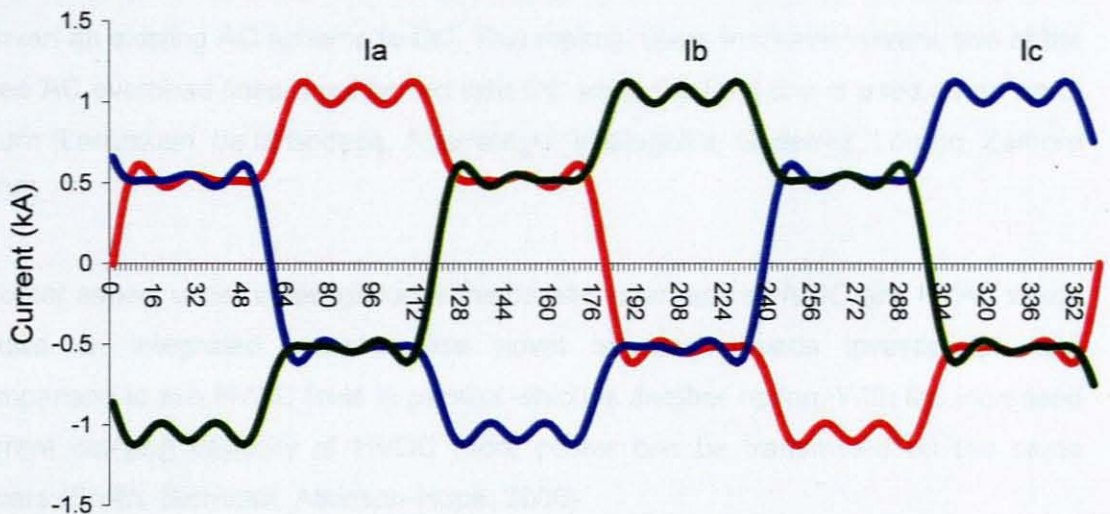
Figure 2.5: Distorted waveforms

HVDC systems at converter stations consume reactive power in the conversion process. Because of this consumption, dedicated capacitors need to be installed to supply this reactive power which may not be forthcoming from the associated HVAC system (Arrillaga, Smith. 1998:15).

2.4 Current research in the field of HVDC

Currently research is being conducted to provide the industry with more reliable and cost effective HVDC transmission systems. Furthermore, as computer technology improves, engineers are making use of software simulation packages to aid them in the design of complex systems (Arrillaga & Arnold 1990:1). The challenge is to develop different models for each of the HVDC components required to make up a complete system such that simulation results match real world results (Woodford, Gole & Menzies 1983: 1616-1623). A thorough understanding is needed of how these elements are modelled and there is a strong need for software users to understand and develop methodologies in which the models are applied so that system responses can be evaluated (Doke & Banerjee 1986: 69-72). Thus more emphasis can be put on system design, operation and analysis.

Traditionally, load flow analyses are conducted on networks which consist only of AC voltages and currents. Now that HVDC systems are being integrated with HVAC systems new methods for load flow calculations are needed that includes both AC and DC elements. This has led to the development of software tools (Reeve, Fahmy, Scott, 1977: 925-933), (Dialynas & Koskolos, 1994:872-878).

In an attempt to optimize ROW, one aspect which is currently researched is to convert an existing AC scheme to DC. This means, using the same towers, two of the three AC overhead lines must be fed with DC while the third line is used as an earth return (Larruskain, de la Bodega, Abarrategui, Iraolagoitia, Gutierrez, Lorono, Zamora 2006).

Another aspect under investigation is the parallel operation a HVDC and HVAC which entails an integrated system. This novel approach needs investigation and comparison to two HVAC lines in parallel which is another option. With the increased current carrying capacity of HVDC more power can be transmitted on the same towers (Smith, Stemmet, Atkinson-Hope, 2008).

As with AC systems, HVDC schemes cause non-sinusoidal currents to flow in the system which are known to increase losses, thus there is a need to investigate power flows in the harmonic domain as well as a need to design harmonic filters to provide solutions to resonance problems (Bathurst, Watson, Arrillaga, 2000: 1034-1038).

2.5   Further research needed

With HVDC systems now incorporated into existing HVAC systems the need is ever growing for research into integrated HVAC/HVDC systems as well as individual HVDC systems. As software tools are now available there is also a great need to evaluate them for their capability to conduct integrated studies. A need is also there to conduct specific case studies to demonstrate different line possibilities, as well as to develop a strategy on how to approach such an investigation.

CHAPTER THREE
HIGH VOLTAGE ALTERNATING CURRENT THEORY

3.1   Transmission line parameters and modelling

In a HVAC system a transmission line can be represented by different models depending upon the accuracy of the results needed. AC transmission lines have the following parameters, resistance, R, capacitance, C and Inductance L. The overhead lines are typically single or three phase. The values of the L and C parameters depend on the type of line configuration used, symmetrical, flat regular or asymmetrical lines. They can be single or bundled lines (Glover & Sarma. 2002:159).

Symmetrical line configuration   Flat regular   Unsymmetrical line configuration

$x = y = z$ $x = y \neq z$ $x \neq y \neq z$
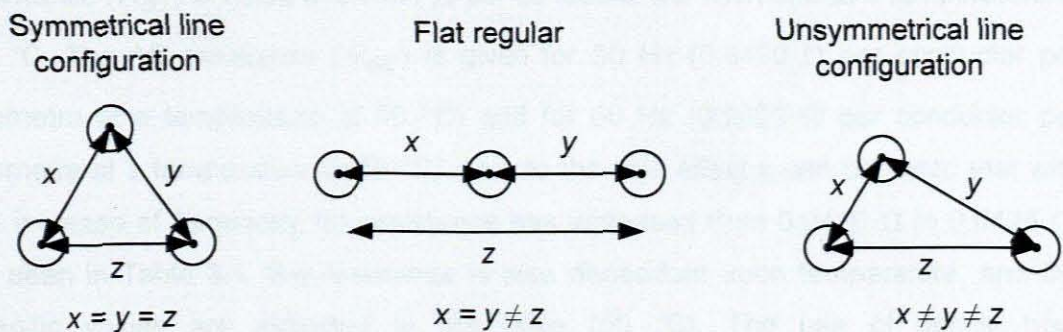
Figure 3.1: Line configurations

The resistance "R" can be DC (R_{dc}) or AC (R_{ac}) resistance, where the AC resistance takes skin effect into account. The uniform current distribution through the cross-section of a conductor exists only for DC. With AC currents the distribution becomes non-uniform. As the frequency increases the current distribution becomes more non-uniform, this phenomenon is called skin effect (Stevenson. 1982:42). The R_{dc} and R_{ac} values are usually obtained from cable manufacturer tables and depend upon whether conductors are solid or aluminium conductor steel reinforced (ACSR) conductors. Figure 3.2 shows an ACSR conductor, which consists of aluminium strands, with a steel core.

Steel strands   Steel strands

Aluminum strands   Aluminum strands
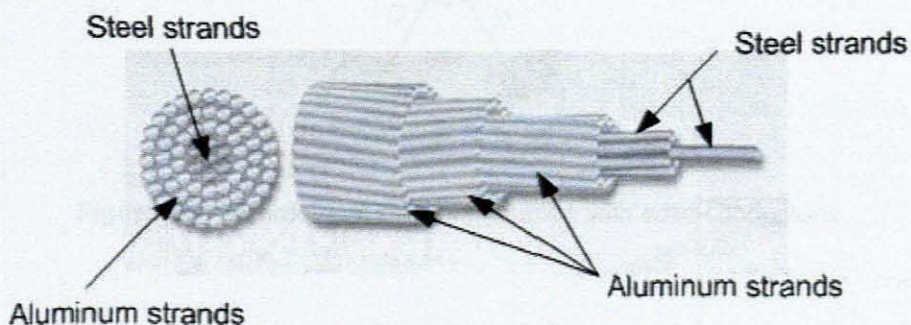
Figure 3.2: ACSR conductor

The manufacturer's data for specific ACSR conductors are shown in Table 3.1.

Table 3.1: Characteristics of aluminium conductor steel reinforced (ACSR)

code words	circular mils (alum)	cm² (Alum)	outside dia. (cm)	GMR (cm)	alum/ steel strands	current carrying capacity (amps)	resistance 50°C (Ω/conductor./km)		
							DC	50 Hz	60 Hz
Falcon	1590000	8.057	3.924	1.585	54/19	1380	0.0401	0.0420	0.0425
Parrot	1510500	7.654	3.825	1.545	54/19	1340	0.0423	0.0441	0.0447
Plover	1431000	7.251	3.721	1.502	54/19	1300	0.0446	0.0466	0.0472
Martin	1351000	6.846	3.617	1.460	54/19	1250	0.0473	0.0492	0.0499
Pheasant	1272000	6.445	3.510	1.417	54/19	1200	0.0502	0.0522	0.0529
Grackle	1192500	6.042	3.399	1.371	54/19	1160	0.0536	0.0556	0.0563

From Table 3.1 it can be seen that for the ACSR conductor, Falcon, the DC resistance (R_{dc}) is equal to 0.0401 Ω per conductor per kilometre at a temperature of 50 °C. The AC resistance (R_{ac}) is given for 50 Hz (0.0420 Ω per conductor per kilometre at a temperature of 50 °C) and for 60 Hz (0.0425 Ω per conductor per kilometre at a temperature of 50 °C). Due to the skin effect it can be noted that with the increase of frequency the resistance has increased from 0.0420 Ω to 0.0425 Ω. As seen in Table 3.1, the resistance is also dependant upon temperature, and the specific values are indicated in the table (50 °C). The use of details from manufacturer's tables is the chosen method for determining resistance values as ACSR conductors rather than solid conductors are used for transmission lines.

Unlike R_{ac} which can be obtained from the manufacturer's tables the inductance (L) and capacitance (C) of an overhead line is dependant on the configuration used, (Figure 3.1).

A symmetrical three phase line with solid conductors is shown in Figure 3.3,

Symmetrical line
configuration
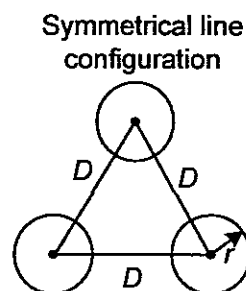
Figure 3.3: Symmetrical line configuration with solid conductors

The inductance per- phase, L_a is calculated as follows:

$$L_a = 2 \cdot 10^{-7} \ln \frac{D}{r'} \quad \text{H/m per phase} \tag{3.1}$$

Where D = the distance between the conductors shown in Figure 3.3, and r' is a fictitious conductor assumed to have no internal flux but with the same inductance as the actual conductor radius r and is calculated as follows (Stevenson. 1982:43):

$$r' = e^{-1/4} \cdot r \tag{3.2}$$

Where r is the radius of the conductor, shown in Figure 3.3.

This only holds true for single solid conductors. When the single solid conductors in Figure 3.3 are replaced with ACSR conductors, the conductor is now known as a composite conductor, which entails one or more solid cylindrical sub-conductors in parallel.

When dealing with composite conductors, r' no longer holds true and the Geometric Mean Radius (GMR) must be used. The GMR (Ds) can be obtained from the manufactures tables as shown in Table 3.1. Thus r' is replaced with Ds in (3.1) and becomes:

$$L_a = 2 \cdot 10^{-7} \ln \frac{D}{Ds} \quad \text{H/m per phase} \tag{3.3}$$

It is very important that the distance between the conductors and the GMR from the table is in the same unit.

With unsymmetrical lines it becomes more difficult to obtain the inductance because the flux linkages and inductances of each phase are not the same, this is shown in Figure 3.4
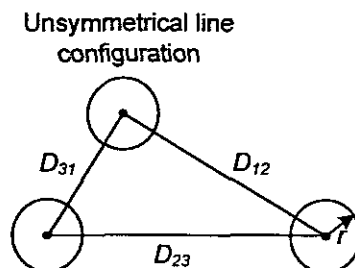
Figure 3.4: Unsymmetrical line configuration with solid conductor

A difference in inductance in each phase will result in the circuit being unbalanced. To balance the circuit the conductor positions are inter-changed at intervals along the line. This is called transposition (Stevenson. 1982:43). With transposition an average inductance per phase can be calculated as follows:

$$L_a = 2 \cdot 10^{-7} \ln \frac{D_{eq}}{D_s} \text{ H/m per phase} \tag{3.4}$$

Where D_{eq} is the geometric mean of the three distances of the unsymmetrical line, which is an equivalent spacing and is calculated as follows:

$$D_{eq} = \sqrt[3]{D_{12} \cdot D_{23} \cdot D_{31}} \tag{3.5}$$

(3.4) is used for ACSR conductors, when dealing with solid conductors D_s is replaced with r'. A flat regular line configuration is shown in Figure 3.1 is also an unsymmetrical configuration and is treated similarly, except two of the distances are equal and the third distance is twice the distance.

It is common in practice for extra high voltages (above 230 kV) to use more than one conductor per phase. When this is done it is called bundling of conductors. The advantages of bundling include (Glover, Sarma. 2002:168):

- Reduction of electric field strength on the conductor surfaces (reduces corona discharges, which entails less power losses, communication interference and audio noise)
- Reduces the series reactance of the line

Figure 3.5 shows different bundle configurations that can be applied to line configurations.

| Two conductor bundle | Three conductor bundle | Four conductor bundle |
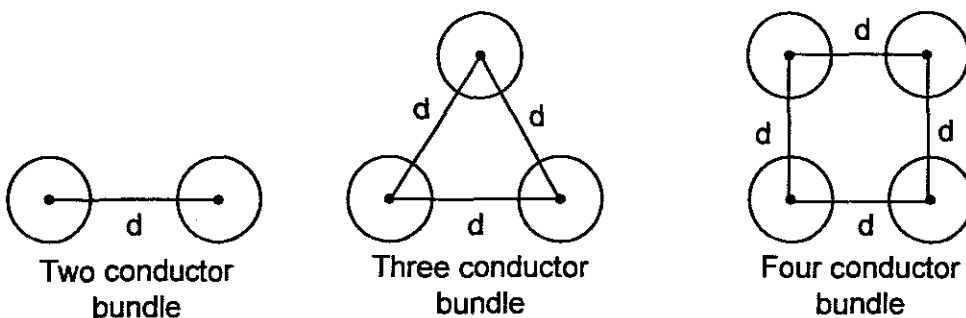
Figure 3.5: Bundle conductor configurations of one phase

15

With bundled conductors a new D_S value must be calculated. The bundle is thus replaced with and single equivalent GMR for the bundle. This equivalent GMR is equal to D_{SL}. This is different for each of the bundle configurations shown in Figure 3.5 (Glover & Sarma. 2002:169).

For two conductor bundle:

$$D_{SL} = \sqrt[4]{(D_S \cdot d)^2} = \sqrt{D_S \cdot d} \qquad (3.6)$$

For three conductor bundle:

$$D_{SL} = \sqrt[9]{(D_S \cdot d \cdot d)^3} = \sqrt[3]{D_S \cdot d^2} \qquad (3.7)$$

For four conductor bundle:

$$D_{SL} = \sqrt[16]{\left(D_S \cdot d \cdot d \cdot d\sqrt{2}\right)^4} = 1.091 \cdot \sqrt[4]{D_S \cdot d^3} \qquad (3.8)$$

D_{SL} represents the GMR of the combination of conductors in a bundle and d is the outer-to-centre distance between the conductors making up a bundle.

This D_{SL} value is now used in (3.3) to obtain the inductance/phase for a symmetrical line that uses bundling and in (3.4) for unsymmetrical lines with bundling. If a line has a length "l" then the inductive reactance for the line is:

$$X_L = 2 \cdot \pi \cdot f \cdot L_a \ \Omega/\text{m per phase} \qquad (3.9)$$

$$X_{LT} = X_L \cdot l \ \Omega/\text{phase} \qquad (3.10)$$

Where f represents the frequency

As with inductance of a transmission line the capacitance of the line must also be calculated and is dependant on the line configuration that is utilized. For a symmetrical three phase line the capacitance in one phase, C_{an} is calculated as follows:

$$C_{an} = \frac{q_a}{V_{an}} = \frac{2\pi\varepsilon}{\ln\left(\dfrac{D}{r}\right)} \quad \text{F/m line-to-neutral} \tag{3.11}$$

Where:

ε = absolute permittivity

q_a = is the charge on phase a

V_{an} = the phase to neutral voltage

D = Distance between the conductors

r = the radius of the conductor

Due to symmetry in this line configuration the capacitance in the b and c phase can be calculated by means of (3.11).

For unsymmetrical lines shown in Figure 3.4, the capacitance can be calculated as follows:

$$C_{an} = \frac{q_a}{V_{an}} = \frac{2\pi\varepsilon}{\ln\left(\dfrac{D_{eq}}{r}\right)} \quad \text{F/m line-to-neutral} \tag{3.12}$$

Where D_{eq} is calculated in (3.5)

For bundled configurations as shown in Figure 3.5 the following equation can be used for unsymmetrical line configurations:

$$C_{an} = \frac{q_a}{V_{an}} = \frac{2\pi\varepsilon}{\ln\left(\dfrac{D_{eq}}{D_{SC}}\right)} \quad \text{F/m line-to-neutral} \tag{3.13}$$

Where D_{SC} for two conductor bundles are:

$$D_{SC} = \sqrt{r \cdot d} \tag{3.14}$$

Three conductor bundles:

$$D_{SC} = \sqrt[3]{r \cdot d^2} \tag{3.15}$$

$$C_{an} = \frac{q_a}{V_{an}} = \frac{2\pi\varepsilon}{\ln\left(\dfrac{D}{r}\right)} \quad \text{F/m line-to-neutral} \qquad (3.11)$$

Where:

ε = absolute permittivity

q_a = is the charge on phase a

V_{an} = the phase to neutral voltage

D = Distance between the conductors

r = the radius of the conductor

Due to symmetry in this line configuration the capacitance in the b and c phase can be calculated by means of (3.11).

For unsymmetrical lines shown in Figure 3.4, the capacitance can be calculated as follows:

$$C_{an} = \frac{q_a}{V_{an}} = \frac{2\pi\varepsilon}{\ln\left(\dfrac{D_{eq}}{r}\right)} \quad \text{F/m line-to-neutral} \qquad (3.12)$$

Where D_{eq} is calculated in (3.5)

For bundled configurations as shown in Figure 3.5 the following equation can be used for unsymmetrical line configurations:

$$C_{an} = \frac{q_a}{V_{an}} = \frac{2\pi\varepsilon}{\ln\left(\dfrac{D_{eq}}{D_{SC}}\right)} \quad \text{F/m line-to-neutral} \qquad (3.13)$$

Where D_{SC} for two conductor bundles are:

$$D_{SC} = \sqrt{r \cdot d} \qquad (3.14)$$

Three conductor bundles:

$$D_{SC} = \sqrt[3]{r \cdot d^2} \qquad (3.15)$$

17

and for four conductor bundles:

$$D_{SC} = 1.091 \cdot \sqrt[4]{r \cdot d^3}$$ (3.16)

When ACSR conductors are used the outside radius of the conductor is obtained from the manufacturers table and this is used as "r" in (3.11)-(3.16). These equations are used to calculate the phase capacitance of the specific line configuration. If a line has a length "l" then the total capacitance (C_T) for the line is obtained by multiplying the capacitance per meter by the length of the line.

$$C_T = \frac{C}{m} \times l \quad F$$ (3.17)

Then the total capacitive reactance (X_{CT}) of the line can be calculated as follows:

$$X_{CT} = \frac{1}{2 \cdot \pi \cdot f \cdot C_T} \quad \Omega \text{ per phase}$$ (3.18)

It was seen that R_{dc} or R_{ac} can be obtained from a manufactures table. The total resistance (R_T) is obtained by multiplying the resistance per meter by the length "l" of the line. These quantities are used to describe transmission line parameters. These are Impedance (Z), Conductance (G), Susceptance (B) and admittance (Y). The total impedance, (Z_T) of a circuit that consists solely of an inductive reactance X_L (3.10) and a resistance R_T is calculated as follows:

$$Z_T \angle \theta_z = R_T + j \cdot X_{LT}$$ (3.19)

for an inductive network

$$Z \angle \theta_z = R_{ac} + j \cdot X_L$$ (3.20)

and

$$Y \angle -\theta_Y = \frac{1}{Z \angle \theta_z} = G - j \cdot B_L$$ (3.21)

where:

Y is the admittance in Siemens (S)

G is conductance (S)

B_L is the inductive susceptance (S)

for a capacitive network

$$Z\angle - \theta_z = R_{ac} - j \cdot X_C \qquad (3.22)$$

and

$$Y\angle\theta_Y = \frac{1}{Z\angle - \theta_z} = G + j \cdot B_C \qquad (3.23)$$

where:

Y is the admittance in Siemens (S)

G is conductance (S)

B_C is the capacitive susceptance (S)

If resistance is assumed negligible then

$$Z = jX_L \qquad (3.24)$$

$$Y = \frac{1}{Z} = -jB_L \qquad (3.25)$$

or

$$Z = -jX_C \qquad (3.26)$$

$$Y = \frac{1}{Z} = +jB_C \qquad (3.27)$$

An AC transmission line can be represented in different ways depending on the accuracy that is required. These different line models depend on how R, L, and C are represented in the model. Three different transmission line models are reviewed namely, the short, medium and long line models. For ease of explanation a single line representation of a three phase system will be described.

3.1.1 Short line model

When an overhead line is shorter than 80 km one can assume that a line has neither capacitance (C) nor skin effect, only a dc resistance R_{dc} (due to the absence of skin effect) and inductance (L) is considered. Figure 3.6 shows an equivalent circuit of a short line model. The advantage of the model is that it simplifies and speeds up calculations. The disadvantage of such a model is that it produces less accurate results than more complex models (Glover, Sarma. 2002:209), (Stevenson. 1982:90).
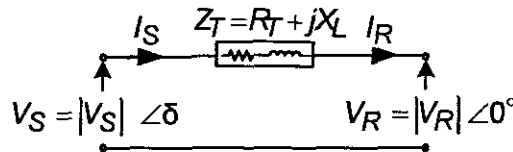
Figure 3.6: Short line model

Where:

Z_T is the impedance of the line

R_T is R_{dc} of the line

X_L is the inductive reactance of the line (3.10)

V_S = Sending-end L-N voltage (V)

V_R = Receiving-end L-N voltage (V)

I_S = Sending-end current (A)

I_R = Receiving-end current (A)

δ = The angle between V_S and V_R

This circuit is solved as a series circuit where $I_S = I_R$ thus (Stevenson. 1982:90):

$$V_S = V_R + I_R \cdot Z_T \qquad\qquad (3.28)$$

If a transmission line length is longer than 80 km the capacitance of the line needs to be taken into account.

3.1.2 Medium line model

If an overhead line is between 80 km and 240 km long a more complex model should be utilized that takes capacitance into account. The capacitance of a medium line can be represented in two different ways. One method is where the capacitance is lumped as a single quantity, this is referred to as a nominal-T network. The second method is where the total line capacitance (C_T) is divided in two and then placed at the two ends of the line. This model is called a nominal-π.

3.1.2.1 Nominal-T model

The nominal-T model is shown in Figure 3.7:
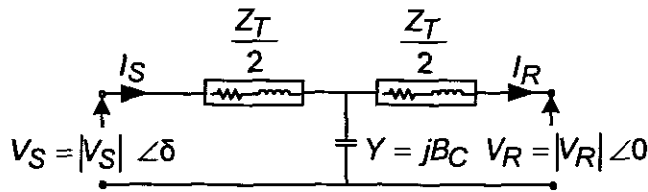
Figure 3.7: nominal-T model

Where:

Y is calculated in (3.27)

$\dfrac{Z_T}{2}$ is the impedance in (3.19) divided by two

With nominal-T networks the total series impedance (Z_T) of the line is divided into two parts and the shunt admittance (Y) of the network is lumped in the middle of the circuit.

3.1.2.2 Nominal-π model

Figure 3.8 shows the nominal-π model.
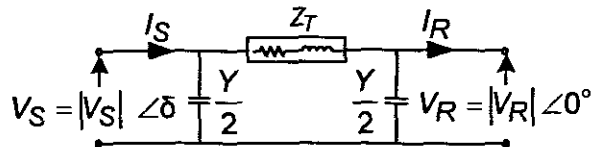
Figure 3.8: nominal-π model

Where:

$\dfrac{Y}{2}$ is the shunt admittance in (3.27) divided by two

Z_T is calculated in (3.19)

With the nominal-π network the total impedance (Z_T) is lumped in the centre of the network and the shunt admittance (Y) is split into two and connected at the two ends of the line. Due to the fact that the shunt admittance is introduced in the medium transmission line model, it becomes a two-port network and the ABCD method is implemented to find the relationships between V_S and V_R as well as between I_S and I_R.

The ABCD method uses generalized circuit constants of a transmission line. They are all complex numbers where, A and D are equal to each other and dimensionless. B and C are ohm and mhos (the inverse of ohms) quantities (Stevenson. 1982:94). They are calculated in the following manner:

$$A = D = 1 + \frac{Y_T \cdot Z_T}{2} = A\angle\theta_A \qquad (3.29)$$

$$B = Z_T = Z_T \angle\theta_Z \qquad (3.30)$$

$$C = Y \cdot \left(1 + \frac{Y_T \cdot Z_T}{4}\right) = C\angle\theta_C \qquad (3.31)$$

From this, the relationship between V_S, V_R I_S and I_R can be found:

$$V_S = A \cdot V_R + B \cdot I_R \qquad (3.32)$$

$$I_S = C \cdot V_R + D \cdot I_R \qquad (3.33)$$

When the line length exceeds 240 km these models prove to be inaccurate and a long line model is utilized to obtain results that compare with those found in a real line (Stevenson. 1982:94).

3.1.3 Long line model

A long line model can be represented by two different models, the one being a distributed model and the other one being an equivalent-π model.

3.1.3.1 Distributed line model

When an overhead line length exceeds 240 km, line parameters can no longer be lumped and are distributed uniformly throughout the entire length of the line. This transmission line model is called a distributed model. One small section of the line (length Δx) is shown in Figure 3.9.

Where x is the length "*l*"
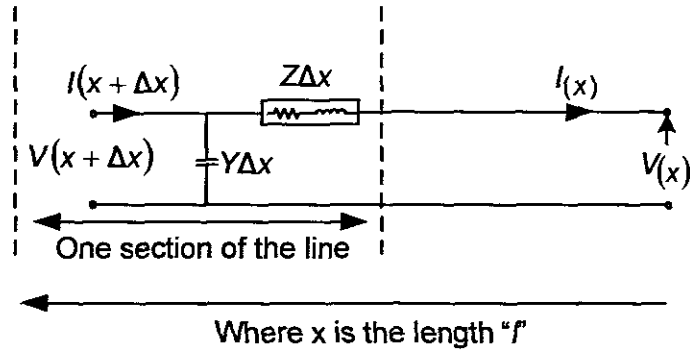
Figure 3.9: Distributed model

The voltage $V_{(x)}$ and the current $I_{(x)}$ are the voltage and currents at position x of the line, where x is the distance in meters from the receiving end of the line. $V(x + \Delta x)$ and $I(x + \Delta x)$ are the voltage and current at the point $(x + \Delta x)$. From Figure 3.9, two equations can be obtained when Kirchoff's voltage law, KVL and Kirchoff's current law, KCL are applied. These are:

$$V(x + \Delta x) = V(x) + Z\Delta x \cdot I(x) \text{ V} \qquad (3.34)$$

$$I(x + \Delta x) = I(x) + Y\Delta x \cdot V(x + \Delta x) \text{ A} \qquad (3.35)$$

If it is assumed that the limit is taken as $(\Delta x) \to 0$, then (3.34) and (3.35) can be rewritten as follows:

$$\frac{dV(x)}{dx} = Z \cdot I(x) \qquad (3.36)$$

$$\frac{dI(x)}{dx} = Y \cdot V(x) \qquad (3.37)$$

These two equations (3.36) and (3.37) are two linear first order differential equations with two unknowns $V_{(x)}$ and $I_{(x)}$.

By differentiating (3.36) and using (3.37), $I_{(x)}$ can be eliminated as follows:

$$\frac{d^2V(x)}{dx^2} - ZY \cdot V(x) = 0 \qquad (3.38)$$

23

This is a second order differential equation with only one unknown $V_{(x)}$. If this is inspected it is found that the solution is (Glover, Sarma. 2002:217):

$$V(x) = A_1 e^{\gamma x} + A_2 e^{-\gamma x} \text{ V}$$

(3.39)

Where A_1 and A_2 are both integration constants and γ is the propagation constant (gamma) whose unit is m^{-1} and is calculated as follows:

$$\gamma = \sqrt{Z \cdot Y} \ m^{-1}$$

(3.40)

If (3.39) and (3.40) is used in (3.38) the solution to the differential equation can be solved. To solve $I_{(x)}$, it is necessary to insert (3.39) into (3.36). When this is done it is found that:

$$I(x) = \frac{A_1 e^{\gamma x} + A_2 e^{-\gamma x}}{\left(\dfrac{Z}{\gamma}\right)} \text{ A}$$

(3.41)

Using (3.40) it becomes (Glover, Sarma. 2002:217):

$$I(x) = \frac{A_1 e^{\gamma x} + A_2 e^{-\gamma x}}{Z_c} \text{ A}$$

(3.42)

Where Z_c is called the characteristic impedance and calculated as follows:

$$Z_c = \sqrt{\frac{Z}{Y}} \ \Omega$$

(3.43)

When the integration constants A_1 and A_2 are evaluated from the boundary conditions at x=0 the receiving end voltage and current, V_R and I_R are:

$$V_R = V(0) \text{ V}$$

(3.44)

$$I_R = I(0) \text{ A}$$

(3.45)

24

It can also be seen that at x=0, (3.39) and (3.42) will become:

$$V_R = A_1 + A_2 \text{ V}$$

(3.46)

$$I_R = \frac{A_1 - A_2}{Z_c} \text{ A}$$

(3.47)

To solve A_1 and A_2 the following is necessary:

$$A_1 = \frac{V_R + Z_c I_R}{2}$$

(3.48)

$$A_2 = \frac{V_R - Z_c I_R}{2}$$

(3.49)

When (3.48) and (3.49) are inserted into (3.39) and (3.42) and written as hyperbolic functions, cosh and sinh, the following are obtained (Glover & Sarma, 2002:217):

$$V(x) = \cosh(\gamma x) V_R + Z_c \sinh(\gamma x) I_R \text{ V}$$

(3.50)

$$I(x) = \frac{1}{Z_c} \sinh(\gamma x) V_R + \cosh(\gamma x) I_R \text{ A}$$

(3.51)

From (3.50) and (3.51) the ABCD parameters of a distributed line can be obtained in the form of a matrix:

$$\begin{bmatrix} V(x) \\ I(x) \end{bmatrix} = \begin{bmatrix} A(x) & B(x) \\ C(x) & D(x) \end{bmatrix} \cdot \begin{bmatrix} V_R \\ I_R \end{bmatrix}$$

(3.52)

At the sending end of the line x is equal to the length of the line (l). That means that $V_{(l)} = V_S$ and $I_{(l)} = I_S$.

If this is inserted into (3.52) then the ABCD parameters for a distributed line are:

$$A = D = \cosh(y \cdot l) \text{ per unit}$$ (3.53)

$$B = Z_c \sinh(y \cdot l) \ \Omega$$ (3.54)

$$C = \frac{1}{Z_c} \sinh(y \cdot l) \ S$$ (3.55)

From this the relationship between V_S, V_R I_S and I_R can be found:

$$V_S = A \cdot V_R + B \cdot I_R$$ (3.56)

$$I_S = C \cdot V_R + D \cdot I_R$$ (3.57)

3.1.3.2 Equivalent- π line model

From section 3.1.3.1 it is clear that obtaining the ABCD parameters of a distributed line is a complex and timely process. A transmission line model was developed that resembles a nominal-π network but produces the same accuracy in results to that of the distributed model, thus simplifying the calculation without sacrificing on the accuracy of the results obtained. This model is called the equivalent- π model. This model is shown in Figure 3.10
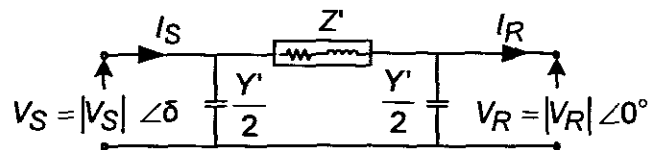
Figure 3.10: Equivalent-π model

In the equivalent-π configuration, the impedance (Z_T) and the admittance (Y_T) from the nominal- π are replaced with Z' and Y' to produce the same ABCD parameters to those of the distributed model. These new quantities, Z' and Y' need to be calculated.

The ABCD parameters of an equivalent-π circuit have the same structure to that of a nominal-π given in section 3.1.22. They are:

$$A = D = 1 + \frac{Y' \cdot Z'}{2} \text{ per unit}$$ (3.58)

$$B = Z' \; \Omega$$ (3.59)

$$C = Y' \cdot \left(1 + \frac{Y' \cdot Z'}{4}\right) S$$ (3.60)

These new quantities, Z' and y' are calculated as follows:

$$Z' = Z_c \sinh(Y \cdot l) \; \Omega$$ (3.61)

To be able to solve the circuit in Figure 3.10:

$$\frac{Y'}{2} = \frac{(Y \cdot l)}{2} \cdot \left[\frac{\tanh\left(\frac{(Y \cdot l)}{2}\right)}{Y \cdot \left(\frac{l}{2}\right)}\right]$$ (3.62)

where:

Y is calculated in (3.40)

l is the line length
Z_c is calculated in (3.37)
Z' is the impedance
Y' is the shunt admittance

These new quantities for the impedance and shunt admittance are now used as the new transmission line parameters. These parameters are used to represent the transmission line when steady-state load-flow studies are conducted.

3.2 Steady-state power flow analysis

Power flow in a HVAC network is dependent on two factors, the angular difference between the sending-end and the receiving-end and/or the voltage magnitude between the sending and receiving-end. The amount of real power that is transmitted across the transmission line is directly proportional to the angular difference and the reactive power is dependent on the difference in voltage magnitude between the sending and receiving-end. A power system is basically composed of generators, transformers and loads all interconnected by transmission lines. The purpose of a power system is to supply real and reactive power to customers at a voltage level within a specified limit. This must be achieved in a way that ensures that the components of the system supplying the customers are not overloaded. The model of a power system consists of all the buses in the system, the generating units and load elements interconnected by transmission lines (Toro, 1992:223).

Power flow studies or also known as load flow studies are extremely important in evaluating the operation of a power system, controlling them, and planning for future expansion.

A bus is an electrical equivalent to a single point on a circuit and it marks the location of one of two things: a generator that injects power, or a load that consumes power. Systems are usually assumed balanced. It is for this reason that the power system can be represented by a one-line- diagram (Von Meier, 2006:195-228).

The main purpose of power flow studies is to calculate bus voltages and power flows in a power system once the network topology is known. For load-flow studies at fundamental frequency, there are four parameters for each bus: voltage magnitude (V), voltage angle (δ), active power (P) and reactive power (Q). The principles involved in load-flow studies are straight forward, but a study relating to a real power system can be extremely complex and is usually done with the help of a digital computer and software.

Different methodologies exist to calculate the power flow in a two port network shown in Figures 3.6-3.10

They are:
- The current conjugate and formula methods
- Power flows by means of ABCD parameters

To be able to solve a multi-bus load-flow study for a power system an iterative procedure is used to calculate the unknowns in a power system. Two of the commonly used iterative numerical procedures are the Gauss-Seidal method and the Newton-Raphson method.

3.2.1   Current conjugate and formula method

In a multi-bus system the power flow across a transmission line between two buses is determined as follows:

Complex power S, in volt-amperes is in general given by

$$S = P + jQ = VI^* \quad \text{VA} \tag{3.63}$$

where:

> P is the active power
>
> Q is the reactive power
>
> I^* is the complex conjugate of I.

Thus, on a per-phase basis of a three phase system (assuming a short line model), the complex power at the receiving-end is (Stevenson, 1982:207):

$$S_R = P_R + jQ_R = V_R I^* \tag{3.64}$$

Similarly the complex power at the sending end is defined by:

$$S_S = P_S + jQ_S = V_S I^* \tag{3.65}$$

This method is called the current conjugate method. Depending on whether the sign of a power is + or -, will define if P or Q value is a supplying or absorbing power. Instead of having to calculate I, the powers can be directly calculated using formulas and the method is called the formula method namely:

$$S_R = \frac{|V_S| \cdot |V_R|}{|Z|} \angle (\theta_Z - \delta) - \frac{|V_S|^2}{|Z|} \angle \theta_Z \tag{3.66}$$

From this

$$P_R = \frac{|V_R| \cdot |V_S|}{|Z|} \cos(\theta_Z - \delta) - \frac{|V_S|^2}{|Z|} \cos\theta_Z \qquad (3.67)$$

and

$$Q_R = \frac{|V_R| \cdot |V_S|}{|Z|} \sin(\theta_Z - \delta) - \frac{|V_S|^2}{|Z|} \sin\theta_Z \qquad (3.68)$$

Similarly at the sending-end

$$P_S = \frac{|V_S|^2}{|Z|} \cos\theta_Z - \frac{|V_R| \cdot |V_S|}{|Z|} \cos(\theta_Z + \delta) \qquad (3.69)$$

and

$$Q_S = \frac{|V_S|^2}{|Z|} \sin\theta_Z - \frac{|V_R| \cdot |V_S|}{|Z|} \sin(\theta_Z + \delta) \qquad (3.70)$$

Using equations (3.67)-(3.70) the power flow across the transmission line (short line model) can be obtained. It must be mentioned that these formuli do not take the capacitance of the line into account. If a medium line model is treated it is usual to use a nominal-π model and the capacitance is placed at either end buses and does not affect flows across the line and these formuli can be used. If a long line model is treated it is used as an equivalent-π model and similarly the capacitance is placed at buses at the end of the line.

3.2.2 Power flows by means of ABCD parameters

The ABCD parameter method takes the capacitance into account and is thus suitable for the equivalent-π transmission model. With this method, four different variables (A, B, C and D) are used to calculate the power flow in a network as discussed in Section 3.1.3.2. They are calculated in (3.58) – (3.60). The variables used, are determined from (3.61) and (3.62).

The method provides the following formuli for calculating power flow at the receiving end of transmission line:

$$S_R = \frac{|V_R| \cdot |V_S|}{Z'} e^{j(\theta_Z - \delta)} - \frac{A \cdot |V_R|^2}{Z'} e^{j(\theta_Z - \theta_A)} \qquad (3.71)$$

$$P_R = \frac{|V_R| \cdot |V_S|}{Z'} \cos(\theta_Z - \delta) - \frac{A \cdot |V_R|^2}{Z'} \cos(\theta_Z - \theta_A) \qquad (3.72)$$

$$Q_R = \frac{|V_R| \cdot |V_S|}{Z'} \sin(\theta_Z - \delta) - \frac{A \cdot |V_R|^2}{Z'} \sin(\theta_Z - \theta_A) \qquad (3.73)$$

In a multi-bus power system the voltages at buses are not usually known, a numerical method is thus needed to solve for these unknown quantities.

For circuits operating in sinusoidal steady-state, Kirchoff's current law (KCL) and voltage law (KVL) apply to phasor currents and voltages. Thus the sum of all phasor currents entering any node is zero and the sum of the phasor-voltage drops around any closed path is zero. Network analysis techniques based on Kirchoff's laws, including nodal analysis, mesh or loop analysis, superposition, source transformations, and Thevenin's theorem or Norton's theorem, are useful for analyzing such circuits. In situations where power systems are composed of many buses (multi-bus systems), power flow solutions are usually based on a nodal equation approach that uses an admittance matrix Y_{bus} (Glover, Sarma. 2002:276):

$$[Y_{bus}] \cdot [V_{bus}] = [I_{bus}] \qquad (3.74)$$

Nodal equations are written in the following three steps:

Step 1 For a system with (N + 1) buses, where V_{bus} is the N vector of bus voltages, select one bus as the reference bus and define the voltages at the remaining buses with respect to the reference bus.

Step 2 Transform each voltage source in series with its impedance to an equivalent current source in parallel with that impedance. Where the I_{bus} is the N vector of source currents injected into each bus. Also, show admittance values instead of impedance values on the diagram, each current source is equal to the voltage source divided by the source impedance.

Step 3 Write nodal equations in matrix format as follows

$$
\begin{bmatrix}
Y_{11} & Y_{12} & Y_{13} & \cdots & Y_{1N} \\
Y_{21} & Y_{22} & Y_{23} & \cdots & Y_{2N} \\
Y_{31} & Y_{32} & Y_{33} & \cdots & Y_{3N} \\
\vdots & \vdots & \vdots & \vdots & \vdots \\
Y_{N1} & Y_{N2} & Y_{N3} & \cdots & Y_{NN}
\end{bmatrix}
\cdot
\begin{bmatrix}
V_{10} \\
V_{20} \\
V_{30} \\
\vdots \\
V_{N0}
\end{bmatrix}
=
\begin{bmatrix}
I_1 \\
I_2 \\
I_3 \\
\vdots \\
I_N
\end{bmatrix}
\qquad (3.75)
$$

Where Y is the N x N bus admittance matrix, V is the column vector of N bus voltages, and I is the column vector of N current sources.

The elements Y_{kN} of the bus admittance matrix Y are formulated as follows:

Diagonal elements: Y_{kk} = the sum of admittances connected to bus k

(k =1,2,...........N) $\qquad$ (3.76)

off-diagonal elements: Y_{kN} = -(the sum of admittances connected between buses k and N) ($k \neq N$) $\qquad$ (3.77)

The diagonal elements Y_{kk} are called the *self-admittances* or the *driving-point admittances* of bus k and the off-diagonal elements Y_{kN} for $k \neq N$ are called the *mutual admittances* or the *transfer admittances* between buses k and n. Since $Y_{kN} = Y_{Nk}$, the matrix Y is symmetric.

Power flow means the determination of voltage magnitudes and phase angle at each bus in a power system under balanced three-phase steady-state conditions. Once known, the real and reactive power flows in equipment such as transmission lines and transformers, as well as equipment losses can be calculated.

The starting point for a multi-bus power-flow problem is a one-line-diagram of the power system. The data needed consists of bus data, transmission line data, and transformer data. As shown below, the four variables are associated with each bus k: voltage magnitude V_k, phase angle δ_k, real power P_k, and reactive power Q_k supplied to the bus (Glover, Sarma. 2002:276):
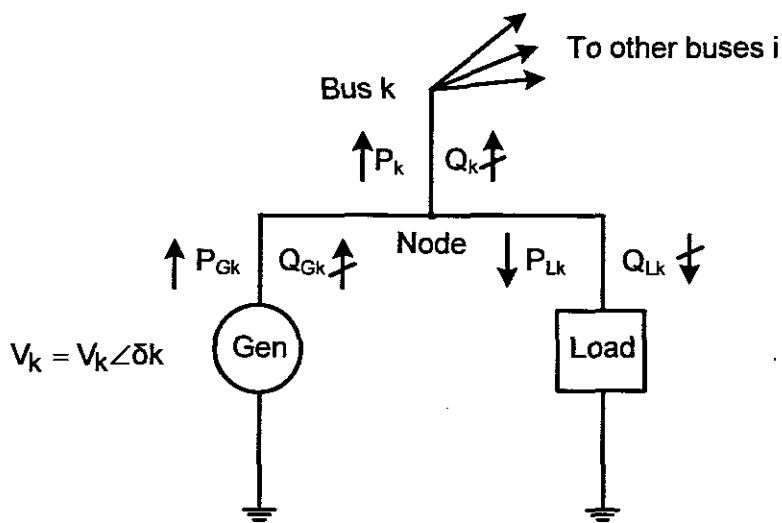
Figure 3.11: Power flow

The power flow solution process begins by starting at each bus, two of these variables are specified as input data, and the other two are unknowns and are to be calculated. At bus k:

$$P_k = P_{Gk} - P_{Lk} \tag{3.78}$$

and

$$Q_k = Q_{Gk} - Q_{Lk} \tag{3.79}$$

Each bus k is categorized into one of the following three bus types:

1. Swing bus- There is only one swing bus and it is numbered bus 1. The swing bus is the reference bus and $V_1 \angle \delta_1$ is typically $1.0 \angle 0°$ per unit. The power-flow solution determines P_1 and Q_1.

2. Load bus- P_k and Q_k are known. The power-flow program finds V_k and δ_k.

3. Voltage controlled bus- are buses to which generators, switched shunt capacitors, or static var systems are connected. P_k and V_k are usually fixed values and the solution calculates Q_k and δ_k. Maximum and minimum var limits Q_{Gkmax} and Q_{Gkmin} that such equipment can handle are also taken into account. Another further example of this type of bus is one to which a tap changing transformer is connected.

Of importance to note is that when bus k is a load bus with no generation then $P_k = -P_{Lk}$ which means the real power supplied to bus k is negative. When the load is inductive, $Q_k = -Q_{Lk}$ is also treated as negative.

The equivalent-π model is used to represent transmission lines and includes the per-unit equivalent-π circuit series impedance Z and shunt admittance Y. Transformers are also represented by equivalent circuits and include per-unit winding impedances Z, the per-unit exciting branch admittance Y and MVA ratings.

For any bus k, the kth nodal equation is (Glover, Sarma. 2002:276):

$$I_k = \sum_{n=1}^{N} Y_{kn} \cdot V_n \qquad (3.80)$$

Power flow solutions by the Gauss-Seidal numerical method are based on the nodal equation (3.80), where each current source I_k is determined from (3.81), that is the complex power delivered to bus k

$$S_k = P_k + jQ_k = V_k I_k^* \qquad (3.81)$$

From this

$$S_k = P_k + jQ_k = V_k \left[\sum_{n=1}^{N} Y_{kn} e^{j\theta_{kn}} \cdot V_n e^{j\delta n} \right]^* \qquad k=1, 2,....,N \qquad (3.82)$$

$$= V_k \left[\sum_{n=1}^{N} Y_{kn} e^{-j\theta_{kn}} \cdot V_n e^{-j\delta n} \right] \qquad (3.83)$$

Using notation

$$V_k = V_k e^{j\delta k} \qquad (3.84)$$

$$P_k + jQ_k = V_k e^{j\delta k} \cdot \left[\sum_{n=1}^{N} Y_{kn} e^{-j\theta_{kn}} \cdot V_n e^{-j\delta n} \right] \qquad (3.85)$$

$$= V_k \sum_{n=1}^{N} Y_{kn} \cdot V_n e^{j\delta kk} \cdot e^{-j\theta kn} \cdot e^{-j\delta n} \qquad (3.86)$$

$$= V_k \sum_{n=1}^{N} Y_{kn} \cdot V_n e^{j(\delta k - \theta kn - \delta n)} \qquad (3.87)$$

$$= V_k \sum_{n=1}^{N} Y_{kn} \cdot V_n e^{j(\delta k - \delta n - \theta kn)} \qquad (3.88)$$

This can be seen
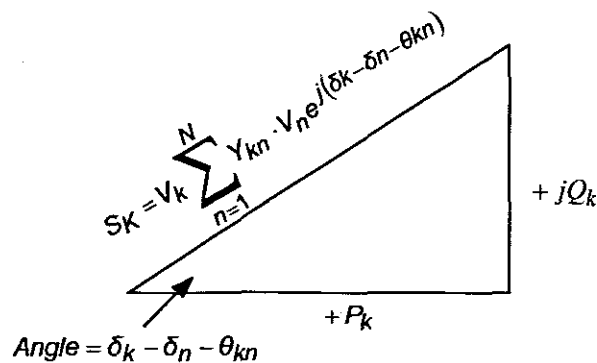
Figure 3.12: Power triangle

35

Taking the real and imaginary part of (3.81)

$$P_k = V_k \sum_{n=1}^{N} Y_{kn} \cdot V_n \cos(\delta k - \delta n - \theta kn) \qquad (3.89)$$

$$Q_k = V_k \sum_{n=1}^{N} Y_{kn} \cdot V_n \sin(\delta k - \delta n - \theta kn) \qquad (3.90)$$

$$k = 1, 2 \ldots \ldots, N$$

Power flow solutions by the second numerical method of Newton-Rapshon are based on the nonlinear load flow equations (3.89) and (3.90).

In both the Gauss-Seidal and the Newton-Raphson method two variables may be specified and the other two calculated (Grady 2007:270-313).

3.2.3 Gauss-Seidal iteration calculation

The Gauss-Seidal method is an iterative procedure for solving simultaneous nonlinear equations using the admittance matrix Y_{bus}. For each load bus, I_k is given as

$$I_k = \frac{P_k - jQ_k}{V_k^*} \qquad (3.91)$$

from which the voltage at a kth bus can be defined as

$$V_k(i+1) = \frac{1}{Y_{KK}} \left[\frac{P_k - jQ_k}{V_k^*(i)} - \sum_{n=1}^{k-1} Y_{kn} V_n(i+1) - \sum_{n=k+1}^{N} Y_{kn} V_n(i) \right] \qquad (3.92)$$

This equation is applied twice during each iteration for load buses first using $V_k^*(i)$ then replacing $V_k^*(i)$, by $V_k^*(i+1)$.

For a voltage controlled bus, Q_k is unknown, but can be calculated from (3.90)

$$Q_k = V_k(i) \sum_{n=1}^{N} Y_{kn} V_n(i) \sin(\delta_k(i) - \delta_n(i) - \theta_{kn}) \tag{3.93}$$

Also

$$Q_{Gk} = Q_k + Q_{Lk} \tag{3.94}$$

If the calculated value of Q_{Gk} does not exceed its limits, then Q_k is used in (3.90) to calculate $V_k(i+1) = V_k(i+1) \angle \delta_k(i+1)$. Then the magnitude $V_k(i+1)$ is updated to V_k which is the input data for the voltage-controlled bus. Thus we use (3.90) to calculate only the angle $\delta_k(i+1)$ for voltage-controlled buses. When calculated values exceed limits $Q_{Gk \, max}$ or $Q_{Gk \, min}$ during any iteration, then the bus type is changed from a voltage controlled bus to a load-bus. For a swing-bus, V_1 and δ_1 fixed, thus no iterations are required for the swing-bus.

3.2.4 Newton-Raphson iteration calculation

To apply the Newton-Raphson method to a power-flow problem, for the kth bus we let (Glover, Sarma. 2002:276):

$$V_k = |V_k| \angle \delta_k, \quad V_n = |V_n| \angle \delta_n, \quad Y_{kn} = |Y_{kn}| \angle Y_{kn} \tag{3.95}$$

Then

$$P_k = V_k \sum_{n=1}^{N} Y_{kn} V_n \cos(\delta_k - \delta_n - Y_{kn}) \tag{3.96}$$

and

$$Q_k = V_k \sum_{n=1}^{N} Y_{kn} V_n \sin(\delta_k - \delta_n - Y_{kn}) \tag{3.97}$$

Having P and Q specified for every bus (accept the swing-bus), we estimate values for V and δ for each bus except the swing-bus, for which they are known.

With these estimated values to calculate values for P_k and Q_k we can compute:

$$\Delta P_k^{(0)} = P_{ks} - P_{kc}^{(0)} \tag{3.98}$$

$$\Delta Q_k^{(0)} = Q_{ks} - Q_{kc}^{(0)} \tag{3.99}$$

where the subscripts s and c mean specified and calculated, respectively.

The change in voltage magnitude and angle for the respective buses can be calculated by the following matrix.

$$\begin{vmatrix} \Delta P \\ \Delta Q \end{vmatrix} = \begin{vmatrix} J_1 & J_2 \\ J_3 & J_4 \end{vmatrix} \times \begin{vmatrix} \Delta \delta \\ \Delta |V| \end{vmatrix} \tag{3.100}$$

Where the Jacobian matrix is defined by:

$$Jacobian = \begin{vmatrix} \dfrac{\partial P_2}{\partial V_2} & \dfrac{\partial P_2}{\partial \delta_2} \\ \dfrac{\partial Q_2}{\partial V_2} & \dfrac{\partial Q_2}{\partial \delta_2} \end{vmatrix} \tag{3.101}$$

It is important to mention that the formulas that are given in (3.96) and (3.97) only hold true for a system where all the buses are specified. If the bus is not specified, the amount of real or reactive power is unknown. Then these formulas don't hold true to calculate the power flow at those unspecified buses. Newton-Rapson will calculate the voltage and angles at those buses and then the formulas given in (3.67)-(3.70) can be utilized to calculate the power flow at those unspecified buses taking the capacitance into account.

3.3 Operating point

As previously discussed, power flow can be determined by means of ABCD parameters. Theses are given in (3.58) – (3.60)

The theoretical maximum real power delivered (or steady-state stability limit) occurs when $\delta = \theta_Z$.

38

From this:

$$P_{max} = \frac{|V_R| \cdot |V_S|}{|Z'|} - \frac{A \cdot |V_R|^2}{Z'} \cos(\theta_Z - \theta_A)$$ (3.102)

This is graphically shown in Figure 3.13. The transmission line represented in Figure 3.6 is a short line which only has inductive reactance ($\theta_Z = 90°$), thus the theoretical maximum real power transfer will occur at 90°. For a transmission line containing capacitance and resistance this point will shift accordingly.
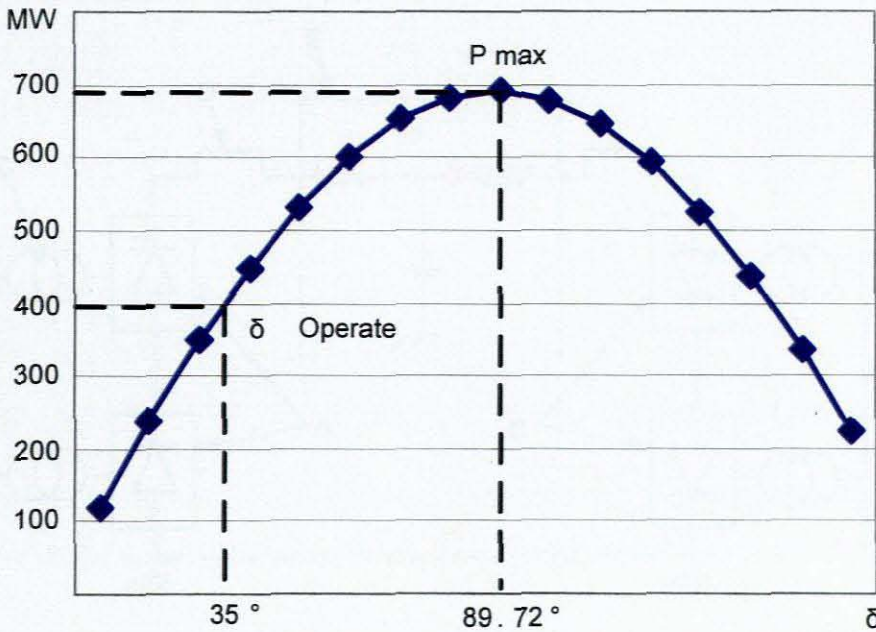
Figure 3.13: Maximum real power delivered

Even though transmission lines can transmit this theoretical maximum power, practically they will never be operated at an angular displacement bigger than 35° due to stability reasons. For this reason any angular displacement larger than 35° is unstable operation (Glover, Sarma. 2002:234).

3.4   Summary

In order for HVAC transmission lines and their interconnection in multi-bus power system to produce power results similar to real world systems it can be seen that models used for studies need to be accurate and for this reason industrial-grade software tools are usually applied to conduct such studies.

CHAPTER FOUR
HIGH VOLTAGE DIRECT CURRENT THEORY

4.1   HVDC system description

Different HVDC system configurations exist, bi-polar, homo-polar, back-to-back, multi-terminal and mono-polar (Padiyar. 1990:8). Only mono-polar is considered in this thesis.

4.1.1   Mono-polar operation

A twelve-pulse mono-polar HVDC system is shown in Figure 4.1.
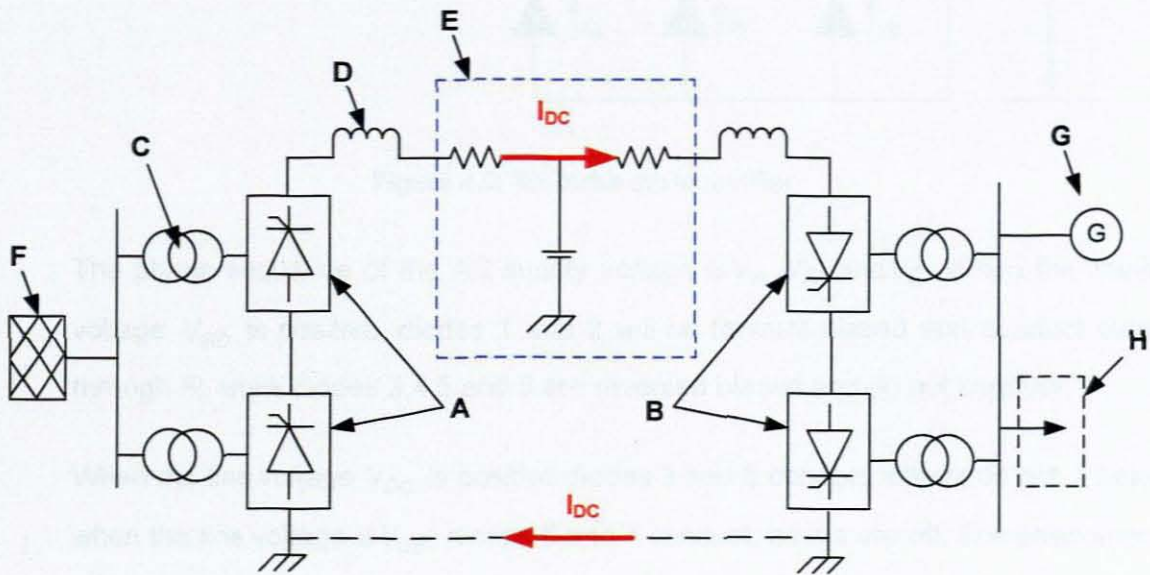
Figure 4.1: Mono-polar operation

The system consists of a rectifier station shown at "A" and an inverter station at "B". These stations are twelve-pulse converter stations which consist of two, six-pulse bridges connected in series. The term converter is the generic term for either a rectifier or an inverter in HVDC systems. These converter stations consists of multiple thyristor valves connected together to form one valve. A thyristor is a semi-conductor that conducts when a firing pulse is applied to its gate. To understand the operation of a six-pulse rectifier bridge which consists of thyristors, it is first necessary to understand the principal of natural commutation and this is best described if we use a (uncontrolled device) diode.

Figure 4.2 shows a six-pulse bridge that consists of diodes.
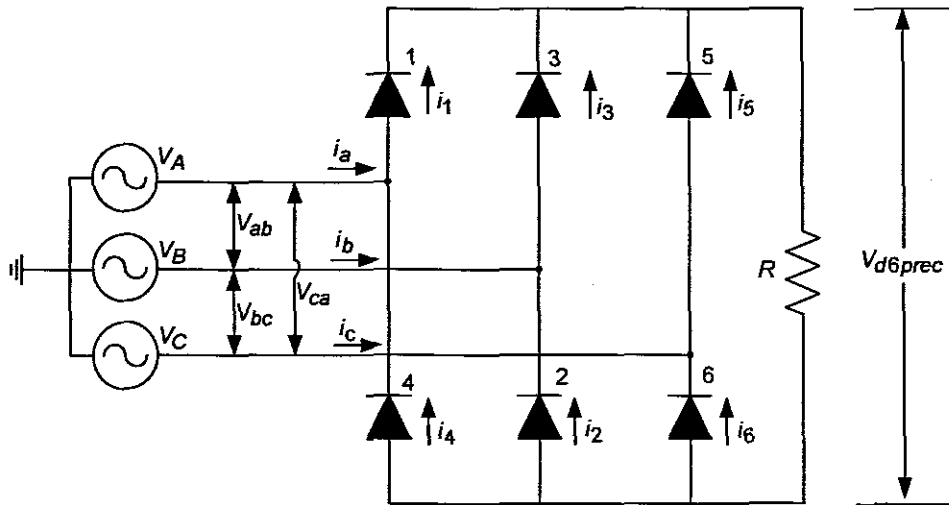
Figure 4.2: Six-pulse diode rectifier

The phase sequence of the AC supply voltage is V_A, V_B and V_C. When the line-line voltage V_{ab} is positive, diodes 1 and 2 will be forward biased and conduct current through R, while diodes 3,4,5 and 6 are reversed biased and do not conduct.

When the line voltage V_{bc} is positive diodes 3 and 6 conduct, others do not. Likewise when the line voltage is V_{ca}, diodes 5 and 4 conduct, others are off. The phenomenon that the most positive voltage will cause corresponding diodes to conduct is called natural commutation. It should also be mentioned that the wave shape of the output voltage leads to an arrangement referred to as a "six-pulse rectifier" because there are six segments to the voltage waveform in one period, each conducts for a duration of 60° (π / 3 radians), the number 6 is used because besides V_{ab}, V_{bc} and V_{ca}, there are also voltage V_{ba}, V_{cb} and V_{ac} present (Fisher 1991:222-223).
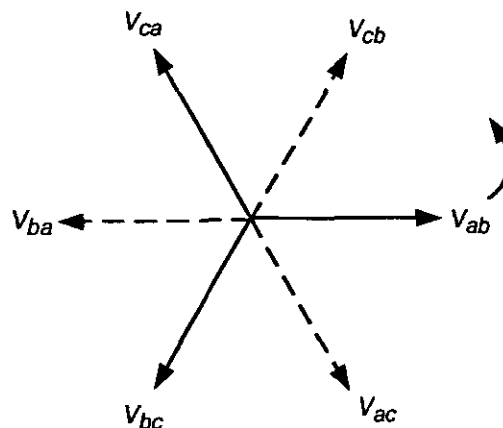
Figure 4.3: Three-phase phasor diagram

The input to the bridge is a sinusoidal three-phase symmetrical voltage shown in Figure 4.4.
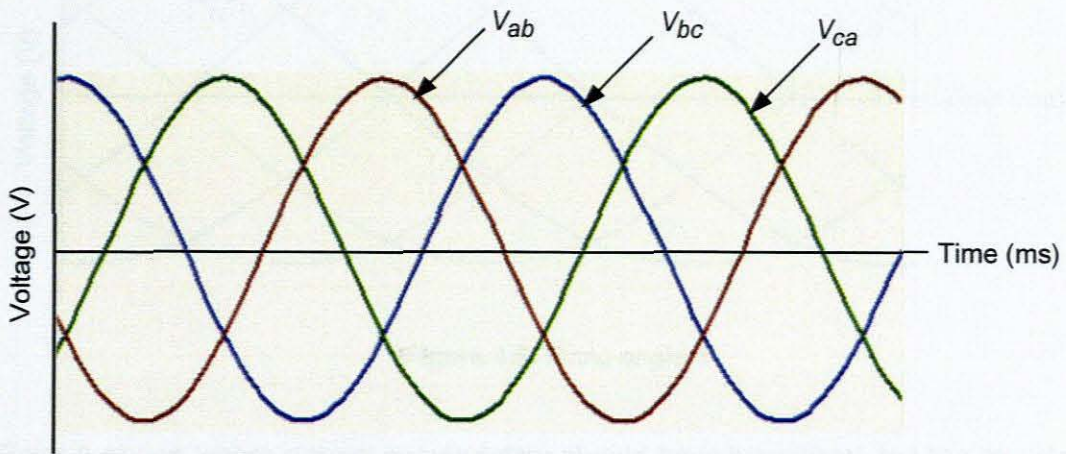
Figure 4.4: Three-phase symmetrical voltage input to the rectifier

The corresponding output from the six-pulse bridge is shown in Figure 4.5
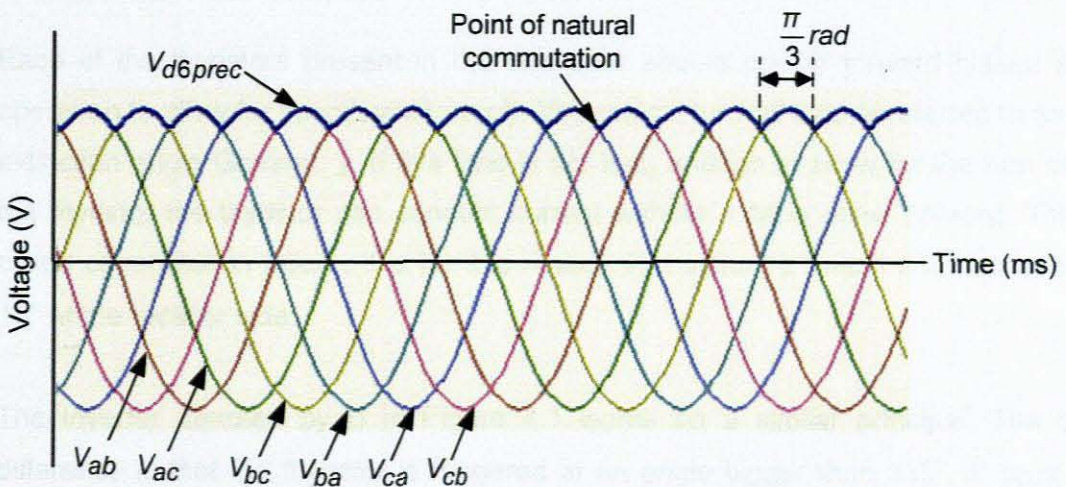
Figure 4.5: Output from the six-pulse bridge

Here, natural commutation can be seen as there is no delay in the changing over from one voltage to the next. In Figure 4.5 all the voltages are indicated, as soon as the one voltage becomes more positive than the next then V_{d6prec} switches over to the next. This is shown at the point of natural commutation.

Now if diodes in Figure 4.2 are replaced with thyristors then as mentioned a thyristor will only conduct if a trigger pulse is supplied to the gate of the thyristor. This pulse is called a firing pulse. The amount of degrees that the signal is delayed is called the firing angle and is denoted with the symbol α. This can be seen in Figure 4.6.
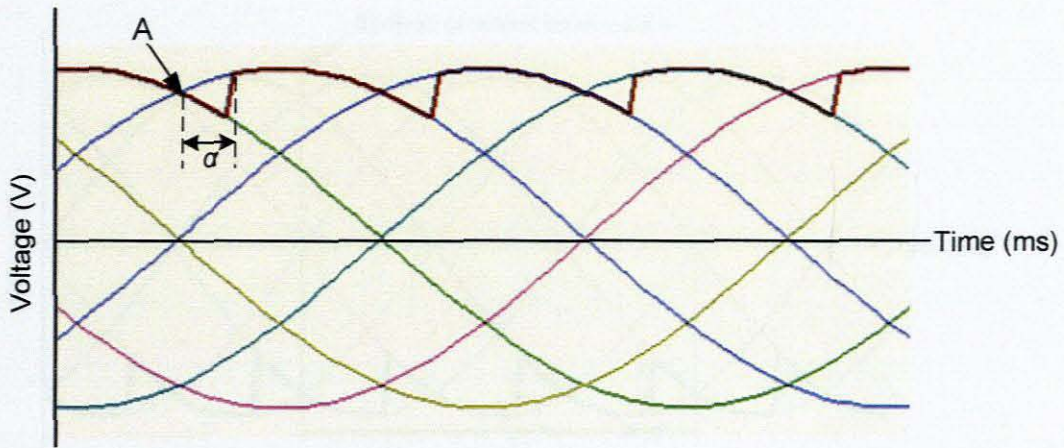
Figure 4.6: Firing angle α

Point A shows where natural commutation should have happened, but the thyristor is controlled and a firing pulse is produced with duration α. In practice this firing angle is never smaller than 15°. When α is operated at 15°, the converter operates as a rectifier, shown as "A" in Figure 4.1 and real and reactive power is absorbed from the AC supply, shown at "F" (Figure 4.1).

Each of the thyristors present in the converter should not be forward biased after operation to allow for successful turn off. This critical turn-off time is referred to as the extinction angle Gamma, γ. If this time is not long enough to allow for the turn off of the thyristor the thyristor can conduct current without a firing pulse present. This is called commutation failure. It is for this reason that alpha "α" must not be less than 15° at the rectifier side.

The inverter denoted by B in Figure 4.1 works on a similar principal. The only difference is that the thyristor is triggered at an angle bigger than 135°. If $α_0$ is the point at which natural commutation would occur then "α" occurs 135° later as shown in Figure 4.7. The firing angle can be expressed as an angle of delay "α" or an angle of advance Beta "β".

When α is fixed at a value greater than 90° a converter operates as an inverter and absorbs DC power delivered by the DC line and delivers AC power to the network, shown by "H" in Figure 4.1.
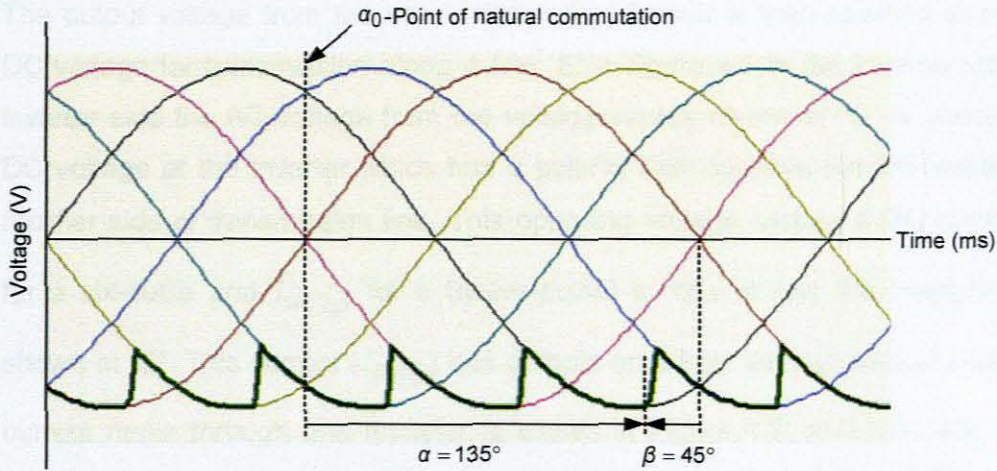
Figure 4.7: Angle of advance β

From this the mono-polar operation can be discussed. When considering Figure 4.1, the sinusoidal three-phase voltage from the grid shown at "F" is changed to the correct voltage level by means of the commutation transformer shown at "C". The transformer reactance hinders the currents transition from one phase to another. This is shown in Figure 4.8. The transition should take place at point A (α_0) but as the transformer reactance delays this change an overlap occurs which is denoted by the angle "μ". The three angles mentioned, α, μ and γ must all add up to 180°, as shown in (4.1)

$$180° = \alpha + \mu + \gamma \qquad (4.1)$$

where:

$$\beta = \mu + \gamma \qquad (4.2)$$

To illustrate the overlap angle, the thyristor firing angle (α) is set to 0 ° (Figure 4.8)
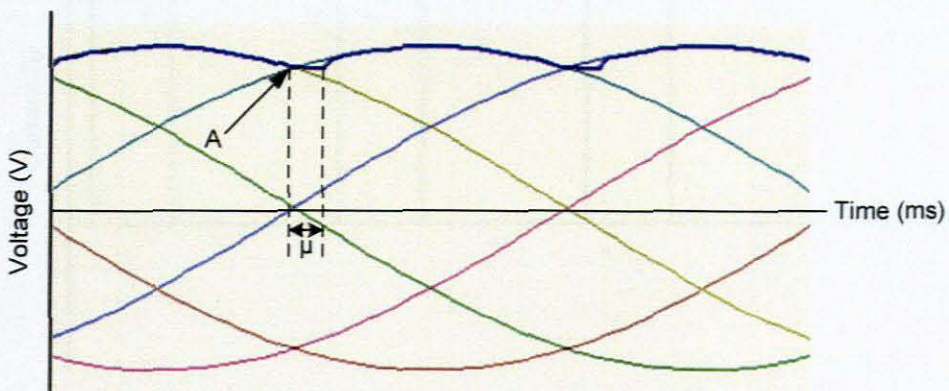
Figure 4.8: Overlap angle, "μ"

44

The output voltage from the commutation transformer is then rectified to produce a DC voltage for transmission along a line "E" in figure 4.1 to the inverter side. At the inverter side the AC voltage from the voltage source shown at "G" is converted to a DC voltage at the inverter which has a polarity that opposes the DC voltage at the rectifier side of transmission line. This opposing voltage causes a DC current (I_{d6p} for a six-pulse and I_{d12p} for a twelve-pulse) to flow across the transmission line shown at "E". This current (I_{d6p}) has a ripple on it from the conversion process. The current ripple through one thyristor is shown in Figure 4.9. Inductors are placed in series with the transmission line shown at "D" to smooth out some of the ripple. A reactor hinders the sudden change in current and in so doing, reduces the ripple of the current.
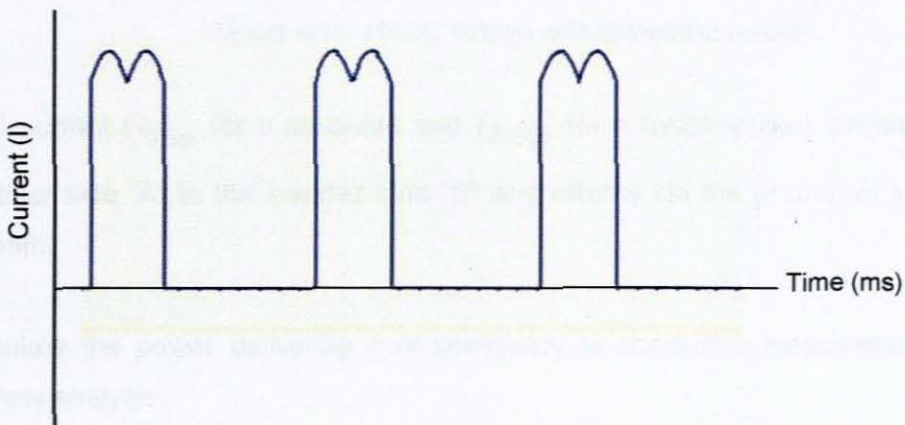
Figure 4.9: HVDC current without smoothing reactors

When the smoothing reactors "D" at both ends of the transmission lines "E" are inserted into the circuit, the resultant current waveform typically obtained through one thyristor are shown in Figure 4.10.
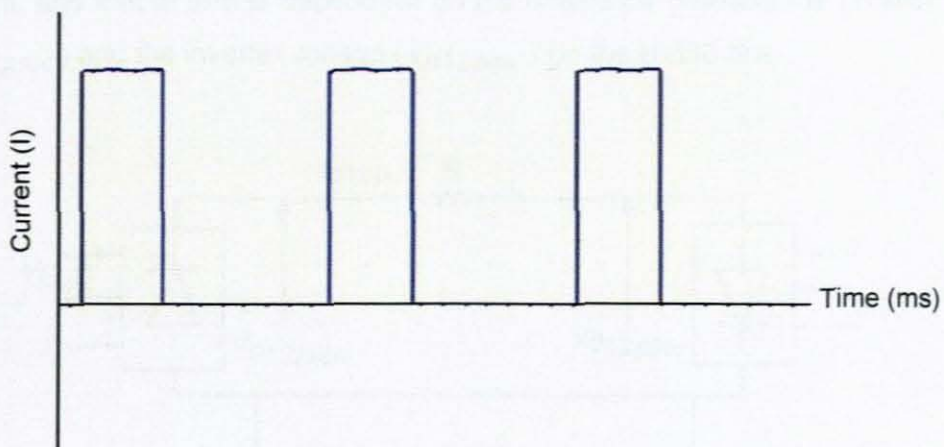
Figure 4.10: HVDC current with smoothing reactor

45

This reactor (D) also produce a more smoothed voltage waveform (Figure 4.11) and increases the average DC voltage and average power that is transmitted across the transmission line (E).
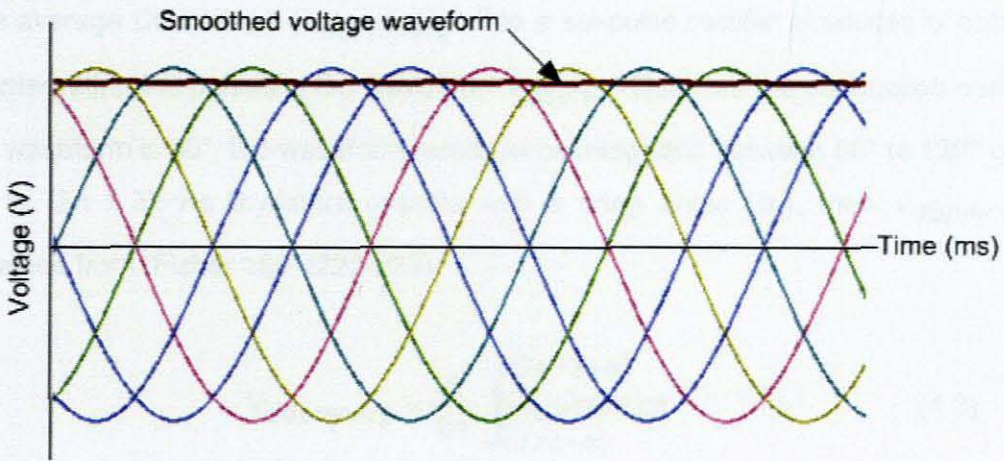
Figure 4.11: HVDC voltage with smoothing reactor

The DC current (I_{d6p} for a six-pulse and I_{d12p} for a twelve-pulse) circulates from the rectifier side "A" to the inverter side "B" and returns via the ground or a metallic return path.

To calculate the power delivering it is necessary to conduct a steady-state HVDC power flow analysis.

4.2   Twelve-pulse HVDC power delivery

4.2.1   DC side power

Unlike HVAC systems the power that is transmitted across HVDC lines is not a function of the angular displacement between buses but rather a function of the DC current, and that in turn is dependent on the difference between the rectifier voltage ($V_{d12prec}$) and the inverter voltage ($V_{d12pinv}$) on the HVDC line.
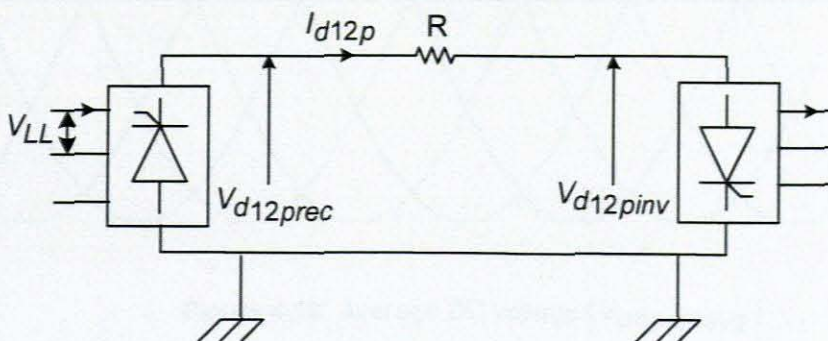
Figure 4.12: Twelve-pulse DC voltages

A twelve-pulse converter is two six-pulse converters connected in series so to be able to calculate the voltages and currents shown in Figure 4.12 a six-pulse must first be considered.

The average DC voltage ($V_{d6precavg}$) that a six-pulse rectifier produces is obtained by integrating the pulsating DC waveform V_{d6prec}. Because the conduction period of the waveform is 60°, the waveform needs to be integrated between 60° to 120° or (π / 3), to (2π / 3). As thyristors operate with a firing angle (α), then $V_{d6precavg}$ is obtained from (Fisher 1991:222-223):

$$V_{d6precavg} = \frac{6}{2\pi} \int_{(\pi/3+\alpha)}^{(2\pi/3+\alpha)} V_M \sin(\omega t) dt \qquad (4.3)$$

This can be simplified to (Fisher 1991:222-223):

$$V_{d6precavg} = \frac{3}{\pi} \cdot V_m \cdot \cos(\alpha) \qquad (4.4)$$

Where V_m is the peak AC voltage.

Figure 4.13 shows the average DC voltage ($V_{d6precavg}$) that a six-pulse rectifier produces.
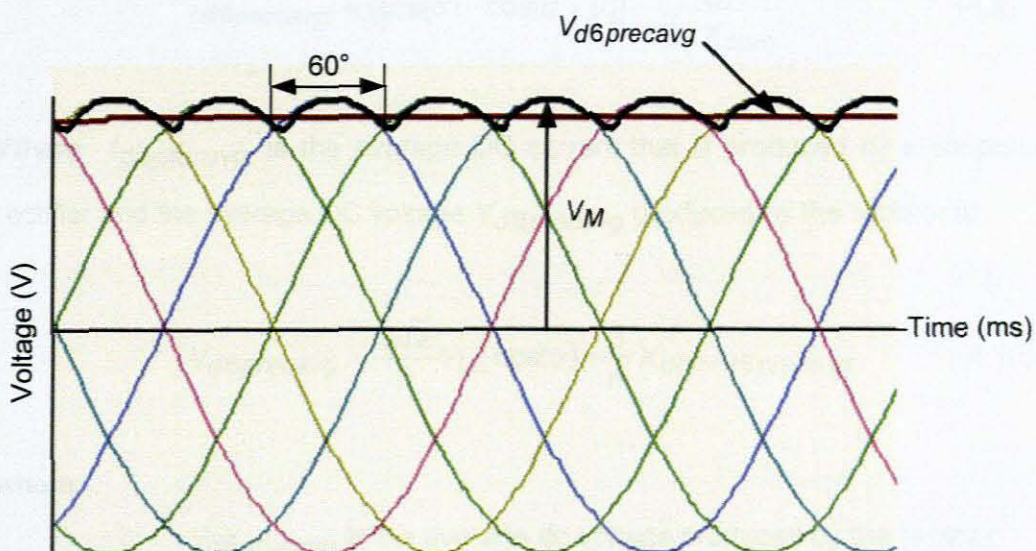
Figure 4.13: Average DC voltage ($V_{d6precavg}$)

47

Because the current ripple is similarly sinusoidal, the average DC current for a six-pulse converter can be expressed as (Fisher, 1991:222-223):

$$I_{d6precavg} = \frac{3}{\pi} \cdot I_m \qquad (4.5)$$

If (4.4) and (4.5) are re-written with the voltage and current specified in line-to-line values (V_{LL} and I_{LL}), they can be written as:

$$V_{d6precavg} = \frac{3\sqrt{2}}{\pi} \cdot V_{LL} \cdot \cos(\alpha) \qquad (4.6)$$

because

$$V_m = \sqrt{2} \cdot V_{LL} \qquad (4.7)$$

and

$$I_{d6precavg} = \frac{3\sqrt{2}}{\pi} \cdot I_{LL} \qquad (4.8)$$

These equations (4.6) and (4.8) only hold true if there is no commutation transformers present in the circuit. As soon as overlap is present in the circuit (commutation transformer present) (Fisher, 1991:222-223):

$$I_{d6precavg} = (\cos(\alpha) - \cos(\alpha + \mu)) \cdot \frac{V_{LL}}{\sqrt{2} \cdot X_{com}} \qquad (4.9)$$

Where $I_{d6precavg}$ is the average DC current that is produced by a six-pulse (6p) rectifier and the average DC voltage $V_{d6precavg}$ produced by the rectifier is:

$$V_{d6precavg} = \frac{3\sqrt{2}}{\pi} V_{LL} \cos(\alpha) - \frac{3}{\pi} X_{com} I_{d6precavg} \qquad (4.10)$$

where:

$V_{d6precavg}$ is the average dc voltage produced by the rectifier

X_{com} is the commutation transformer reactance in pu.

To calculate the DC side voltage for a twelve-pulse rectifier the following equations is used.

$$V_{d12precavg} = 2 \cdot V_{d6precavg} \qquad (4.11)$$

where, $V_{d6precavg}$ is the average six-pulse DC voltage.

The current produced by a twelve-pulse rectifier ($I_{d12precavg}$) which flows to the inverter side ($I_{d12pinvavg}$) of the HVDC system and which is common to both sides of the line is:

$$I_{d12precavg} = (\cos(\alpha) - \cos(\alpha + \mu)) \cdot \frac{V_{LL}}{\sqrt{2} \cdot X_{com}} \qquad (4.12)$$

Thus:

$$I_{d12precavg} = I_{d12pinvavg} \qquad (4.13)$$

When the average DC voltage on the inverter side ($V_{d12pinvavg}$) is calculated the DC rectifier voltage $V_{d12precavg}$ and the DC current $I_{d12precavg}$ is usually known and from this $V_{d12pinvavg}$ can be calculated as follows:

$$V_{d12pinvavg.} = V_{d12precavg.} - I_{d12precavg} \cdot R \qquad (4.14)$$

where R is the DC resistance of the line (E)

If these quantities ($V_{d12precavg}$ and $I_{d12precavg}$) is not known then (4.10) can be re-written in terms of inverter quantities:

$$V_{d6pinvavg} = \frac{3\sqrt{2}}{\pi} V_{LL} \cos(\alpha) - \frac{3}{\pi} X_{com} I_{d6pinvavg} \qquad (4.15)$$

and from this:

$$V_{d12pinvavg} = 2 \cdot V_{d6pinvavg} \qquad (4.16)$$

The power that is being transmitted from the rectifier side for a twelve-pulse converter can be calculated as:

$$P_{DCrec} = V_{d12precavg} \cdot I_{d12precavg} \qquad (4.17)$$

and the DC power that is absorbed by the inverter:

$$P_{DCinv} = V_{d12pinvavg} \cdot I_{d12pinvavg} \qquad (4.18)$$

If it is assumed that the power losses are negligible in a converter, then it can be assumed that the AC power is equal to the DC power. This is shown in (4.19):

$$P_{AC} = \sqrt{3} \cdot V_{LL} \cdot i_{LL} \cdot \cos(\theta) = P_{DC} \text{ W} \qquad (4.19)$$

where θ is the angle between the phase voltage and current and P_{AC} can be expressed as P_{ACrec} and P_{ACinv} and P_{DC} as P_{DCrec} and P_{DCinv}. From this:

$$P_{DCrec} = P_{ACrec} \qquad (4.20)$$

and

$$P_{DCinv} = P_{ACinv} \qquad (4.21)$$

4.2.2 Reactive power flow analysis

Due to the firing delay and commutation angles, the converter (both rectifier and inverter) fundamental frequency currents in each phase always lags its voltage by angle "θ" (Arrillaga & Smith, 1998:15). The converter therefore absorbs lagging current which means it consumes reactive power.

From (4.19) the angle θ can be calculated as follows (Arrillaga & Smith. 1998:15):

$$\cos(\theta) = \frac{1}{2} \cdot (\cos\alpha + \cos(\alpha + \mu)) \qquad (4.22)$$

Where, α is the rectifier firing angle and μ is the overlap angle for the converter (both rectifier and inverter).

The reactive power that is absorbed by the converter (in this case a rectifier) is expressed in terms of the AC power and that is (Arrillaga, Smith. 1998:16):

$$Q_{rec} = P_{ACrec} \cdot \tan(\theta) \tag{4.23}$$

and for an inverter:

$$Q_{inv} = P_{ACinv} \cdot \tan(\theta) \tag{4.24}$$

where $\tan(\theta)$ is calculated as:

$$\tan(\theta) = \frac{(\sin(2\alpha + 2\mu) - \sin 2\alpha - 2\mu)}{\cos 2\alpha - \cos(2\alpha + 2\mu)} \tag{4.25}$$

In the case of a rectifier α will be smaller than 90° and for an inverter it will be larger.

The rectifier absorbs AC power P_{ACrec} and delivers P_{DCrec} where the inverter absorbs DC power P_{DCinv} and delivers AC power P_{ACinv} to the AC network. Both the rectifier and the inverter absorb reactive power and this is calculated in (4.23) and (4.24). In industry the relationship between the real power (both rectifier and inverter) P_{AC} delivered and Q absorbed is typically 0.6, which means for every 1000 MW delivered 600 Mvar is absorbed (Arrillaga, 1988:35). As the AC system may not be able to supply this reactive power it is usually necessary to connect a source of reactive power to both the rectifier and inverter stations. This is usually done by connecting capacitors to the converter buses (Padiyar, 1990:12), (Arrillaga, 1988:33).

4.3 Harmonic analysis

The presence of waveform distortion in both current and voltage is generally expressed in harmonic frequencies which are integers of the fundamental frequency (Arrillaga, Smith, Watson, Alan, 1997:135). As HVDC converter stations are non-linear devices they contribute harmonics of larger magnitudes than typically found in plain HVAC power systems.

Generally a converter has considerable more inductance on the DC side than on the AC side and the station acts like a source of harmonic voltage on the DC side and a source of harmonic current on the AC side (Arrillaga, Smith, Watson, Alan, 1997:134).

As the DC voltage waveform is pulsating, it can be decomposed into voltage harmonics, namely (Arrillaga, Smith, Watson, Alan, 1997:134):

$$DC_{harmonics} = n \cdot p \cdot f \qquad (4.26)$$

where

p = the pulse number of the converter

n = is an integer (1, 2, 3 and 4)

f = the fundamental frequency of the AC system

This means if $n=1$ and $p=12$ and the frequency is 50 Hz, the $DC_{harmonic}$ produced for this integer will be equal to:

$$DC_{harmonics} = 1 \cdot 12 \cdot 50 = 600 \, Hz$$

$$\frac{600}{50} \, Hz = 12^{th} \text{ harmonic which is an even harmonic}$$

If $n=2$ it will be the 24th harmonic (also an even harmonic).

The DC harmonics are typically even harmonics and this is different to harmonics on the AC side of converters.

On the AC side the distorted current waveform can be decomposed into (Arrillaga, Smith, Watson, Alan, 1997:135):

$$AC_{harmonics} = (n \cdot p) \pm 1 \qquad (4.27)$$

This means if $n=1$ and $p=12$, the $AC_{harmonics}$ for the integer will be equal to:

$$AC_{harmonics} = (1 \cdot 12) + 1 = 13^{th} \text{ harmonic (odd harmonics)}$$

and

$$AC_{harmonics} = (1 \cdot 12) - 1 = 11^{th} \text{ harmonic (odd harmonics)}$$

Likewise for n = 2, 3 and 4 odd harmonics are produced. This is only true if the AC side is symmetrical and the system loading is balanced. For this reason they are called characteristic harmonics.

This means a twelve-pulse converter produces a 11th harmonic which is the lowest characteristic harmonic generated. From (4.27) a six-pulse converter produces:

$$AC_{harmonics} = (n \cdot 6) \pm 1$$

The 5th harmonic is thus its lowest characteristic harmonic generated.

When unsymmetrical or unbalance is present in the network then odd, triplen and even harmonics can occur.

4.3.1 Harmonic cancellation

There are several problems associated with these harmonics and they are (Padiyar, 1990:145):

- Telephone interference
- Extra power losses and heating in machines and capacitors connected to the system
- Over-voltages due to resonances
- Instability of converter controls

These problems make it imperative to eliminate or reduce these harmonics.

In twelve-pulse converters two solutions are typically used to eliminate these harmonics, the one being the implementation of commutation transformer topologies (e.g. delta windings) and the other being the installation of harmonic filters.

4.3.1.1 Transformer topologies

From (4.27) and the example given it can be seen that a six-pulse converter station produces AC harmonics, inter-alia 5th and 7th harmonic will be present. A twelve-pulse converter has the inter-alia 11th and 13th present but because the converter consists of two six-pulse converter stations connected in series, the 5th and 7th will also be present. It was found that when certain transformer connections are used the 5th and 7th, can be eliminated (Fisher, 1991:247).

The transformer topology used to eliminate harmonics is shown in Figure 4.14. They are a star-delta connected to the one six-pulse and a star-star connected to the other one.
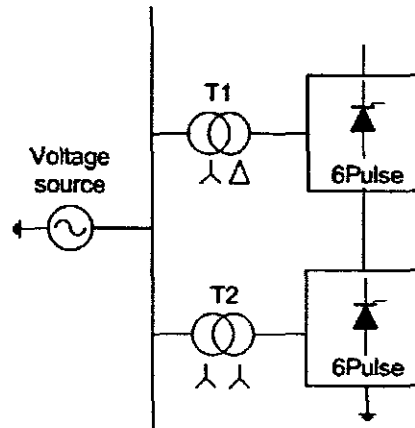
Figure 4.14: Twelve-pulse bridge configuration

The reason for this is because the AC currents from the Y-Y and Y-D groups are identical in shape, but displaced by $30°$ on account of the phase shift in the Y-D transformer. Their summation cancels out all six-pulse harmonics. All that is left is a twelve-pulse resultant waveform with harmonics of the order, 11th and 13th and the lower order 6p harmonics (5th and 7th) are eliminated in the twelve-pulse arrangement.

The general equation for the current on the secondary side of T1 can be expressed as (Fisher, 1991:247):

$$i_{YD2} = A_1 \cos(\omega t) + A_5 \cos(5\omega t) + A_7 \cos(7\omega t) + A_{11} \cos(11\omega t)$$
$$+ A_{13} \cos(13\omega t) + \ldots \tag{4.28}$$

And the current on the secondary side of T2 can be expressed as:

$$i_{YY2} = A_1 \cos\left(\omega t + \frac{\pi}{6}\right) + A_5 \cos 5\left(\omega t + \frac{\pi}{6}\right) + A_7 \cos 7\left(\omega t + \frac{\pi}{6}\right)$$
$$+ A_{11} \cos 11\left(\omega t + \frac{\pi}{6}\right) + A_{13} \cos 13\left(\omega t + \frac{\pi}{6}\right) + \ldots \tag{4.29}$$

The Y-D connected transformer has a $30°$ phase shift from secondary to primary for the fundamental current, and with the 5th harmonic being a negative sequence component, the phase shift is $-30°$ and for the 7th harmonic being a positive sequence component, the phase shift is $30°$.

54

The primary side current of T1 can be expressed in terms of the secondary side current taking the turns ratio of the transformer into account. The primary side current is:

$$i_{YD1} = B_1 \cos\left(\omega t + \frac{\pi}{6}\right) + B_5 \cos\left(5\omega t - \frac{\pi}{6}\right) + B_7 \cos\left(7\omega t + \frac{\pi}{6}\right)$$
$$+ B_{11} \cos\left(11\omega t - \frac{\pi}{6}\right) + B_{13} \cos\left(13\omega t + \frac{\pi}{6}\right) + \dots$$

(4.30)

The Y-Y connected transformer has no phase shift from the secondary to primary side of the transformer and the primary side current of T2 is defined as:

$$i_{YY1} = B_1 \cos\left(\omega t + \frac{\pi}{6}\right) + B_5 \cos\left(5\omega t + \frac{5 \cdot \pi}{6}\right) + B_7 \cos\left(7\omega t + \frac{7 \cdot \pi}{6}\right)$$
$$+ B_{11} \cos\left(11\omega t + \frac{11 \cdot \pi}{6}\right) + B_{13} \cos\left(13\omega t + \frac{13 \cdot \pi}{6}\right) + \dots$$

(4.31)

The total current is obtained from the sum of the transformer primary side currents, (4.30) and (4.31).

$$i_T = i_{YD1} + i_{YY1}$$
$$i_T = C_1 \cos\left(\omega t + \frac{\pi}{6}\right) + C_{11} \cos\left(11\omega t - \frac{\pi}{6}\right) + C_{13} \cos\left(13\omega t + \frac{\pi}{6}\right)$$

(4.32)

The 5th and 7th harmonic current components in the total current are zero.

From (4.32) that the lower order, 5th and 7th harmonics are eliminated and only higher order harmonics are present, inter-alia 11th and 13th. Harmonic filters will need to be installed to eliminate these harmonics if levels are unacceptable, that is, if levels prescribed in harmonic standards e.g. IEEE 519 standard are exceeded (IEEE Std. 519-1992:75-79).

4.4   Control of HVDC systems

The power that is being transmitted across a HVDC transmission line is not a function of the angular displacement between the sending and receiving end voltages, but rather a function of the DC current and voltage (Wildi, 2000: 748). The DC current of a twelve-pulse rectifier of a HVDC network is calculated for the rectifier side by (4.12) and this is common to the inverter side (4.13). The DC voltage for a rectifier is calculated by (4.11) and for an inverter by (4.16).

The DC voltage at the rectifier is directly proportional to the cosine function of the delay angle α, which entails that the minimum value for α will result in a maximum DC voltage and when α is increased to 90° the rectifier DC voltage will become 0.

The inverter operates for a delay angle α in the range between 90°> α <175°, this means that with α close to 180° its DC voltage will approach maximum value.

The rectifier is dependant on α and typically operates in the range 5°> α <90°. A minimum of 5° is typically chosen because the voltage across the device has to be large enough to guarantee a successful turn-on for firing angles beyond this value. If α drops below 5° and this is set as the minimum value, the rectifier runs the risk of commutation failure. On the other hand, 90°> α <180° is the typical range for an inverter. The inverter is also dependant upon γ, where the relationship is (4.1). As α is usually large, γ will have a small value. If γ (extinction angle, EA) drops below a minimum set value of 5°, there is insufficient time for the thyristor to switch off and this will result in commutation failure. It is for this reason that α is controlled on the rectifier side and γ is the deciding factor for control on the inverter side (Padiyar, 1990:80).

When controlling a two terminal HVDC system shown in Figure 4.12, the rectifier is responsible for controlling the common DC current and the inverter is responsible for controlling the DC voltage at the inverter side (Woodford, 1998:20).

To explain this graphically, a V-I characteristic of the operation of the HVDC link is shown in Figure 4.15 and depends on (4.10) to (4.14).

Figure 4.15: V-I characteristics of a two terminal HVDC link

The V-I characteristics are typically drawn for α_{min} (rectifier side) and for a 1 pu V on the inverter side. An α_{min} is used as this is the firing angle required to turn the thyristor on and this will deliver maximum DC voltage. Line 1-2 represents the rectifier voltage (4.10)) and (4.11) and this decreases with a slope $-\frac{3}{\pi}X_{com}I_{d6precavg}$ with α_{min} kept constant.

Similar equations are used for inverter DC voltage (4.15) and (4.16) and also have $-\frac{3}{\pi}X_{com}I_{d6precavg}$ as a slope. Line 4-8 is drawn using a constant α for the inverter and commences at 1 pu V for the inverter (point 4).

The DC rectifier and inverter voltages cause a common current $I_{d12precavg}$ to flow through them (4.14).

The rectifier side uses a current controller to fix the current at 1 pu A. This mode of operation is called constant current mode and indicated by line 2-3. Thus lines 1-2 and 2-3 define the V-I characteristics for the rectifier.

In its simplest mode the inverter uses two controllers. It uses a gamma controller and a current controller that operate together to control the inverter firing angle.

The inverter voltage is kept at 0 V until 0.9 pu A is reached (point 6). At this point inverter voltage rises up to point 5.

Thus lines 6-5 and 5-8 define the V-I characteristics for the inverter. Thus with the inverter controllers two set points are predefined. The one is the voltage set point (point 4), which is set to 1 pu voltage, and the other is a 0.9 pu A DC current that is set to point 6.

The difference between the rectifier current set point (point 3) and inverter set point (point 6) is called the current margin. This is so that the rectifier and inverter constant current modes do not interact due to any current harmonics which may be superimposed on the DC current. This control strategy is called the current margin method (Sood, 2004:78).

The point where the two curves intersect (point 7) is called the operating point of the two port HVDC network. This point causes the inverter to deliver power based on the product of 1 pu V and 1 pu A.

4.4.1 Rectifier side controller

A current controller is implemented at the rectifier side to control the common current and keep it at 1 pu A (Woodford, 1998:20). This is called constant current operation (Sood. 2004:76).

In current control mode the rectifiers firing angle is controlled by means of a feedback control system which is shown in Figure 4.16.
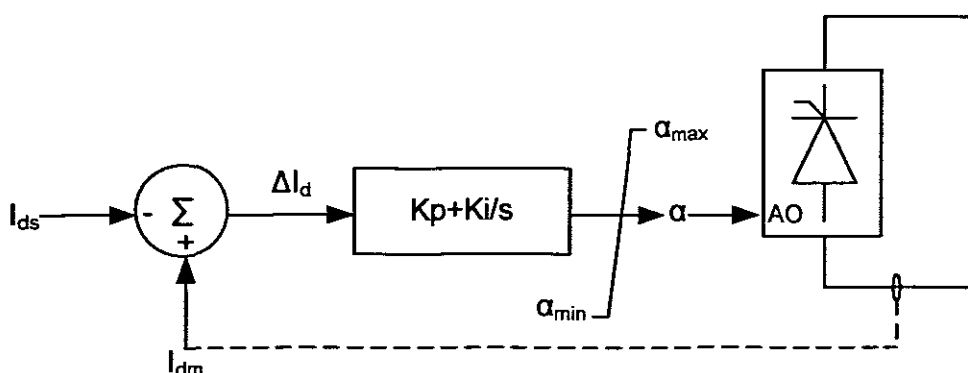
Figure 4.16: Current control

The first stage of the current controller uses a comparator that compares a measured current (I_{dm}) to a specified current (I_{ds}). The difference (ΔI_d) is then fed to a Proportional, Integral controller (PI controller) to control the current.

The PI controller is set to operate between a minimum and a maximum value for the firing angle. It will adjust the firing angle in such a way that ΔI_d will become zero and the rectifier will operate at specified current values which is equal to 1 pu A.

4.4.2 Gamma control

To control the voltage on the inverter side and eliminate commutation failure a gamma controller is implemented on the inverter side. It works on the same principal as the current control with the only difference being that Gamma "γ" is being specified in such a way that the inverter will produce a DC voltage on its output that will be equal to 1 pu V. This specified γ is then compared to the measured γ and this difference is then fed into the PI controller and Alpha is then varied between its set limits to eliminate the difference between the two. This is shown in Figure 4.17 (Sood, 2004:78).
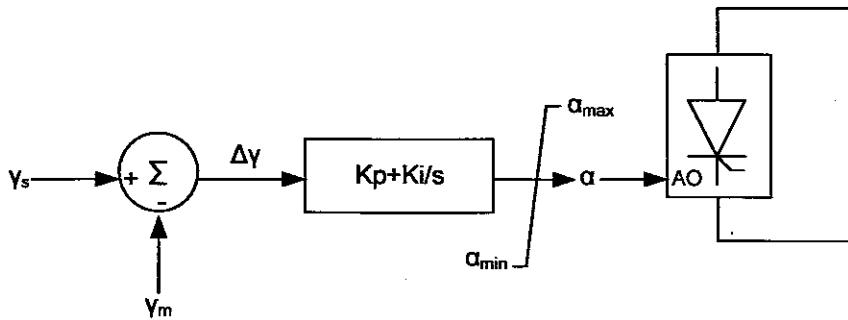
Figure 4.17: Gamma control

4.4.3 Current error control

When only current control and gamma control is present in a HVDC network the risk exists that changes on the AC voltage of the rectifier side will have a big impact on the operating point of the HVDC network. This is shown in Figure 4.18 (Sood, 2004:78).
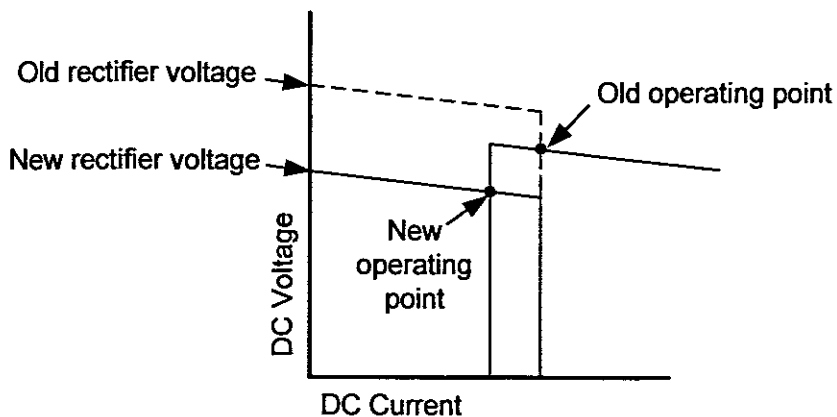
Figure 4.18: New operating point

To eliminate this problem, current error control is used. This control system includes gamma and current control. This is shown in Figure 4.19.
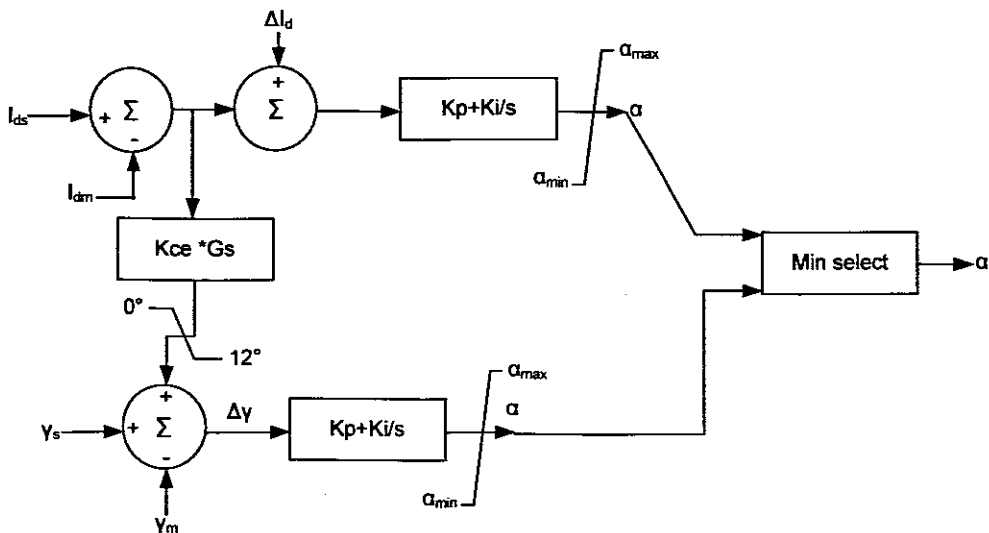
Figure 4.19: Current error control

Current error control controls the slope of the inverter voltage as shown in Figure 4.20.
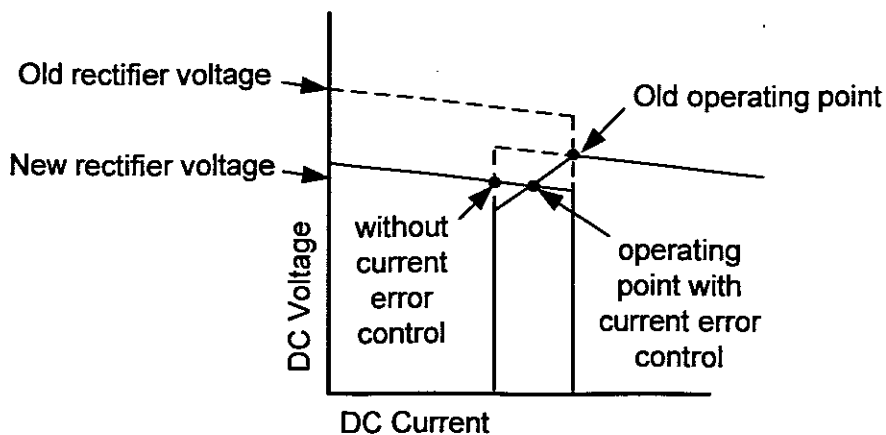
Figure 4.20: Operating point with current error control

This slope will keep the operating point closer to its desired value when the AC rectifier voltage decreases (Sood. 2004:78).

4.4.4   Voltage dependant current order limit

If a fault occurs, for instance a short circuit fault in the converter, the above mentioned controls may not operate fast enough. It is for this reason that a voltage monitoring control is also included. This control is then called voltage dependant current order limit (VDCOL).

When this is present the fault clearing time is dramatically reduced. With this control the DC current is limited as a function of either the DC Voltage or in some cases the AC voltage (Sood, 2004:80). This control helps the HVDC network to recover from faults. The V-I characteristics of this system is shown Figure 4.21.
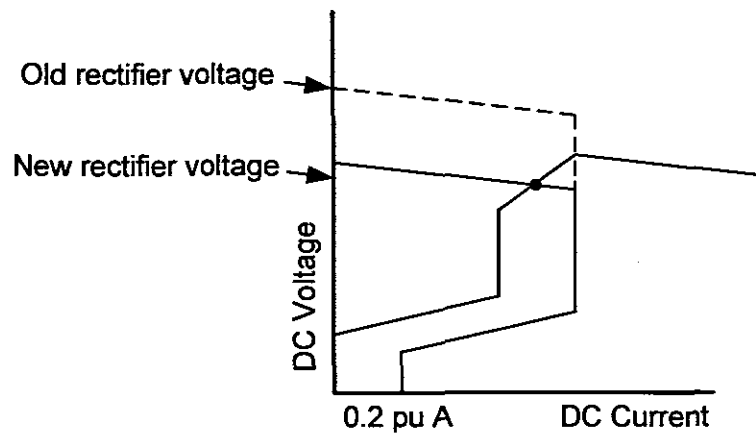
Figure 4.21: VDCOL control

4.5   Summary

From the described HVDC theory it can be seen that it differs in operation largely from that of a HVAC system. When these two systems, HVAC and HVDC systems are integrated it can be deduced that their combined operation to deliver power to a localized area of a national grid is complex. For this reason software tools have been developed so that such studies can be conducted.

CHAPTER FIVE
SOFTWARE TOOLS

5.1 Modern Software tools

One of the innovations of this research is that three different software packages are evaluated and adaptive tools are developed to conduct the necessary simulation studies from which their results are compared and analysed. Two of these are costly industrial-grade software packages for power system analysis and are selected as they are marketed as having capabilities to conduct HVAC and/or HVDC studies. These packages are called DIgSILENT PowerFactory (frequency domain) and PSCAD/EMTDC (time domain). The third software package is an academic mathematical computational software package (MathCAD) that is used to write a HVAC load flow program and apply it to conduct the necessary hand calculations to verify the simulation results.

5.1.1 PSCAD/EMTDC

PSCAD®/EMTDC™, is an electromagnetic time domain transient simulation package and is commonly referred to as PSCAD (Power System Computer Aided Drawing) (PSCAD 2006:2).
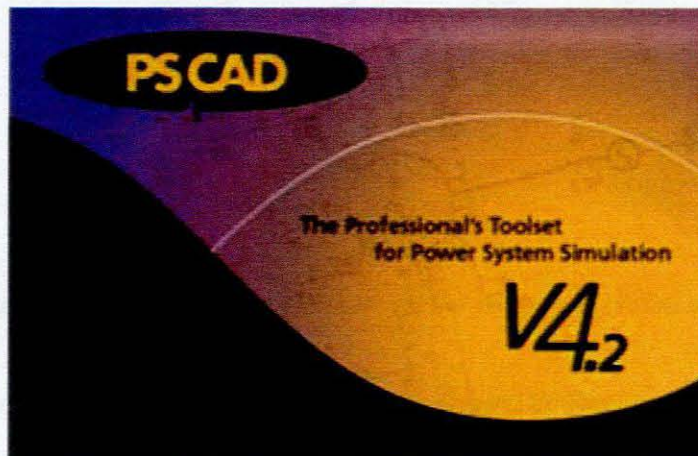
Figure 5.1: PSCAD logo

After investigation it was found that PSCAD's main purpose is to conduct time domain studies with no direct capabilities to conduct steady-state studies. Thus PSCAD needed to be evaluated with the intention to assess if it can be applied in a manner to conduct steady-state HVAC studies and ultimately to conduct steady-state HVDC studies and finally steady-state integrated HVAC/HVDC studies.

5.1.1.1 Evaluation and adaptation when using PSCAD/EMTDC

PSCAD uses root mean square, (rms) values as default to generate results. These default values are used for HVAC studies. These default values are not appropriate when comparing the DC side of the HVDC system simulation study results with that of hand calculations. This will later be discussed in more detail in Case study 4. The results obtained from hand calculations are average values for DC quantities (see Appendix B). Thus it was necessary to research the workings of the software and develop and implement adaptive tools so that comparative DC side studies become possible.

After evaluating all the tools available in PSCAD and after empirical studies it was found that steady-state results could be obtained and that the obtaining of average values was possible. Thus the following tool was developed to measure the average power transmitted across the DC side of a HVDC system. This measuring element makes use of and combines the following devices from the PSCAD toolbox (PSCAD library) and is self developed. This adaptive simulation measurement tool is shown in Figure 5.2 together with a metering panel (a positive feature of PSCAD).
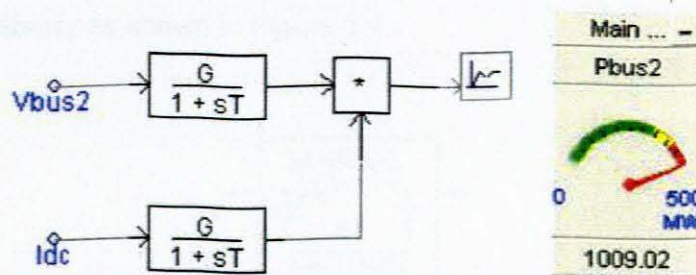
Figure 5.2: Adapted tool to measure on the DC side of HVDC system

This adaptive simulation measurement tool is shown in Figure 5.2 together with a metering panel (a positive feature of PSCAD).

The average power, voltage and current signals received from measuring devices (e.g. Vbus2 and Idc) are firstly put through integrators and the outputs are then put through a multiplier to obtain the average DC power that is calculated in (4.18). An average value of 1009.02 MW is shown (see Appendix B). The hand calculation agrees with the simulation result proving the effectiveness of this innovation.

Another shortcoming found with PSCAD is that it has no default Grid supply model in its PSCAD library (tool box).

It was found that the voltage source device in the toolbox needs to be selected and adapted in such a way to react in a similar manner as a Grid supply model typically found in other software packages (e.g. DIgSILENT). To achieve a Grid supply model the following tool is used so comparative studies can be conducted.
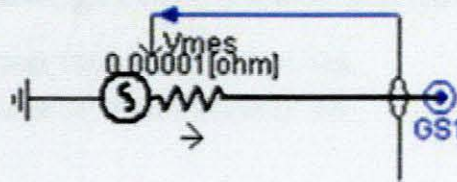
Figure 5.3: Adapted tool to represent a grid model (voltage source)

The measured output voltage from the voltage source is measured by a loop element and this is fed back to the voltage source, enabling the voltage source to keep the output voltage to its internally set specified value. This is shown in Figure 5.3.

The effectiveness of this element will be demonstrated in the case studies that follow.

On evaluation of the package it was further found that PSCAD has a π-transmission line model in its library as shown in Figure 5.4.
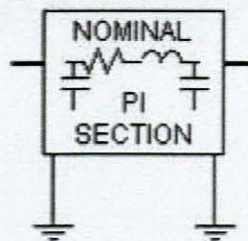
Figure 5.4: π-transmission line model

This model however doesn't allow for equivalent-π or distributed transmission line modelling. However, it was found that PSCAD has in its toolbox a T-line element and a Bergeron line device. To be able to model an equivalent-π line (equivalent π = distributed line model) it was found through empirical investigations that the T-line element combined together with the Bergeron model gives the desired results. This model is shown in Figure 5.5 and its effectiveness will be demonstrated in subsequent case studies.

Bergeron Model Options

Travel Time Interpolation: On
Reflectionless Line (ie Infinite Length): No
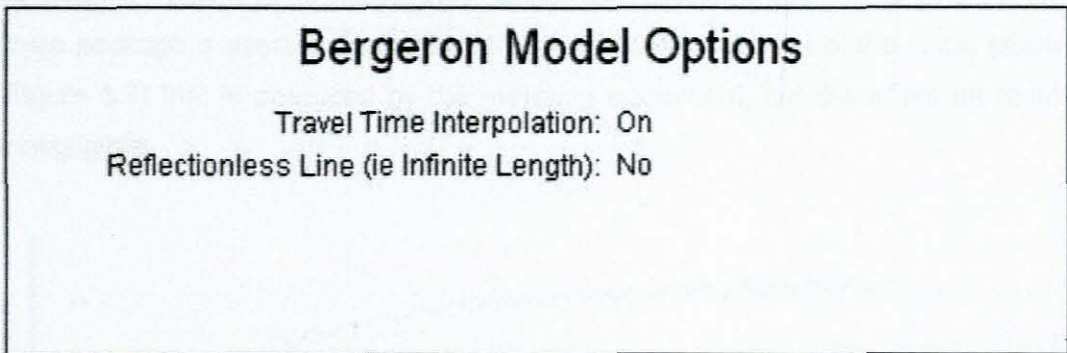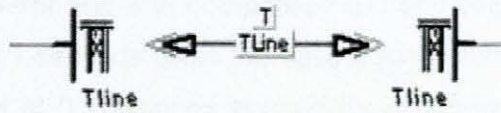
Figure 5.5: Equivalent-π model

It was also found that when using a time domain package the time constants applied to an analogue measuring device significantly affects the results. The smaller the time constant the sooner the varying waveform reaches a steady state.

Figure 5.6 shows a typical voltage output from an analogue measuring device with a time constant of 0.001s applied to the meter.
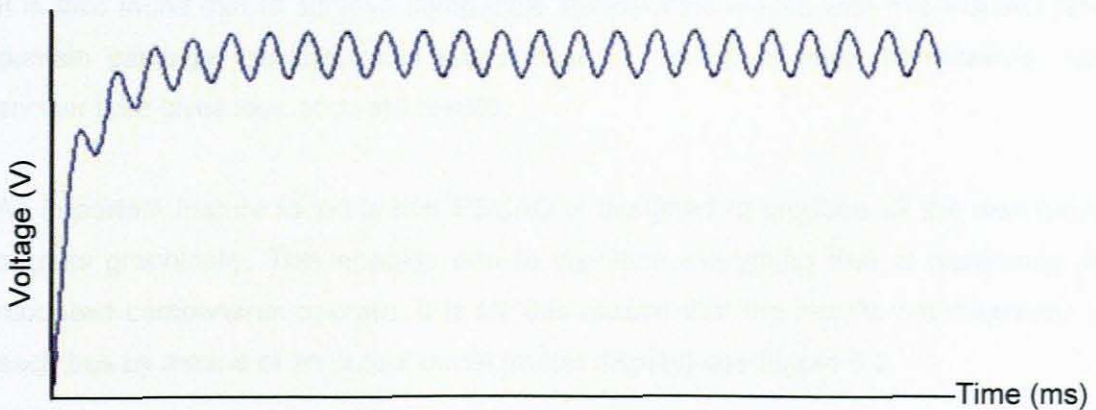
Figure 5.6: Small time constant (0.001 seconds)

It is found that when this time constant is increased, the time it takes for the signal to reach steady-state is longer but the ripple is less, producing a more accurate result. The upside of using a larger time constant is the simulation study must be set to run for a longer time period to allow for steady-state. The time constant that is selected is left to the discretion of the user who is conducting the simulation and this discretion is a general shortcoming as it can lead to less accurate results, if not aware of this shortcoming.

After much trial and error and with comparison to hand calculations it was found that a time constants of 0.1 seconds gives the best result and this is shown in Figure 5.7. Thus a time constant of 0.1 seconds is used for all studies conducted in this work. This gives a ripple that is acceptable. Small discrepancies are found when a time domain package is used to display steady-state results, because of the ripple (shown in Figure 5.7) that is produced by the metering equipment, but the effect on results are negligible.
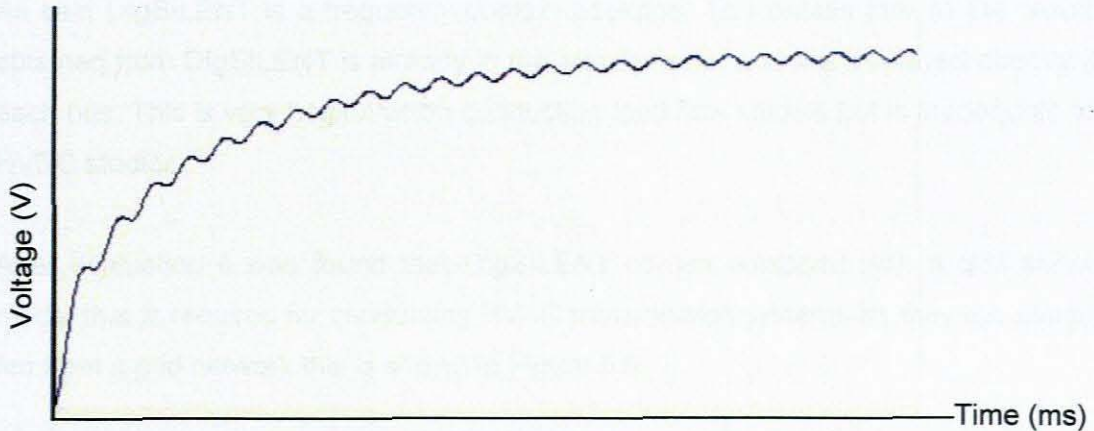
Figure 5.7: 0.1 second time constant

It is also found that to achieve compatible steady-state results with this PSCAD time domain package the simulation study must be run for at least 10 seconds. Any shorter time gives less accurate results.

An important feature found is that PSCAD is designed to produce all the measuring outputs graphically. This enables one to visualize everything that is happening as modelled components operate. It is for this reason that the results are displayed at each bus by means of an output panel (meter display) see Figure 5.2.

5.1.2 DIgSILENT PowerFactory

DIgSILENT PowerFactory (DIgSILENT PowerFactory 2005:1) is the second package used in this work and its purpose is to verify the results that are obtained by PSCAD and the hand calculations conducted. This version of DIgSILENT is a frequency domain software package and it is found only to be capable of conducting HVAC power system studies. It cannot conduct integrated HVAC/HVDC power flow studies. A much more expensive version is available from DIgSILENT but was not available for this research. This will form the basis of future work. For this research DIgSILENT will only be used to verify the HVAC results The name **DIgSILENT** stands for "**DIg**ital **SImu**Lation and **E**lectrical **NeT**work calculation program".

Figure 5.8: DIgSILENT PowerFactory logo

As said DIgSILENT is a frequency domain package. This entails that all the results obtained from DIgSILENT is already in the steady-state, and are displayed directly at each bus. This is very helpful when conducting load flow studies but is inadequate for HVDC studies.

After evaluation it was found that DIgSILENT comes equipped with a grid supply model that is required for conducting HVAC transmission systems as they are usually fed from a grid network this is shown in Figure 5.9
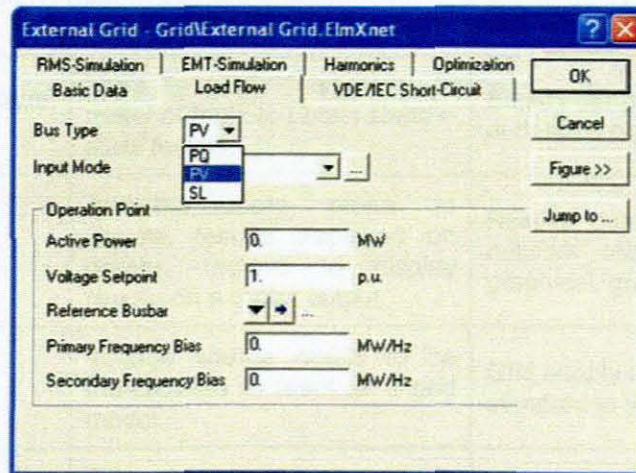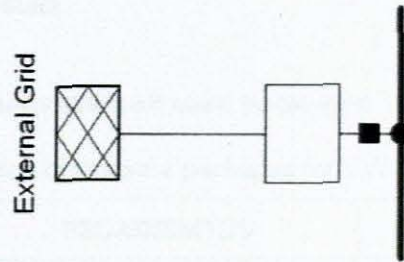
Figure 5.9: DIgSILENT Grid supply model

It was found that the transmission line model supplied by DIgSILENT provides for a selection between lumped parameter (nominal-π model) or distributed parameters (equivalent- π) this is shown in Figure 5.10.

```
┌ Out of Service
┌ Number of
  parallel Lines        [1

┌ Parameters
  Length of Line        [500.        km
  Derating Factor       [1.

  Type of Line          Overhead Line

  ┌ Line Model
    ⃝ Lumped Parameter (PI)
    ⦿ Distributed Parameter

    Routes/Cubicles/Sections
```

Figure 5.10: DIgSILENT distributed or π-model

Thus the developed PSCAD tools (e.g. adaptive simulation measurement tool) and the models found in DIgSILENT make these two packages comparable and therefore suitable for comparative studies. To ensure that the software packages generate correct HVAC results, hand calculations by means of MathCAD program are conducted to prove the results.

5.2   Comparison of Industrial-grade software packages

Table 5.1: Comparison of software packages for HVAC/HVDC studies

Modelling	PSCAD/EMTDC	DIgSILENT
Modelling in the time or frequency domain	Time domain package.	Frequency domain package
Displaying of Steady-state results	Have to apply integrators to meter outputs to obtain steady-state results.	Steady-state results obtained at desired place on bus bars
Difficulty in displaying results	Software more prone to visuals, results displayed on graphs, tedious to display results on a meter output.	Results easily displayed on network tedious do obtain graphical, graph results.
Grid supply modelling	Voltage source needs to be manipulated to react as a grid model.	Grid supply model come standard in library.
Transmission line modelling	Equivalent-π model not in library but found that Bergeron model reacts similar to an equivalent-π model.	Default model allows for equivalent-π modelling.
HVDC modelling	Comes standard with program	EMT added licence necessary to conduct HVDC studies.
HVDC control file construction	Easily accessible and easy to manipulate or change functions, reason for choosing PSCAD for HVDC studies.	

PSCAD and DIgSILENT are compared in their capabilities to conduct steady-state results, difficulty in displaying results, grid supply modelling, transmission line modelling, HVDC modelling and HVDC control file construction.

DIgSILENT has the ability to show steady-state results on the one line diagram and this is an advantage over PSCAD.

However these two tools are found very effective and complement each other.

5.3 MathCAD

MathCAD (MathCAD 2007:1) is used to conduct all the necessary hand calculations. MathCAD is evaluated and it is found that it is (see Appendix A) a mathematical computational software package with the advantage that all the calculations can be stored in a text format.
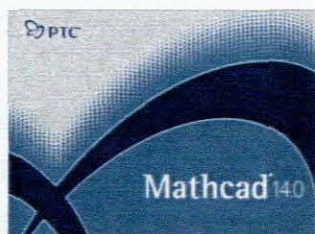
Figure 5.11: MathCAD logo

5.4 Summary

The three simulation tools utilized to perform the necessary studies were found to be effective and are recommended for conducting studies on the topic investigated.

69

CHAPTER SIX
DEVELOPMENT OF A STRATEGY

6. **Development of a strategy for solving power delivery problems**

From the literature review conducted a need was found to develop a strategy in the form of a flow chart to guide engineers in their approach (methodology) to decide on a solution to increase the power delivery to a localized area of a national grid. All possible transmission line solutions need to be stated and proven, and each of their pros and cons needs to be highlighted. The purpose of this flow chart is to establish a method for doing just that and thus finding a solution to a power delivery shortage to a localized area of a national grid.

The advantage of the utilization, once proven of such a developed strategy, is the saving of time. This strategy shows the advantages and disadvantages for each of the solutions given, so that it can be taken into consideration, when a decision is made on what solution to apply.

What makes this developed strategy novel is the fact that specific case studies are conducted to demonstrate the plan as well as prove the different solutions. Furthermore hand calculations are used to verify the results obtained as well as the use of two software packages to compare their results.

The case specific studies involving individual and combinations of HVAC and HVDC lines are conducted to demonstrate their effectiveness as solutions to the problem encountered.

This strategy that is developed only considers the transmission lines supplying the localized area, the option of upgrading of generation capacity in the localized area is not considered.

The developed workflow strategy is given in Figure 6.1 and is labelled "A" to "U" for the ease of explanation:

It starts at A. The question asked in B: Is there sufficient power delivery? If yes, then the solution is to go directly to U as no problem exists. If no, the next question (C) is asked: Is the angular displacement limit of $\delta > 35°$ exceeded due to the load demand increasing beyond acceptable level?

If yes, (D) then the following solutions should be considered (E, F and G).

The first possible solution is to add a similar HVAC transmission line in parallel with the existing one shown in block E.

The second solution is to replace to HVAC transmission line with a completely new HVDC scheme (block F).

The third solution proposed is the construction of a new HVDC transmission line in parallel with the existing HVAC transmission line. This solution is then an integrated HVAC/HVDC system (block G).

Now questions are asked for each of the possible solutions (E, F, and G): Does the two HVAC parallel lines meet the demand (H)? Likewise, does a HVDC system (F) provide adequate power delivery (I)? Also, will an integrated HVAC/HVDC system (G) provide the solution (J)?

If the answers to these questions are yes, then the increased load demand is met (K) and any of these can be implemented. However, other factors need to be considered before making any decision, namely (L).

The factors needed to be considered are shown in blocks M-S:

- Cost (M)
- Right of Way (N)
- Line losses (O)
- Reactive power support (P)
- Harmonic impact (Q)
- HVDC configurations (R)
- Contingency analysis (S)

Once these factors have all been evaluated, a scenario is selected as the solution and the strategy ends at U.

To prove the effectiveness of this developed strategy (flow chart), 5 different case studies are conducted to evaluate solutions and point out some of the considerations associated with each solution.

The first case study will show a healthy system so the flow chart is fast tracked from B-U.

The second will illustrate the problem where the angular displacement is exceeded due to load demand exceeding that which was originally planned.

The remaining three case studies will evaluate the proposed solutions in blocks E-G.

In this thesis the effectiveness of this developed strategy will be implemented applying blocks A to K only with the emphasis on evaluation of integrated HVAC/HVDC to provide the desired solution. The other factors M to S will form part of future work.

The developed strategy that is developed to solve a power delivery problem to a localized area of a national grid is shown in Figure 6.1
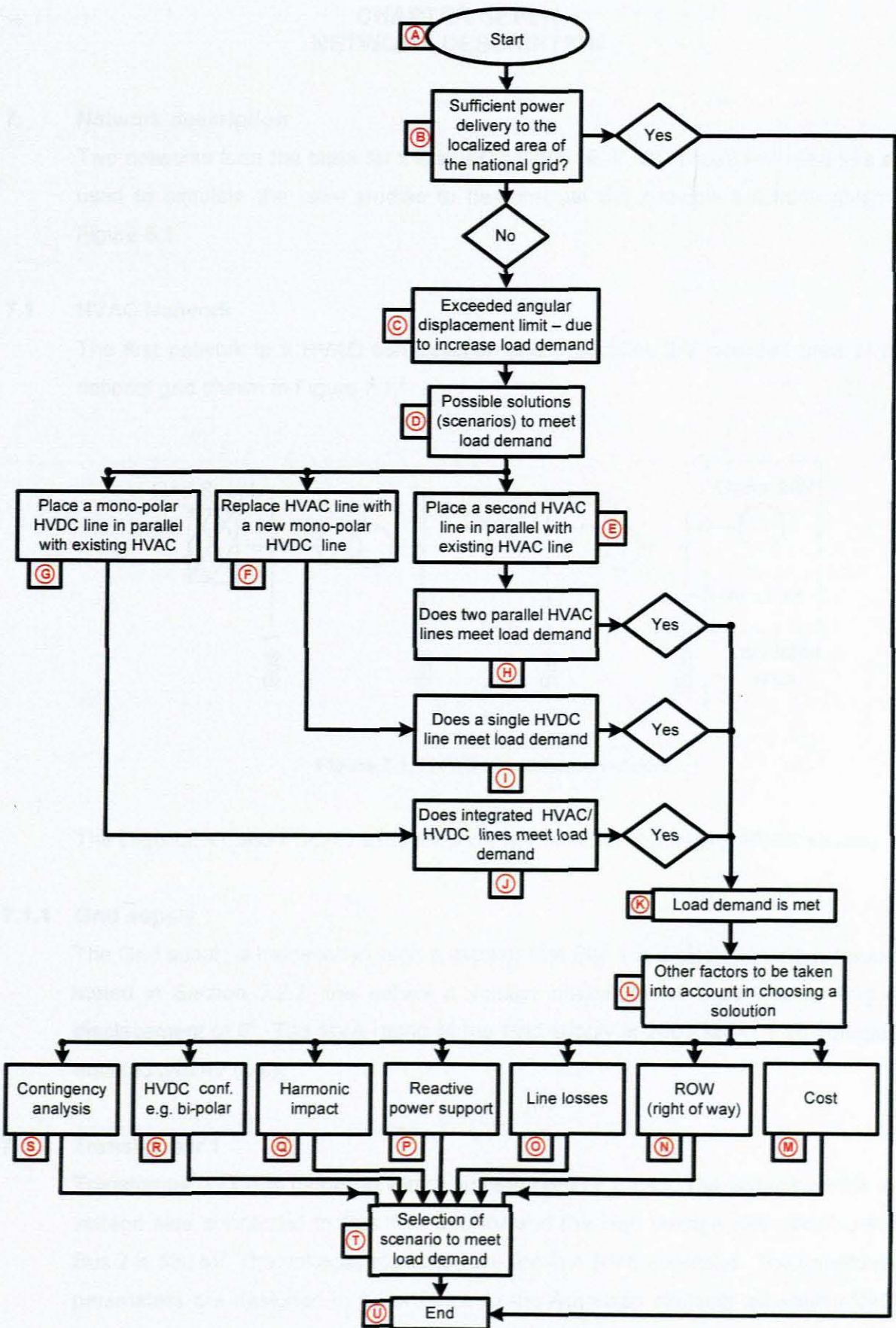
Figure 6.1: Strategy for solving power delivery problems

CHAPTER SEVEN
NETWORK DESCRIPTION

7. Network description

Two networks form the basis for the investigations (E, F, G). These two networks are used to simulate the case studies to demonstrate the possible solutions given in Figure 6.1.

7.1 HVAC Network

The first network is a HVAC configuration and it supplies the localised area of the national grid shown in Figure 7.1.
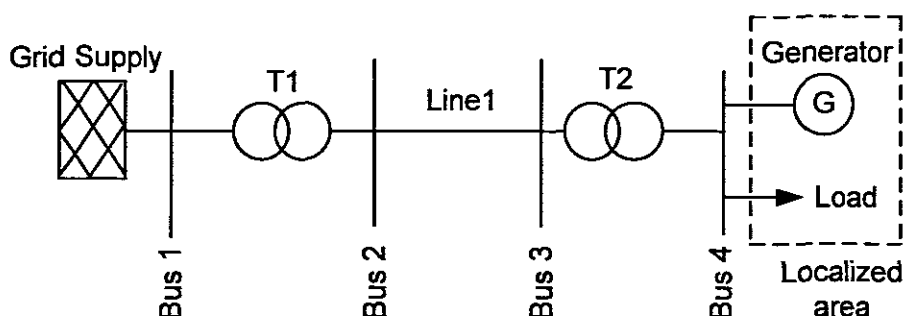
Figure 7.1: HVAC transmission network

The DIgSILENT and PSCAD software tools are used for conducting HVAC studies.

7.1.1 Grid supply

The Grid supply is modelled in such a manner that Bus 1 is a slack bus. As previously stated in Section 3.2.2, this entails a voltage magnitude of 1 pu and an angular displacement of 0°. The MVA rating of the Grid supply is 2000 MVA. 1 pu voltage is equal to 345 kV (L-L).

7.1.2 Transformer 1

Transformer 1 (T1) is modelled with a voltage ratio of 1:1.45. The voltage on the low voltage side connected to Bus 1 is 345 kV and the high voltage side connected to Bus 2 is 500 kV. The voltages stipulated are line-line RMS quantities. The transformer parameters are designed in accordance to the American National standard (ANSI). To be able to model transformer (T1) in DIgSILENT the following data is used which is shown in Figure 7.2.
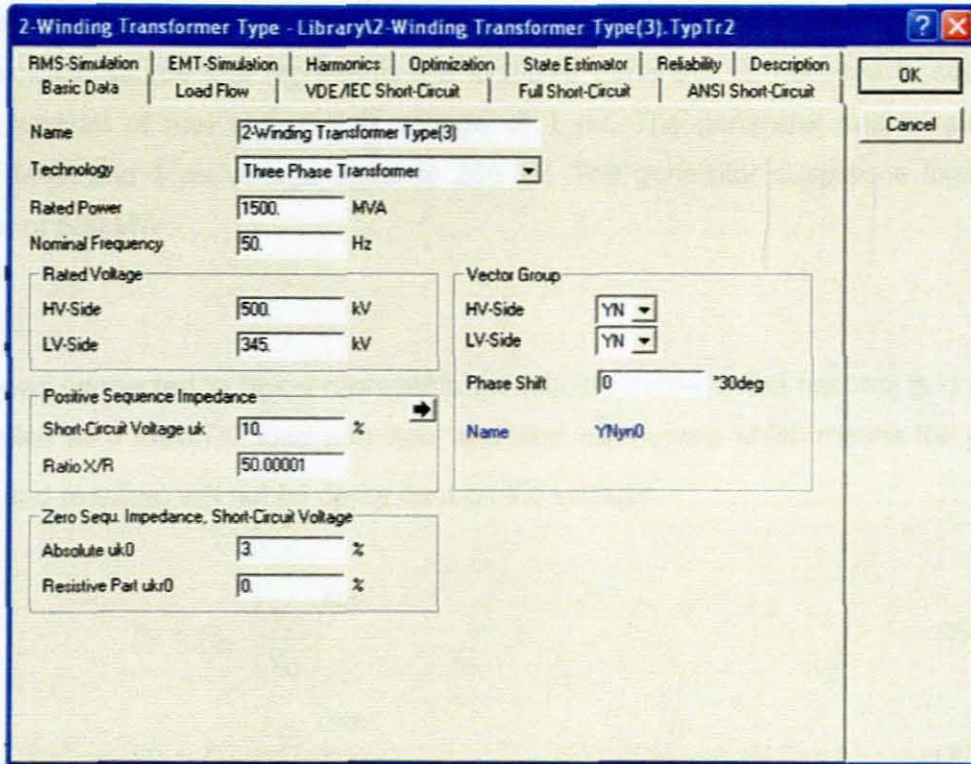
Figure 7.2: DIgSILENT transformer model

The X/R ratio is equal to 50 and a short circuit voltage (uk) of 10 %, with a absolute uk0 value of 3 % is used for T1. The transformer has a rating of 1500 MVA, and is modelled as a star, star transformer with available models.

7.1.3 Transmission line

The transmission line (Line 1) chosen is 500 km long. The positive sequence resistance of the line is 0.01Ω/km and the reactance is 0.75Ω/km. The susceptance of the line is 1.634 µS/km. The line can be modelled as a distributed model or equivalent-π as previously discussed (Section 3.1.3). An equivalent-π model is used and its parameters for the line are $Z' = 4.501 + j356.146\,\Omega$. The susceptance ($\frac{Y'}{2}$) is equal to j0.0004 Ω. This is calculated in detail in Appendix A.

7.1.4 Transformer 2

Transformer 2 (T2) is modelled with a voltage ratio of 1:2.174. The voltage on the low voltage side connected to Bus 4 is 230 kV and the high voltage side connected to Bus 3 is 500 kV. The quantities for the model are X/R ratio is equal to 50, and a short-circuit voltage (uk) of 10 %, with an absolute uk0 value of 3 %. The transformer has a rating of 1500 MVA, and is modelled as a star-star.

7.1.5 Generator

The voltage source that represents the localized generator is modelled to supply a fixed amount of real power at a voltage of 1 pu. The generator has a rating of 2000 MVA and 1 pu voltage equal to 230 kV. The generator supplies a fixed real power of 500 MW.

7.1.6 Load

The load connected to Bus 4 represents the localized area of the national grid and is modelled as a fixed PQ load with *kpu* and *kqu* set to zero which means the power (real and reactive) will not be dependant on the voltage:

$$P_r = P_o \cdot \left(\frac{V_r}{V_o}\right)^{kpu} \tag{7.1}$$

$$Q_r = Q_o \cdot \left(\frac{V_r}{V_o}\right)^{kqu} \tag{7.2}$$

Where:

P_r is the rated active power

P_o is the specified active power

V_r is the rated L-L voltage

V_o is the specified L-L voltage

Q_r is the rated reactive power

Q_o is the specified reactive power

kpu is the static voltage dependency constant (Voltage dependency on P)

kqu is the static voltage dependency constant (Voltage dependency on Q)

The load consumes 700 MW of real power and 368.75 Mvar of reactive power, giving a power factor of 0.85 lagging.

7.2 HVDC network

For HVDC and integrated HVAC/HVDC studies, only PSCAD software is used. The HVDC network that is to be utilized to supply the localized area of the national grid is the CIGRE Benchmark system (Szechman, Wess, Thio, 1991:54-73). This network is shown in Figure 7.3 but to make explanation easier, the system diagram is sub-divided into blocks and labelled.

Block Diagram: HVDC Cigre Benchmark

A Supply voltage or grid in feed	**H** Invertor
B Reactive compensation	**I** Inverter Transformer.
C Harmonic filters	**J** Smoothing reactor.
D Rectifying convertor.	**K** Supply voltage or grid in-feed
E Rectifier Transformer.	**L** Reactive compensation
F Smoothing reactor.	**M** Harmonic Filter
G Convertor control.	**N** Invertor control.
	O HVDC line

Figure 7.3: CIGRE benchmark system.

The HVDC elements from the PSCAD toolbox is used to construct the software model necessary to simulate the CIGRE benchmark network. The parameters for each of the components are as follows.

7.2.1 Grid supply

The Grid supply is modelled in such a manner that Bus 1 is a slack bus. As previously stated in Section 3.2.2, this entails a voltage magnitude of 1 pu and an angular displacement of 0°. The MVA rating of the Grid supply is 2000 MVA. 1 pu voltage is equal to 345 kV (L-L).

7.2.2 Reactive compensation.

The converter stations consume reactive power in the conversion process (4.24). It is for this reason that a capacitor bank is included in the system to assist with supplying reactive power as insufficient is typically not forthcoming from the localized area network, Figure 7.3 block B (C=3.342 µF) and L (C=7.522 µF). The capacitor element is found on the shortcut toolbar in PSCAD.

7.2.3 Harmonic filters

A drawback of a HVDC system (Section 4.3) is the production of harmonics. A six-pulse converter station injects harmonics in the order 6n ± 1, (4.27), where the lowest pair are the 5th and 7th harmonic. A twelve-pulse converter injects a lowest pair of 11th and 13th harmonics. With certain transformer configurations as discussed (Section 4.3.1), the 5th and 7th, can be eliminated when the converter is twelve-pulse. As they are typically the largest harmonics, two harmonic filters are installed to eliminate the 11th and 13th harmonics. These are shown at C and M. The harmonic filters are constructed in PSCAD using the inductor, resistor and the capacitor elements. These elements can be found on the shortcut toolbar or in the "passive elements" toolbox. The parameters which are used are shown in Figure 7.3.

7.2.4 Rectifying converter

The converter station shown at D is a twelve-pulse converter. It is two six-pulse stations connected in series together. It is configured in such a way that it produces an output HVDC voltage of 500 kV. PSCAD has a compact representation of a six-pulse converter which can be modelled as a rectifier or an inverter. This element is found in the "HVDC, facts & power electronics" toolbar.

7.2.5 Rectifier transformer

There are two rectifier transformers. Both the transformers have a rating of 600 MVA. The voltages ratios are as indicated in Figure 7.3. These transformers are situated at E. They are modelled as star-star (on the one six-pulse converter) and star-delta (on the other). This is used for harmonic cancellation.

7.2.6 Smoothing reactors

As discussed (Section 4.1.1), on the transmission line, two big reactors are inserted. These reactors are used for smoothing purposes and are the same reactors found on the shortcut toolbar, and the model used uses an inductance of 0.5968 H. These reactors are represented by F and J

7.2.7 Rectifier control

The rectifier control system used in modelling is shown in Figure 7.4.

Figure 7.4: Rectifier control system

In this system a current controller is used (see Section 4.4.1). The specified current is selected to the desired value and the controller will produce a firing angle that will produce this current. This is represented by G in Figure 7.3.

7.2.8 Inverter

The inverter is modelled as a holistic model similar to the rectifier except, it is operated as a line commutated inverter. The voltage level is 500 kV on the HVDC side and the HVAC voltage is 230 kV. The inverter model is applied with similar transformer configuration models as specified for the rectifier accepted a lower rating of 590 MVA is used.

7.2.9 Inverter control

In order to obtain the desired firing angle, the HVDC control for the inverter is more complex than that for the rectifier. The control file that is used is shown in Figure 7.5.
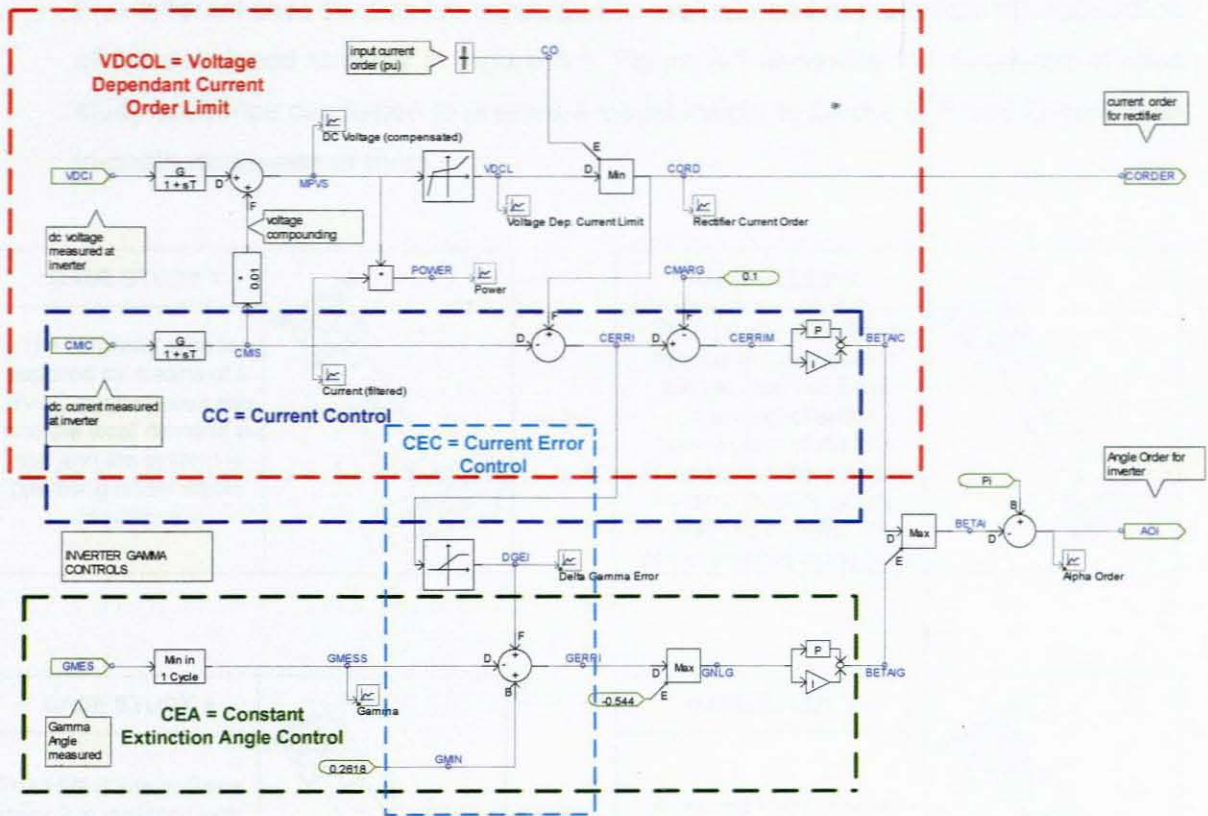
Figure 7.5: Inverter control system

The various control elements that were described in Chapter 4 can now be identified in this control system. In essence it comprises of three parts, a VDCOL, CC and a CEA part.

7.2.10 Generator

The generator that represents the localized generation is modelled to supply a fixed amount of real power at a voltage of 1 pu. The generator has a rating of 2000 MVA and 1 pu voltage equal to 230 kV. The generator supplies a fixed real power of 500 MW. The Reactive power and angular displacement are variables.

7.2.11 HVDC transmission line

The transmission line model uses the parameters that are given in the CIGRE benchmark model. The transmission line has a DC resistance of 5 Ω and a capacitor (26 µF). It is necessary to include a capacitor on the DC side as converters generate pulsating (ripple) voltages.

8   Case studies

Five different case studies are conducted to evaluate and demonstrate the application of the developed strategy in Figure 6.1. Figure 8.1 illustrates the sequence of case study scenarios conducted to present a visual insight to blocks E, F and G before an in-depth discussion of them.

CASE STUDY 1

The localized area is supplied by means of a HVAC transmission line and the local demand is met and the system is operating under stable conditions

CASE STUDY 2

The system is similar to the one in Case study 1 but the load has been increased causing overloading of the line and instability in the system ($\delta > 35°$), giving reason to increase the power delivery to the load

CASE STUDY 4

The HVAC line in Case study 2 is replaced with a HVDC line to increase the power delivered to the localized area of the national grid

CASE STUDY 3

A second HVAC line is added to increase the power delivered to the localized area of the national grid

CASE STUDY 5

A integrated HVAC (Case 2) and HVDC line (Case 4 with less power delivery) is utilized to increase the power delivered to the localized area of the national grid

Figure 8.1: Case study sequence

These case studies are now fully described.

8.1   Case study 1

In Case study 1, the localized area of the national grid is supplied by means of a HVAC transmission network as shown in Figure 8.2.
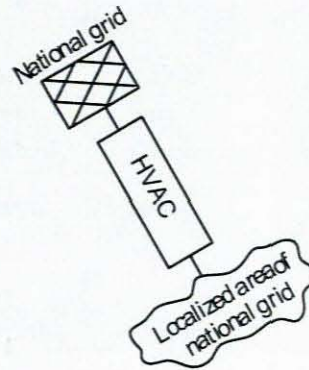
Figure 8.2: Case study 1

The localized area of the national grid is represented by a load and a local generating station Figure 7.1. This is typically how a large localized area is supplied (e.g. Cape Town, South-Africa). In case study 1, the load for the localized area is 700 MW and 368.75 Mvar giving a power factor for the load of 0.85 lagging. The network is described in Chapter 7. This HVAC transmission system was first modelled in PSCAD/EMTDC using the following PSCAD one-line-diagram representation shown in Figure 8.3.
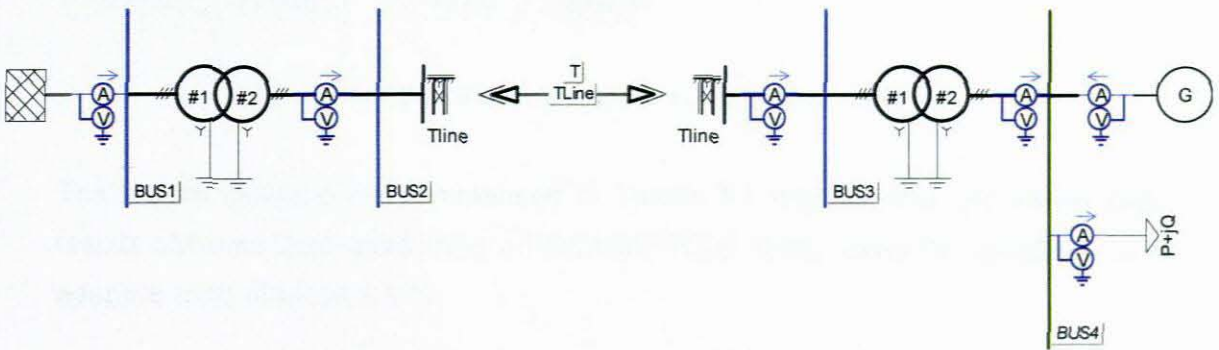
Figure 8.3: PSCAD network model of Case study 1

To generate results in PSCAD, measuring devices are added to the network. The results obtained from the simulation study conducted are displayed on instrument panels inside the graphic window of PSCAD. Each measuring device uses an arrow as well as a number to present results and this can be seen in Figure 8.3. A meter is placed in the network in the direction that the power (active and reactive) is most likely to flow. If a power flows in the opposite direction to that of the anticipated direction, the results will be negative. Figure 8.4 shows the results for each of the buses as well as the generator and load elements obtained for Case study 1.
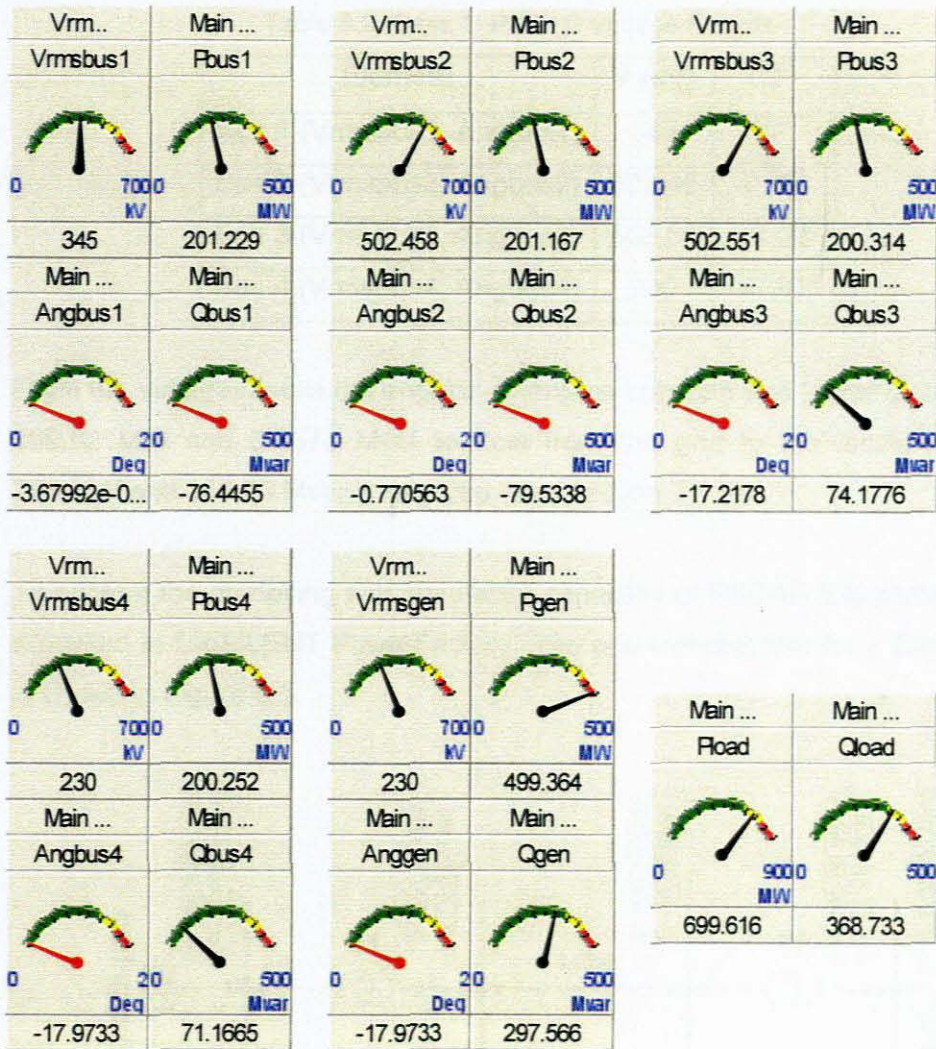
Figure 8.4: PSCAD network model results of Case study 1

The results obtained are summarised In Tables 8.1 and 8.2 and are steady-state results obtained from conducting a PSCAD/EMTDC study, using the developed and adaptive tools (Section 5.1.1).

Table 8.1: Case 1: PSCAD Power Results

Element	P (MW)	Q (Mvar)
Grid supply (Pbus1, Qbus1)	201.23	-76.45
T1 (Pbus2, Qbus2)	201.17	-79.53
Line (Pbus3, Qbus3)	200.31	74.18
T2 (Pbus4, Qbus4)	200.25	71.17
Gen (Pgen, Qgen)	499.36	297.57
Load (Pload, Qload)	699.62	368.73

Table 8.2: Case 1: PSCAD Voltage Results

Element	V (kV)	δ
Bus 1 (Vrmsbus1, Angbus1)	345	0°
Bus 2 (Vrmsbus2, Angbus2)	502.46	-0.77°
Bus 3 (Vrmsbus3, Angbus3)	502.55	-17.22°
Bus 4 (Vrmsbus4, Angbus4)	230	-17.97°

From the voltage results the angular difference between Bus 2 and 3 causes power of 699.62 MW and 3.6873 Mvar to flow from the grid to the localized area where 700 MW and 368.75 Mvar is required (see Section 7.1.6).

To confirm the modelling and simulation capability of PSCAD this same network was modelled in DIgSILENT PowerFactory. The one-line-diagram for a DIgSILENT study is shown in Figure 8.5.
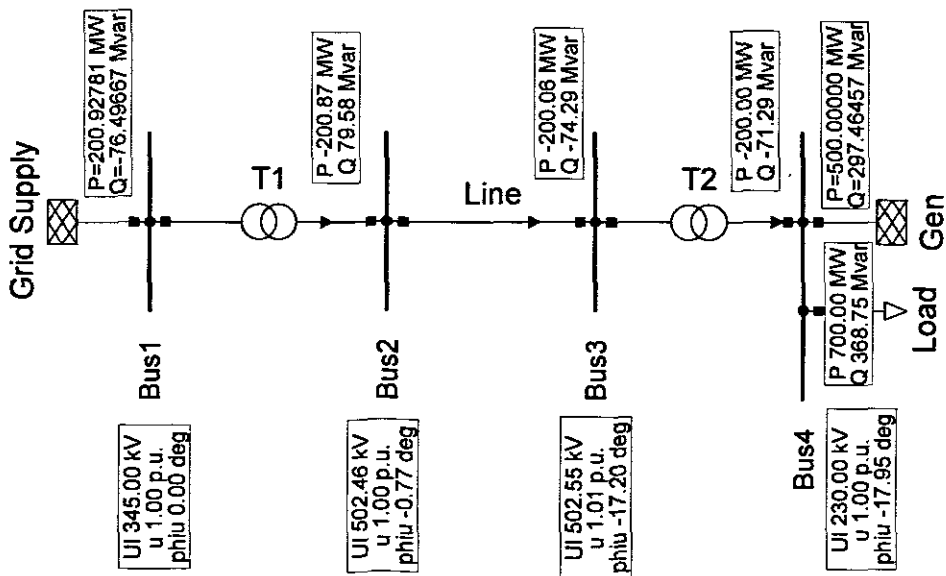
Figure 8.5: DIgSILENT PowerFactory network model of Case study 1

With DIgSILENT a + or - sign is used in front of a power result to indicate the direction of the power flow.

The results obtained after conducting a load-flow analysis in DIgSILENT are summarized in Tables 8.3 and 8.4

Table 8.3: Case 1: DIgSILENT Power Results

Element	P (MW)	Q (Mvar)
Grid supply	200.93	-76.49
T1	200.87	-79.58
Line	200.06	74.29
T2	200.00	71.29
Gen	500	297.46
Load	700	368.75

Table 8.4: Case 1: DIgSILENT Voltage Results

Element	V (kV)	δ
Bus 1	345	0°
Bus 2	502.46	-0.77°
Bus 3	502.55	-17.19°
Bus 4	230	-17.95°

Similar results to that of PSCAD were obtained. The results show that 700 MW and 368.75 Mvar are delivered to the localized area. To further confirm the accuracy of the PSCAD and DIgSILENT results, a hand calculation was performed using MathCAD. The Newton-Raphson load flow technique together with the current conjugate method (Section 3.2.1) was used to obtain results (See Appendix A for the details of this hand calculation). A 5x5 Jacobian matrix (8.1) is used and the values obtained for each element after the second iteration are shown (Appendix A, Section A.6.3).

$$
\text{Jacobian} := \begin{pmatrix} J_{11} & J_{12} & J_{13} & J_{14} & J_{15} \\ J_{21} & J_{22} & J_{23} & J_{24} & J_{25} \\ J_{31} & J_{32} & J_{33} & J_{34} & J_{35} \\ J_{41} & J_{42} & J_{43} & J_{44} & J_{45} \\ J_{51} & J_{52} & J_{53} & J_{54} & J_{55} \end{pmatrix} \qquad (8.1)
$$

$$
\text{Jacobian} = \begin{pmatrix} 10.4967 & -0.455 & 0 & 0.2068 & 0.1272 \\ -0.4516 & 10.5005 & -10.0489 & -0.1387 & 0.2069 \\ 0 & -10.0436 & 10.0436 & 0 & -0.3316 \\ -0.2079 & -0.1279 & 0 & 10.4453 & -0.4527 \\ 0.1393 & -0.2079 & 0.0686 & -0.4494 & 10.4472 \end{pmatrix}
$$

The change in voltage magnitude and angle are calculated, using (8.2):

$$
\begin{pmatrix} \Delta\delta_2 \\ \Delta\delta_3 \\ \Delta\delta_4 \\ \Delta V_2 \\ \Delta V_3 \end{pmatrix} := \begin{pmatrix} J_{11} & J_{12} & J_{13} & J_{14} & J_{15} \\ J_{21} & J_{22} & J_{23} & J_{24} & J_{25} \\ J_{31} & J_{32} & J_{33} & J_{34} & J_{35} \\ J_{41} & J_{42} & J_{43} & J_{44} & J_{45} \\ J_{51} & J_{52} & J_{53} & J_{54} & J_{55} \end{pmatrix}^{-1} \begin{pmatrix} \Delta P_2 \\ \Delta P_3 \\ \Delta P_4 \\ \Delta Q_2 \\ \Delta Q_3 \end{pmatrix}
\qquad (8.2)
$$

$$
\begin{pmatrix} \Delta\delta_2 \\ \Delta\delta_3 \\ \Delta\delta_4 \\ \Delta V_2 \\ \Delta V_3 \end{pmatrix} = \begin{pmatrix} -0 \\ -0 \\ -0 \\ -0 \\ -0 \end{pmatrix}
\qquad (8.3)
$$

In (8.3) it can be seen that there is no change thus the tolerance of 0.001 is met. The voltage magnitude and angle are then calculated. These values are then used in the current conjugate method to calculate the power at each of the respective buses. The results obtained from the hand calculation are shown in Tables 8.5 and 8.6 (Appendix A, Section A.7).

Table 8.5: Case 1: Hand Calculation Power Results

Element	P (MW)	Q (Mvar)
Grid sup	200.85	-76.54
T1	200.79	-79.62
Line	200.06	74.34
T2	199.99	71.33
Gen	500	297.42
Load	700	368.75

Table 8.6: Case 1: Hand Calculation Voltage Results

Element	V (kV)	δ
Bus 1	345	0°
Bus 2	502.46	-0.77°
Bus 3	502.55	-17.19°
Bus 4	230	-17.95°

From the results obtained in Case study 1, it can be seen that the angular difference between the sending and receiving end voltages is all well within the ($\delta < +/-35°$) limit. The first stage block B (Figure 6.1) in the developed strategy is completed.

As the demand of 700 MW and 367 Mvar is delivered, the answer to the question in the study after block B is yes, and this scenario fulfils the solution in T and U. The next stage in the application of the strategy is to evaluate the scenario where the stability limit is exceeded due to the increases demand level (block C).

8.2 Case study 2

In Case study 2 the load in the localized area of the national grid is increased due to a bigger load demand as a result of population growth and industrial as well as commercial expansion. For this scenario it is assumed that the load increases from (700+j368.75) MVA to (1000+j527) MVA having the same power factor of 0.85 lagging as before.

This network was again modelled in PSCAD/EMTDC as well as in DIgSILENT and then verified by hand (MathCAD). Case study 2 uses the same technique and network as that of Case study 1 (Figure 8.3). The PSCAD results are shown in Figure 8.6 and Tables 8.7 and 8.8, respectively:
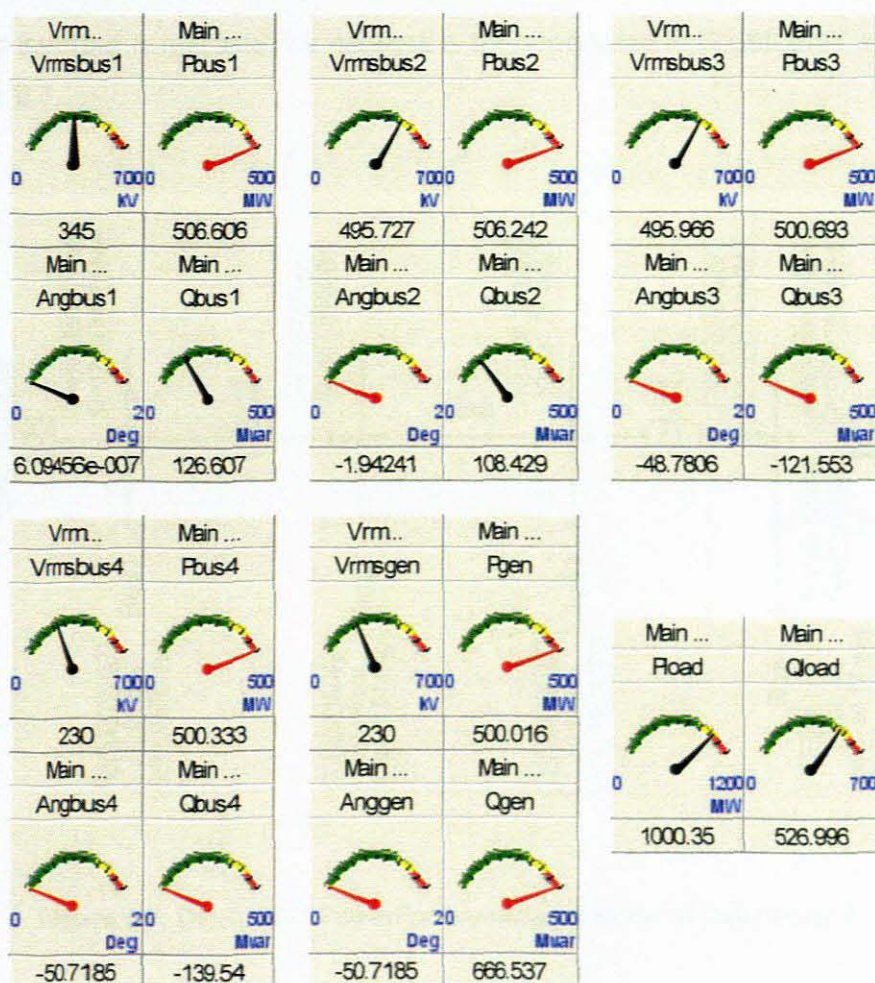
Figure 8.6: PSCAD network model results of Case study 2

Table 8.7: Case 2: PSCAD Power Results

Element	P (MW)	Q (Mvar)
Grid supply (Pbus1, Qbus1)	506.61	126.61
T1 (Pbus2, Qbus2)	506.24	108.43
Line (Pbus3, Qbus3)	500.69	-121.55
T2 (Pbus4, Qbus4)	500.33	-139.54
Gen (Pgen, Qgen)	500.02	666.54
Load (Pload, Qload)	1000.35	526.99

Table 8.8: Case 2: PSCAD Voltage Results

Element	V (kV)	δ
Bus 1 (Vrmsbus1, Angbus1)	345	0°
Bus 2 (Vrmsbus2, Angbus2)	495.23	-1.94°
Bus 3 (Vrmsbus3, Angbus3)	495.97	-48.78°
Bus 4 (Vrmsbus4, Angbus4)	230	-50.72°

The load demand is met and the network is then modelled in DIgSILENT and shown in Figure 8.7.
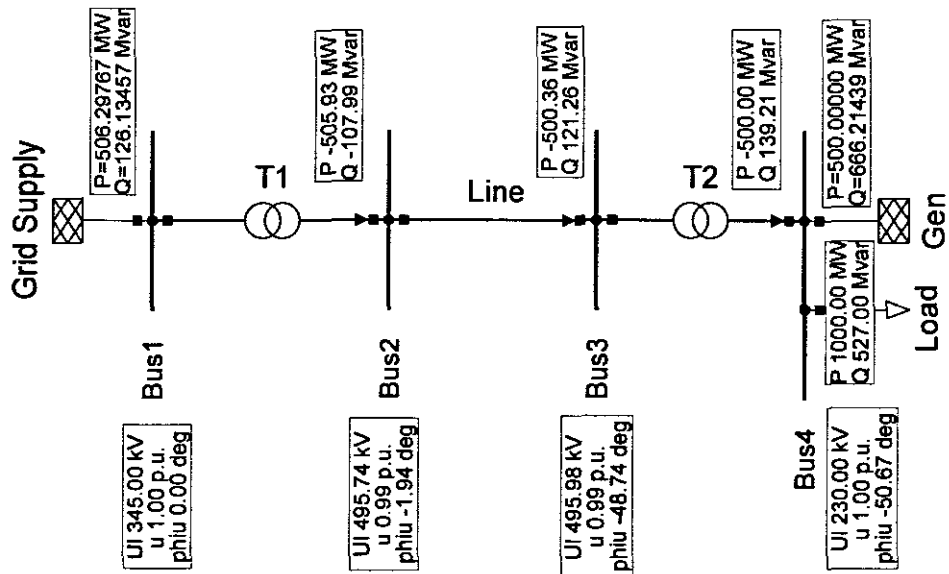
Figure 8.7: DIgSILENT PowerFactory network model of Case study 2

The results obtained from the load-flow study conducted are shown in Tables 8.9 and 8.10.

Table 8.9: Case 2: DIgSILENT Power Results

Element	P (MW)	Q (Mvar)
Grid sup	506.30	126.13
T1	505.93	107.99
Line	500.36	-121.26
T2	500.00	-139.21
Gen	500.00	666.21
Load	1000.00	527.00

Table 8.10: Case 2: DIgSILENT Voltage Results

Element	V (kV)	δ
Bus 1	345	0°
Bus 2	495.74	-1.94°
Bus 3	495.97	-48.73°
Bus 4	230	-50.67°

Same load results as PSCAD were obtained. MathCAD is used to prove that the modelling and simulation study methods of both industrial-grade software packages were correct. The results obtained by MathCAD are shown in Tables 8.11 and 8.12 (Appendix B).

Table 8.11: Case 2: Hand Calculation Power Results

Element	P (MW)	Q (Mvar)
Grid sup	506.22	126.05
T1	505.86	105.12
Line	500.36	-121.18
T2	499.99	-139.14
Gen	500.01	666.14
Load	1000.00	527.00

Table 8.12: Case 2: Hand Calculation Voltage Results

Element	V (kV)	δ
Bus 1	345	0°
Bus 2	495.74	-1.94°
Bus 3	495.98	-48.73°
Bus 4	230	-50.67°

From the studies conducted in Case study 2 it can be seen in Tables 8.8, 8.10 and 8.12 that the angular difference between the sending end (Bus 1) and the receiving end (Bus 4) exceeds the allowed maximum stability displacement of +/-35°. This indicates that the transmission line is not stable and thus the power delivery to the localized area of the national grid should be increased. This illustrates block C in the developed strategy (Figure 6.1). The next step is to evaluate possible solutions given in block D to increase the power delivery.

8.3   Case study 3

In Case study 3 the first possible solution is evaluated as suggested in Figure 6.1 (Block E). This solution considers the parallel operation of two HVAC transmission lines and this is shown in Figure 8.8.
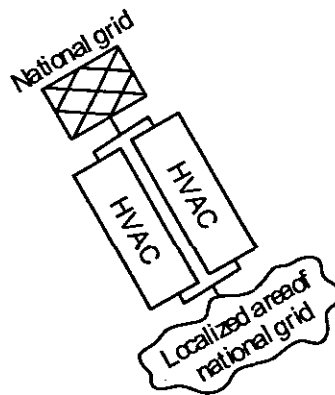
Figure 8.8: Case study 3: HVAC parallel operation

In Case study 2, one transmission was inadequate to supply the localized area, another identical line is placed in parallel with the first one. The advantage of such a system is that if the one line is out of commission then at least some of the load demand can be met. Parallel HVAC operation is evaluated to solve the power delivery problem highlighted in Case study 2.

The parallel operation is modelled in both PSCAD and DIgSILENT to compare the results from both software packages. Figure 8.9 shows the one-line-diagram required for the PSCAD simulation study. The results obtained in this study are shown on the one-line-diagram.

Vrm..	Main ...	Vrm..	Main ...	Vrm..	Main ...	Vrm..	Main ...	Vrm..	Main ...
Vrmsbus1	Pbus1	Vrmsbus2A	Pbus2A	Vrmsbus3A	Pbus3A	VrmsT2A	PT2A	Vrmsgen	Pgen
345	503.157	501.851	251.489	501.968	250.216	230	250.129	230	499.889
Main ...	Main ...	Main ...	Main ...	Main ...	Main ...	Main ...	Main ...	Main ...	Main ...
Angbus1	Qbus1	Angbus2A	Qbus2A	Angbus3A	Qbus3A	AngT2A	QT2A	Anggen	Qgen
-5.63034e-0..	-116.963	-0.96209	-62.9294	-21.7421	56.3135	-22.6901	51.9614	-22.6901	423.594

Figure 8.9: Case study 4 PSCAD one-line-diagram

Again a negative sign indicates a power flow in the opposite direction to that of the measuring device.

When looking at Figure 8.9 it is seen that the physical space (usage of property) that will be utilized to insert a second overhead line is in the region of twice the size, Thus, in real life ROW is a constraint when this option is used and this, inter-alia one of the factors (Figure 6.1) that needs consideration.

The results from this study are documented in Tables 8.13 and 8.14, and show that the load demand of 1000 MW and 527 Mvar is met.

These two lines are identical, and will share the load equally ((500 + j 263.5) MVA).

91

Table 8.13: Case 3: PSCAD Power Results

Element	P (MW)	Q (Mvar)
Grid sup (Pbus1, Qbus1)	503.16	-116.96
T1A (Pbus2A, Qbus2A)	251.49	-62.93
T1B (Pbus2B, Qbus2B)	251.49	-62.93
Line1 (Pbus3A, Qbus3A)	250.22	56.31
Line2 (Pbus3B, Qbus3B)	250.22	56.31
T2A (Pbus4A, Qbus4A)	250.13	51.96
T2B (Pbus4B, Qbus4B)	250.13	51.96
Gen (Pgen, Qgen)	499.89	423.54
Load (Pload, Qload)	1000.15	527.52

Table 8.14: Case 3: PSCAD Voltage Results

Element	V (kV)	δ
Bus 1 (Vrmsbus1, Angbus1)	345	0°
Bus 2A (Vrmsbus2A, Angbus2A)	501.85	-0.96°
Bus 2B (Vrmsbus2B, Angbus2B)	501.85	-0.96°
Bus 3A (Vrmsbus3A, Angbus3A)	501.96	-21.74°
Bus 3B (Vrmsbus3B, Angbus3B)	501.96	-21.74°
Bus 4 (Vrmsbus4, Angbus4)	230	-22.69°

In Figure 8.10 the-one-line diagram for the DIgSILENT study is shown.
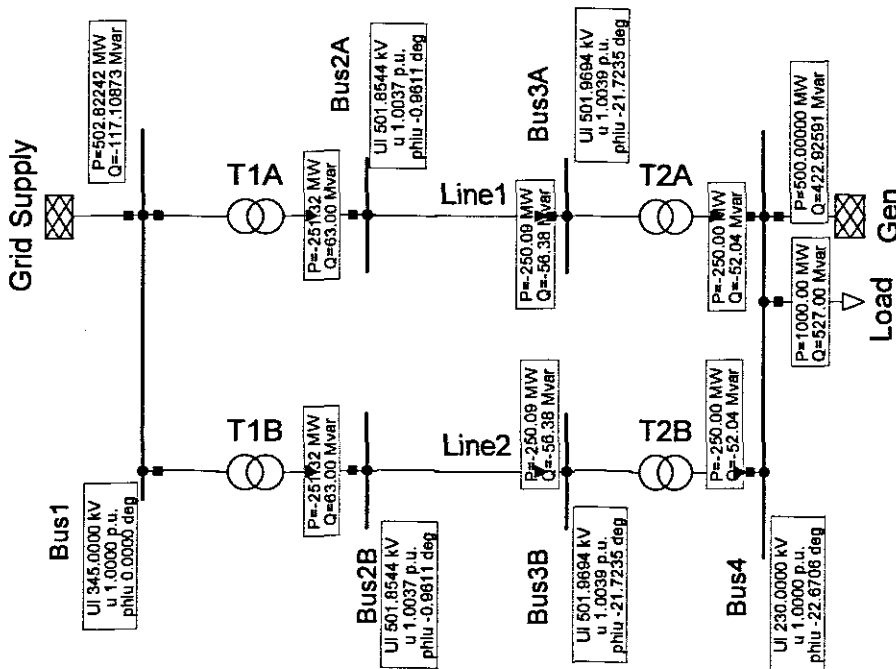
Figure 8.10: Case study 3 DIgSILENT one-line-diagram

92

The challenge with modelling a parallel HVAC line with the same parameters in DIgSILENT is that the program needs to distinguish between the two transmission lines. It is for this reason that the user should take precaution when labelling any variable in DIgSILENT to ensure that none of them corresponds between the two lines.

With DIgSILENT only one library element is used to represent an overhead transmission line where whereas PSCAD, three elements are needed to perform this task.

Tables 8.15 and 8.16 summarises the results obtained for Figure 8.10

Table 8.15: Case 3: DIgSILENT Power Results

Element	P (MW)	Q (Mvar)
Grid sup	502.82	-117.11
T1A	251.32	-63.00
T1B	251.32	-63.00
Line1	250.09	56.38
Line2	250.09	56.38
T2A	250.00	52.04
T2B	250.00	52.04
Gen	500.00	422.93
Load	1000.00	527.00

Table 8.16: Case 3: DIgSILENT Voltage Results

Element	V (kV)	δ
Bus 1	345	0°
Bus 2A	501.85	-0.96°
Bus 2B	501.85	-0.96°
Bus 3A	501.97	-21.72°
Bus 3B	501.97	-21.72°
Bus 4	230	-22.67°

From Table 8.16 it can be seen that the angular displacement limit is well within the stability limit of $\delta < +/- 35°$ while at the same time meeting the load demand.

No MathCAD hand calculation was conducted as the correctness of the modelling has been established in Case study 1 and 2.

8.4   Case study 4

In Case study 4 the single HVAC transmission line (from Case study 2) is completely replaced with a mono-polar HVDC transmission line as shown in Figure 8.11. This is the second proposed solution, (Block F) in Figure 6.1 requiring evaluation.
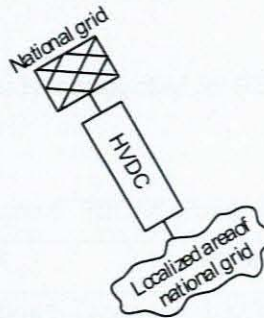
Figure 8.11: Case study 4

The HVDC model used is the CIGRE HVDC benchmark model described in Chapter 7 (Section 7.2).

As only PSCAD/EMTDC can conduct HVDC studies it is used for this evaluation. The results obtained will be proven by hand (MathCAD) to verify the results from the software package (see Appendix C).

When the HVDC transmission line is modelled in PSCAD the one-line-diagram is as follows:
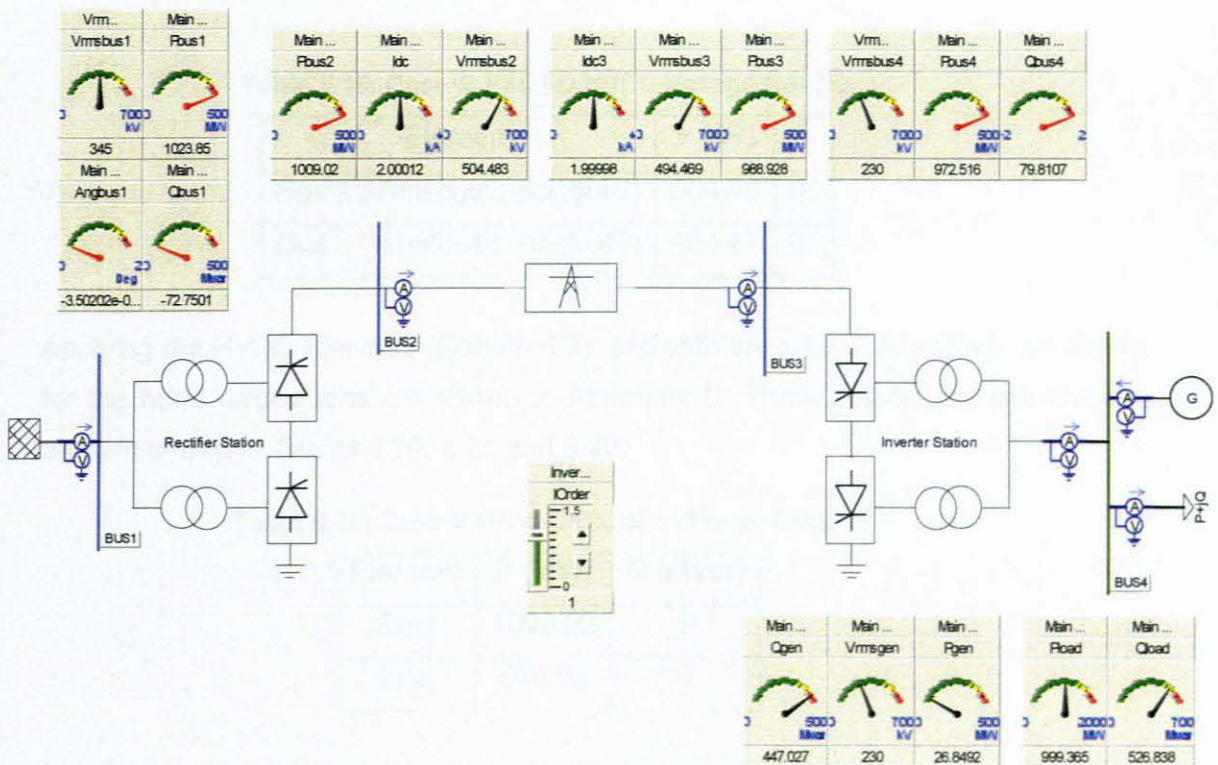
Figure 8.12: Case study 4 one-line-diagram in PSCAD

The HVDC control scheme (Sections 7.2.7 and 7.2.8) allows one to set the DC current on the line to a specific value. When this is done the control file adjusts the firing angles of both the inverter and rectifier to keep this value constant. The power that is being transmitted across the overhead line is directly proportional to the DC current.

The results of the simulation study conducted in PSCAD are shown in Tables 8.17, 8.18 and 8.19:

Table 8.17: Case 4: PSCAD Power Results

Element	P (MW)	Q (Mvar)
Grid sup Grid sup (Pbus1, Qbus1)	1023.85	-72.75
Rect (Pbus2, Qbus2)	1009.02	0
Line (Pbus3, Qbus3)	988.92	0
Inv (Pbus4, Qbus4)	972.52	-79.81
Gen (Pgen, Qgen)	26.84	447.03
Load (Pload, Qload)	999.37	526.84

Table 8.18: Case 4: PSCAD HVAC Voltage Results

Element	V (kV)	δ
Bus 1 (Vrmsbus1, Angbus1)	345	0°
Bus 4 (Vrmsbus4, Angbus4)	230	0°

Table 8.19: Case 4: PSCAD HVDC Voltage Results

Element	V (kV)	δ
Bus 2 (Vrmsbus2, Angbus2)	504.48	0°
Bus 3 (Vrmsbus3, Angbus3)	494.47	0°

Applying the HVDC formulas (Section 4.2), and with the help of MathCAD the results for the hand calculations are shown in Appendix C. These results are extrapolated and are shown in Tables 8.20, 8.21 and 8.22.

Table 8.20: Case 4: Hand Calculation Power Results

Element	P (MW)	Q (Mvar)
Rect	1009.02	0
Line	988.92	0

Table 8.21: Case 4: Hand Calculation HVAC Voltage Results

Element	V (kV)	δ
Bus 1	345	0°
Bus 4	230	0°

Table 8.22: Case 4: Hand Calculation HVDC Voltage Results

Element	V (kV)	δ
Bus 2	504.52	0°
Bus 3	495.33	0°

It is important to note that the angular difference between sending and receiving-end buses (buses 2 and 3) has no effect on the power that is transmitted across the HVDC transmission line. From Table 8.22 it can be seen that there is no angular difference between the sending and receiving-end buses, and from Table 8.17 it is seen that the load demand is fully met.

8.5 Case study 5

The third possible solution that needs to be explored to increase the power delivery to a localized area is an integrated HVAC/HVDC system. Block G in Figure 6.1 represents this part of the strategy. This scenario has the advantage that if the HVAC or HVDC line is out of commission some load demand can still be met. The networks used in Case studies 2 and 4 are connected in parallel to form an integrated HVAC/HVDC system. This is shown in Figure 8.13.
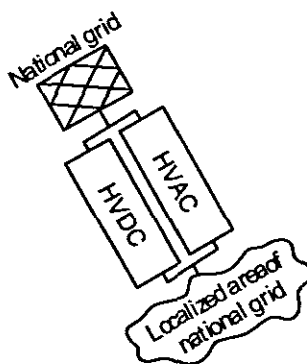
Figure 8.13: Case study 5: HVAC/HVDC parallel operation

The HVDC system that was used in Case study 4 had its firing angle set to deliver a 1000 MW. Now that is operated as an integrated HVAC/HVDC system and the HVAC line also delivers power the combination of delivery will be more than what is required for the localized area. If 1000 MW transfer, is maintained the excess will be transferred back into the grid across the HVAC line.

There is a limit to the amount of power that can be transferred back. It is for this reason the HVDC line in this case study is set to deliver 0.8 pu rated DC current.

This is performed in PSCAD only. The one-line-diagram of this study is shown in Figure 8.14.
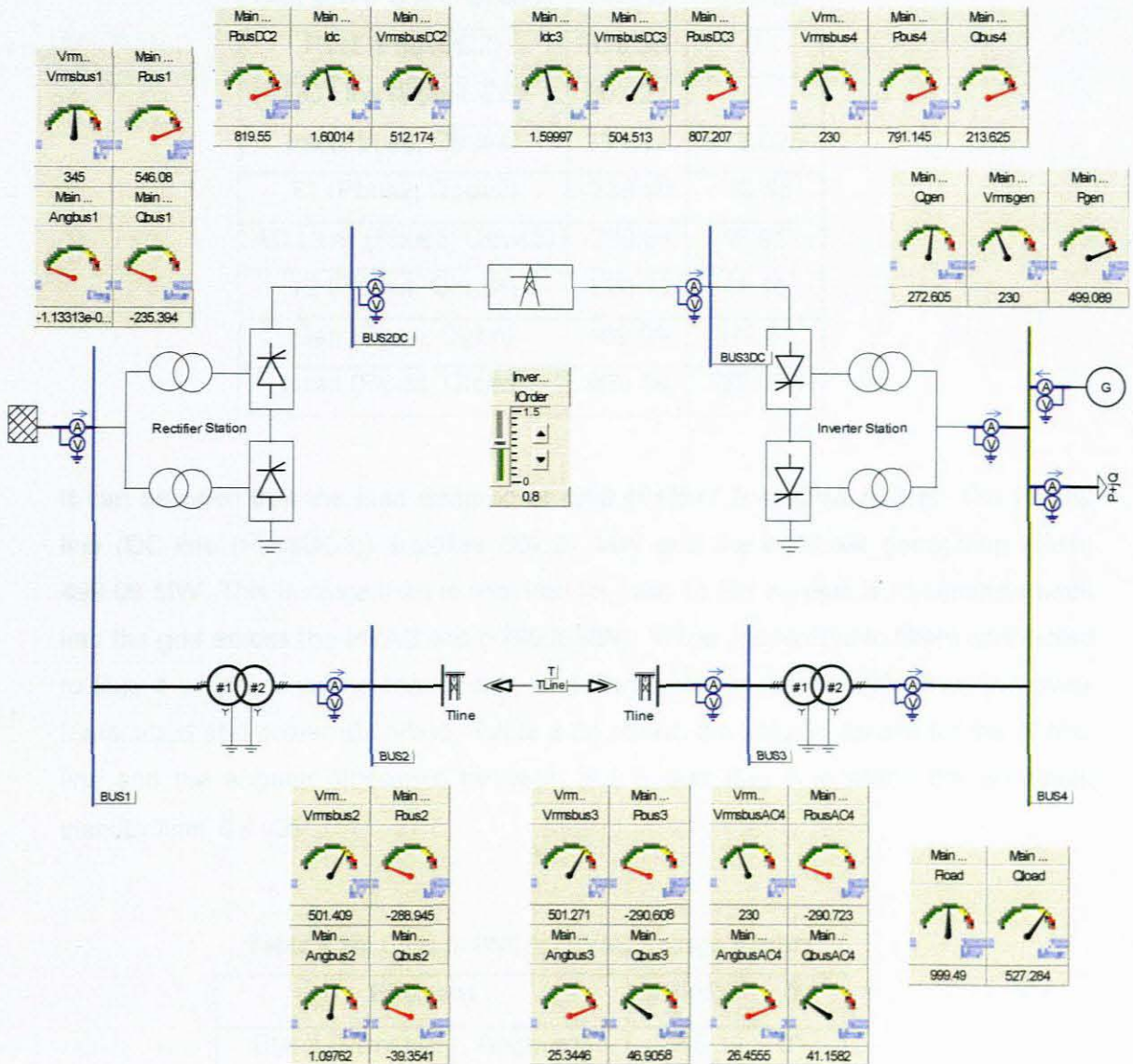
Figure 8.14: Case study 5 PSCAD one-line-diagram

This integrated system uses a mono-polar HVDC line (parameters in Chapter 7 with reduced power transfer), and a HVAC line. Both of these lines are 500 km long. The firing angles are determined by the pre-decided DC current which is now set to 0.8 pu (1.6 kA see IORDER in Figure 8.14). The HVDC commutation transformers that are used have much higher reactance to that of the HVAC system transformer. The reason for this is that a converter station needs a high reactance to protect it from sudden current changes, as it limits the rate of current change.

The results obtained from the study in shown in Figure 8.14 and are tabulated in Tables 8.23, 8.24 and 8.25.

Table 8.23: Case 5: PSCAD Power Results

Element	P (MW)	Q (Mvar)
Grid sup (Pbus1, Qbus1)	546.08	-235.39
Rect (PbusDC2)	819.55	0
DC Line (PbusDC3)	807.21	0
Inv (Pbus4, Qbus4)	791.14	213.625
T1 (Pbus2, Qbus2)	-288.95	-39.55
AC Line (Pbus3, Qbus3)	-290.61	46.91
T2 (Pbus4, Qbus4)	-290.72	41.16
Gen (Pgen, Qgen)	499.09	272.61
Load (Pload, Qload)	999.49	527.284

It can be seen that the load demand of (999.49+j527.284) MVA is met. The HVDC line (DC line (PbusDC3)) supplies 807.21 MW and the localized generation (Gen) 499.09 MW. This is more than is required for load so the surplus is transmitted back into the grid across the HVAC line (-290.6 MW). There are harmonic filters connected to Bus 4 which consume real power, and they account for the difference in power transmitted and power absorbed. Table 8.24 shows the voltage results for the HVAC line and the angular difference between Bus 1 and Bus 4 is within the allowable stability limit $\delta < -35°$.

Table 8.24: Case 5: PSCAD HVAC Voltage Results

Element	V (kV)	δ
Bus 1 (Vrmsbus1, Angbus1)	345	0°
Bus 2AC (Vrmsbus2, Angbus2)	501.41	1.09°
Bus 3AC (Vrmsbus3, Angbus3)	501.27	25.34
Bus 4 (Vrmsbus4, Angbus AC4)	230	26.46°

Table 8.25: Case 5: PSCAD HVDC Voltage Results

Element	V (kV)	δ
Bus 2DC (VrmsbusDC2)	512.17	0°
Bus 3DC (VrmsbusDC3)	504.51	0°

From Table 8.25 it can again be seen that there is no angular difference between the sending- and receiving-end (Bus 2DC and Bus 3DC) of the HVDC transmission line showing its difference to a HVAC line operation, that requires an angular displacement.

In this chapter the results obtained from all the different case studies are given and it is now necessary to analyse them in terms of the strategy to block K (Figure 6.1) then moving to the final stage of the strategy "U" to make recommendations.

CHAPTER NINE
ANALYSIS OF RESULTS

9.1   Case specific analysis of results

9.1.1   Case study 1

For evaluation of the developed strategy in Figure 6, Case study 1 was utilized to portray a healthy system (Block B). The power flow for this case study is visually shown in Figure 9.1.
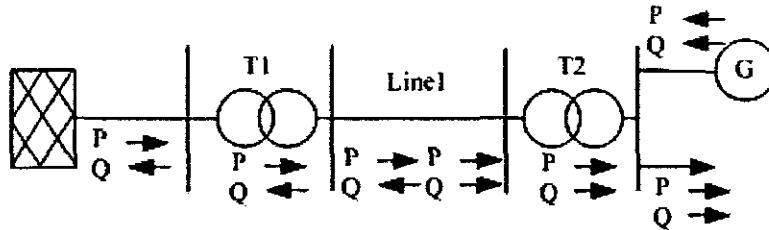
Figure 9.1: Case study 1 power flows

Two software packages were evaluated as well as a mathematical program namely, PSCAD, DIgSILENT, and MathCAD and they were used to obtain the power flow diagram shown in Figure 9.1. The results from the two software packages as well as the hand calculation for Case study 1 are shown in Tables 9.1 and 9.2 making for ease of comparison from which findings can be made.

In Table 9.2 power flow results from all there tools used are compared.

Table 9.1: Case 1: Power Results

Element	PSCAD P (MW)	Dig. P (MW)	Hand P (MW)	PSCAD Q (Mvar)	Dig. Q (Mvar)	Hand Q (Mvar)
Grid sup	201.23	200.93	200.85	-76.45	-76.49	-76.54
T1	201.17	200.87	200.79	-79.53	-79.58	-79.62
Line	200.31	200.06	200.06	74.18	74.29	74.34
T2	200.25	200.00	199.99	71.17	71.29	71.33
Gen	499.36	500	500	297.57	297.46	297.42
Load	699.62	700	700	368.73	368.75	368.75

The load is absorbing 700 MW and 368.75 Mvar, which is correct due to the fact that it is modelled as a fixed PQ load (Section 7.1.6) with a rating of (700+j368.75) MVA.

The generator situated in the localized area is supplying 500 MW and the remaining load demand is supplied over the overhead line from the Grid supply step–up through a transformer (T1) and then stepped down again (T2) and is equal to 200 MW.

In Table 9.2 the voltage results for Case study 1 are compared.

Table 9.2: Case 1: Voltage Results

Element	PSCAD V (kV)	Dig. V (kV)	Hand V (kV)	PSCAD δ	Dig. δ	Hand δ
Bus 1	345	345	345	0°	0°	0°
Bus 2	502.46	502.46	502.46	-0.77°	-0.77°	-0.77°
Bus 3	502.55	502.55	502.55	-17.22°	-17.19°	-17.19°
Bus 4	230	230	230	-17.97°	-17.95°	-17.95°

It is found that the results obtained from the two software packages and mathematical tool, produce results with discrepancies lower than 0.19 %. This indicates that the simulation approach is correct. The results obtained from DlgSILENT are the closest to the hand calculation results. The reason PSCAD has small discrepancies is due to the time domain nature of the program, and because the developed method explained in Section 5.1.1.1 and shown in Figure 5.2 is time constant dependant so a small ripple exists on the output signal causing the small discrepancies. These discrepancies are so small they can be ignored.

From Table 9.2 it can be seen that the voltage are 502.46 kV at the sending-end of the transmission line and 502.55 kV at the receiving-end, this means there is a voltage increase of 0.09 kV. This increase in voltage is caused by the capacitance on the transmission line.

The angular difference between the sending and receiving-end is equal to -17.95°. This is 17.05° within the allowable limit (-35°). This indicates that the system is operating normally because the angular displacement limit is not exceeded, and the power (active and reactive) that is measured at the load indicates that the load demand is met. This proves Block B in Figure 6.1

This angular difference of -17.95° indicates that a difference should exist when real power is transmitted across a transmission line. The network is thus healthy.

9.1.2 Case study 2

Block C, Figure 6.1 describes a scenario where the angular displacement limit of $\delta < +/-35°$ is violated due to the increase in load demand in the localized area of a national grid. The load demand was increased above that in Case study 1 and this is shown in Case study 2.

The power flow directions again obtained from the two software packages and mathematical tool (hand calculations) are drawn in a power flow diagram and shown in Figure 9.2.
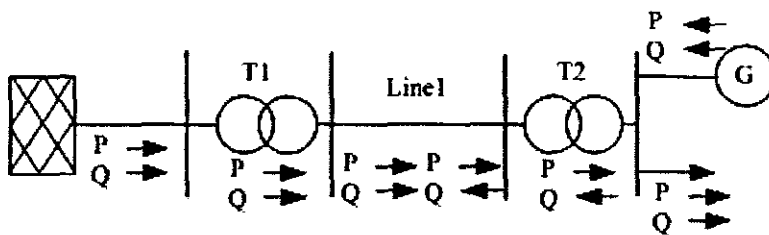
Figure 9.2: Case study 2 power flows

All the results from the three mentioned tools which were used to draw the power flow diagrams are tabulated for ease of comparison. This is shown in Tables 9.3 and 9.4.

Table 9.3: Case 2: Power Results

Element	PSCAD P (MW)	Dig. P (MW)	Hand P (MW)	PSCAD Q (Mvar)	Dig. Q (Mvar)	Hand Q (Mvar)
Grid sup	506.61	506.30	506.22	126.61	126.13	126.05
T1	506.24	505.93	505.86	108.43	107.99	105.12
Line	500.69	500.36	500.36	-121.55	-121.26	-121.18
T2	500.33	500.00	499.99	-139.54	-139.21	-139.14
Gen	500.02	500.00	500.01	666.54	666.21	666.14
Load	1000.35	1000.00	1000.00	526.99	527.00	527.00

The load has been increased from (700+j368.75) MVA to (1000+527) MVA. It is still modelled as a fixed PQ load so it is understandable that the load will be drawing 1000 MW and 527 Mvar. The generator can only supply 500 MW of the needed power so to be able to meet this increased load demand the Grid supply needs to supply more power and thus supplying 506 MW. With the losses subtracted the power delivered to the localized area across the transmission line is 500 MW.

In Table 9.4 the combined voltage results for Case study 2 are compared.

Table 9.4: Case 2: Voltage Results

Element	PSCAD V (kV)	Dig. V (kV)	Hand V (kV)	PSCAD δ	Dig. δ	Hand δ
Bus 1	345	345	345	0°	0°	0°
Bus 2	495.23	495.74	495.74	-1.94°	-1.94°	-1.94°
Bus 3	495.97	495.97	495.98	-48.78°	-48.73°	-48.73°
Bus 4	230	230	230	-50.72°	-50.67°	-50.67°

To supply the increased load demand to the localized area the power transfer across the line should increase. To increase the real power transfer across the transmission line the angular difference between the sending-end (Bus 1) and receiving-end should increase, it is for this reason that the angular displacement is now -50.67° and this is -15.67° more than the allowable limit (-35°).

This proves Block C, because it illustrates that there is a problem (angular displacement exceeded). Demonstrating the problem leads to Block D which follows with three possible solutions to solve this problem.

9.1.3 Case study 3

Case study 3 evaluated the first possible solution to solve the power delivery problem associated with a localized area of a national grid. The solution is the erection of two identical HVAC lines in parallel. Table 9.5 shows a comparison between the power results obtain in PSCAD and DigSILENT.

Table 9.5: Case 3: Power Results

Element	PSCAD P (MW)	Dig. P (MW)	PSCAD Q (Mvar)	Dig. Q (Mvar)
Grid sup	503.16	502.82	-116.96	-117.11
T1A	251.49	251.32	-62.93	-63.00
T1B	251.49	251.32	-62.93	-63.00
Line1	250.22	250.09	56.31	56.38
Line2	250.22	250.09	56.31	56.38
T2A	250.13	250.00	51.96	52.04
T2B	250.13	250.00	51.96	52.04
Gen	499.89	500.00	423.54	422.93
Load	1000.15	1000.00	527.52	527.00

With the load of (1000+527) MVA and the Generator supplying 500 MW, it is found that the remaining 500 MW needed is equally shared across the two lines and each supplies 250 MW. This is shown in Table 9.5. The voltage results obtained are shown in Table 9.6.

Table 9.6: Case 3: Voltage Results

Element	PSCAD V (kV)	Dig. V (kV)	PSCAD δ	Dig. δ
Bus 1	345	345	0°	0°
Bus 2A	501.85	501.85	-0.96°	-0.96°
Bus 2B	501.85	501.85	-0.96°	-0.96°
Bus 3A	501.96	501.97	-21.74°	-21.72°
Bus 3B	501.96	501.97	-21.74°	-21.72°
Bus 4	230	230	-22.69°	-22.67°

The power flow diagram representing these results is shown in Figure 9.3
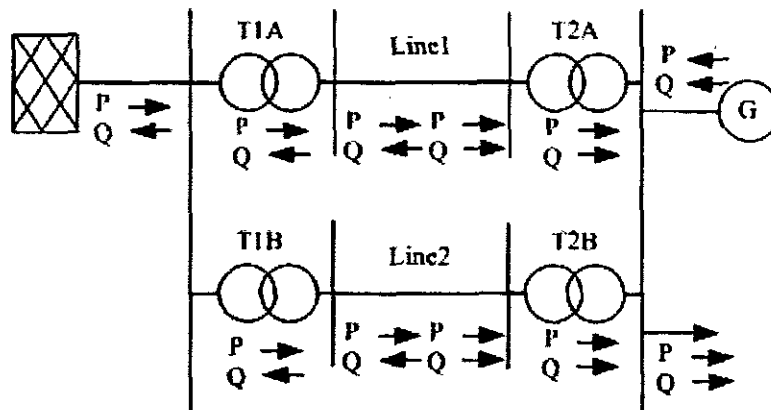
Figure 9.3: Case study 3 power flows

The power flow across the two transmission lines is identical, and from the voltage results shown in Table 9.6 it can be seen that the angular displacement across both the lines are -22° and that is within the allowable limit. It must be noted that the results obtained from both software packages (PSCAD and DIgSILENT) produce results with negligible differences, this proves the operation of both software packages as well as the first solution (increases the power delivery to the localized area) and that the angular displacement limit is not exceeded. Furthermore Block E (Figure 6.1) is thus correct.

9.1.4 Case study 4

The second possible solution indicated by Block F (Figure 6.1), is to replace the HVAC line in Case study 2 with a HVDC line. From the literature review HVDC was pointed out as a good alternative to that of HVAC lines. This was evaluated in Case study 4. The objectives was to replace the single HVAC (inadequate to supply the localized area with power) with a single HVDC system and evaluate the software used. Table 9.7 shows only the sending end HVDC voltage as well as the receiving end voltage. The comparison between the simulation conducted in PSCAD and that of the hand calculation is shown in Table 9.7.

Table 9.7: Case 4: Power Results

Element	PSCAD P (MW)	Hand P (MW)	PSCAD Q (Mvar)	Hand Q (Mvar)
Rect	1009.02	1009.02	0	0
Line	988.92	988.92	0	0

The voltage results are shown in Table 9.8

Table 9.8: Case 4: HVDC Voltage Results

Element	PSCAD V (kV)	Hand V (kV)	PSCAD δ	Hand δ
Bus 2	504.48	504.52	0°	0°
Bus 3	494.47	495.33	0°	0°

The amount of power that is being transmitted across the transmission line is substantially higher (1009.02 MW) than that of the parallel HVAC operation (250 MW x 2 = 500 MW) which gives an advantage to the HVDC system to that of the single and parallel HVAC transmission systems. The power that is transmitted across the transmission line is calculated by the equations given in Section 4.2.1 and more specifically (4.12). The power flow diagram is shown in Figure 9.4
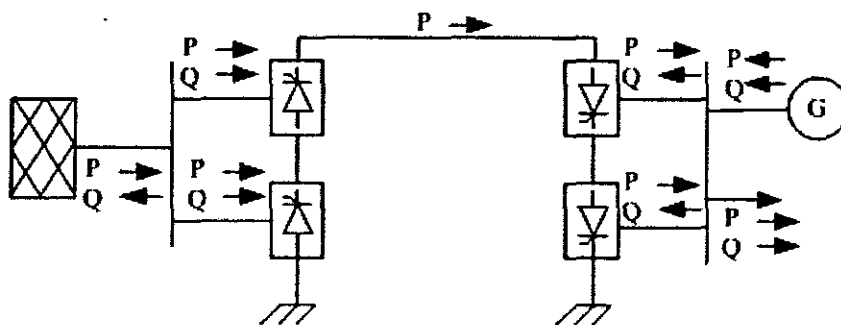
Figure 9.4: Case study 4 power flows

As mentioned in the section describing the operation of a HVDC transmission system (Chapter 4) the rectifier as well as the inverter are absorbing reactive power. This can be seen from Figure 9.4. No reactive power is transmitted across the line. The reason that the Grid supply is absorbing reactive power is a result of the Var compensation, in the form of a capacitor that is connected to Bus 1, supplying reactive power.

The results obtained from the simulation study that is shown in Table 9.7 show that this model is more than capable of supplying the localized area. This proves the effectiveness of the proposed solution in Block F in the proposed strategy (Figure 6.1).

9.1.5 Case study 5

In Case study 5 the final proposed solution is given. This is an integrated HVAC/HVDC network which entails a HVAC transmission network operated in parallel with the HVDC network. The results obtained for Case study 5 are tabulated in Chapter 8 (Tables 8.23, 8.24 and 8.25), but the flow diagram of this complex integrated network is given in Figure 9.5.
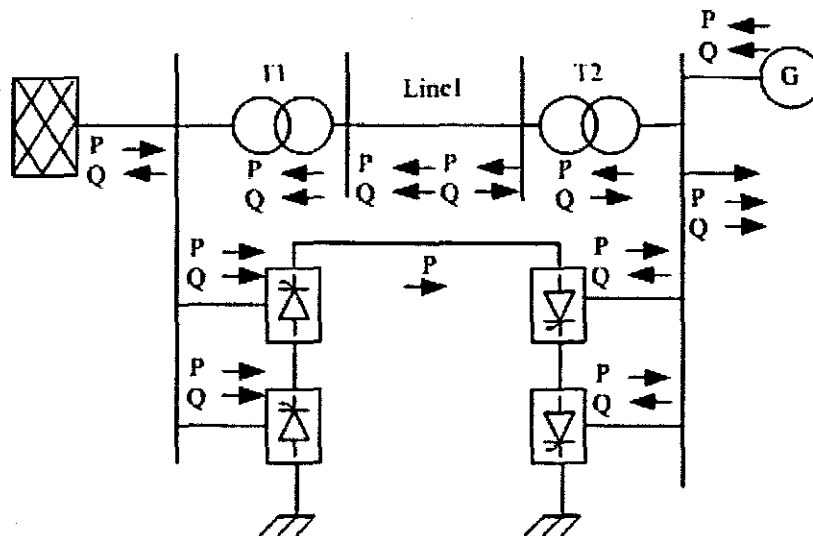
Figure 9.5: Case study 5 power flows

Even though the HVDC is only operated at 0.8 pu DC current and only approximately 800 MW is being transmitted the excess power is transmitted back to the Grid supply.

This makes this arrangement extremely good for the reason that when too much power is transmitted to the localized area the excess can be transmitted back to the grid.

The advantage of this integration is that contingency plans are in place with this circuit, because if a line is lost the other can still supply some of the load. One problem with this type of HVDC configuration is that if the generator is switched off, no commutation can take place and therefore the HVDC cannot transmit any power, as the converters are line commutated, leaving the HVAC line to still transmits some of the power. This is a perfect scenario when there is a prospect of further industrial and population growth in the localized area. One of the positive things in this case study is that the HVAC transmission line can supply some of the reactive power that is needed by the HVDC conversion process, reducing the need for large reactive compensation.

This proves that the final proposed solution is well suited to alleviate the power delivery problems.

9.2   Comparison and analysis of case study results

9.2.1   Load demand

In all the case studies the load resembles the amount of power (real and reactive) that is absorbed by the localized area of the national grid. Figure 9.6 shows the amount of power that is drawn for each of the case studies.
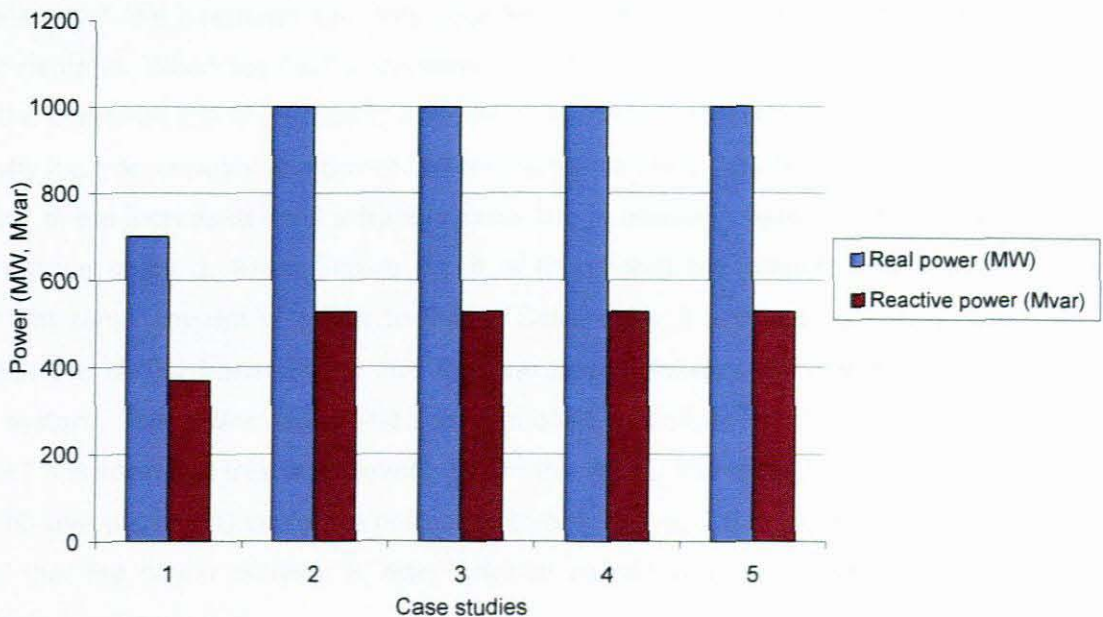
Figure 9.6: Power absorbed by the load

From Figure 9.6 it can be seen that the load increases from Case study 1 to Case study 2 and for the remaining case studies the power rating of the load was (1000+j527) MVA.

The generator in Case studies 1-5 is limited to 500 MW and the balance of the load demand is supplied by the grid supply via overhead lines (HVAC and/or HVDC). Figure 9.7 shows the real power delivered by the different overhead lines.
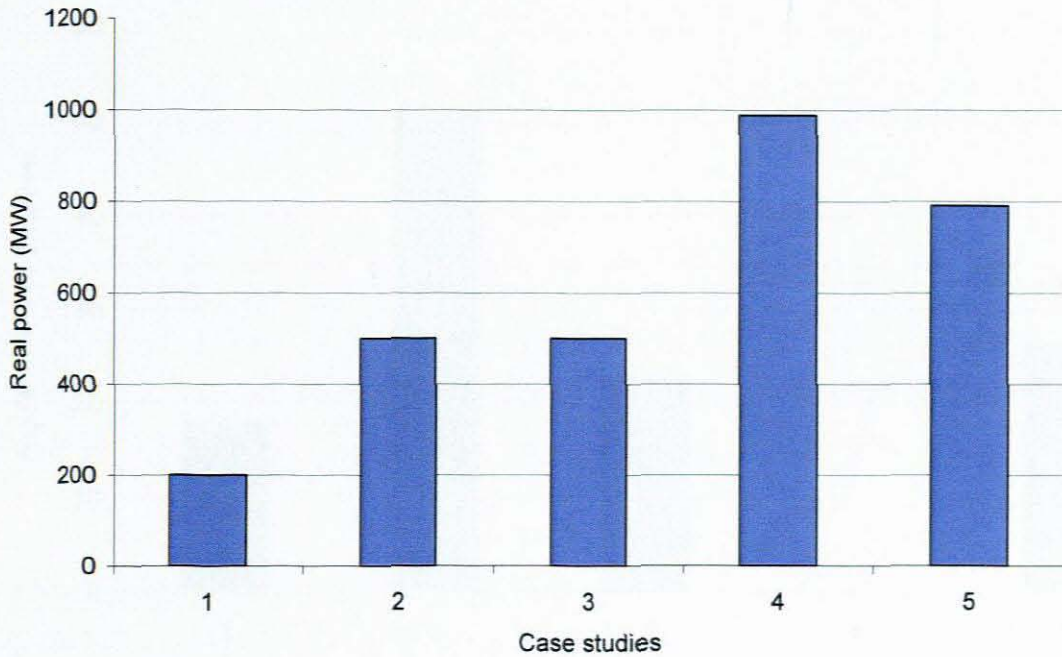
Figure 9.7: Real power delivered by the line

In Case study 1 the overhead line only supplies 200 MW, which is enough to meet the load demand. When the load is increased in Case study 2 the power transmitted across the overhead line increases to 500 MW. The load increased with 300 MW and this is why the transmission line power delivery increased with 300 MW. With the load remaining at the increased level a transmission line is added in parallel with the one given in Case study 2. From Figure 9.7 it is found that the parallel combination delivers the same amount of power to that in Case study 2 and is thus sharing the load. With the HVDC transmission line the real power delivery is controlled via its control system. The power transmitted is controlled to deliver 1000 MW and from Figure 9.7 it is seen that this is achieved. When the HVAC line is placed in parallel to the HVDC line, the HVDC system is controlled to only deliver 0.8 pu A and from this it is found that the power delivery is also reduced as can be seen when examining Case study 5 in Figure 9.7.

The power that is transmitted across a HVAC transmission line is a function of the angular difference between the sending- and receiving-end voltages. It is thus also necessary to investigate the angular difference across the transmission line. This is done in Figure 9.8.
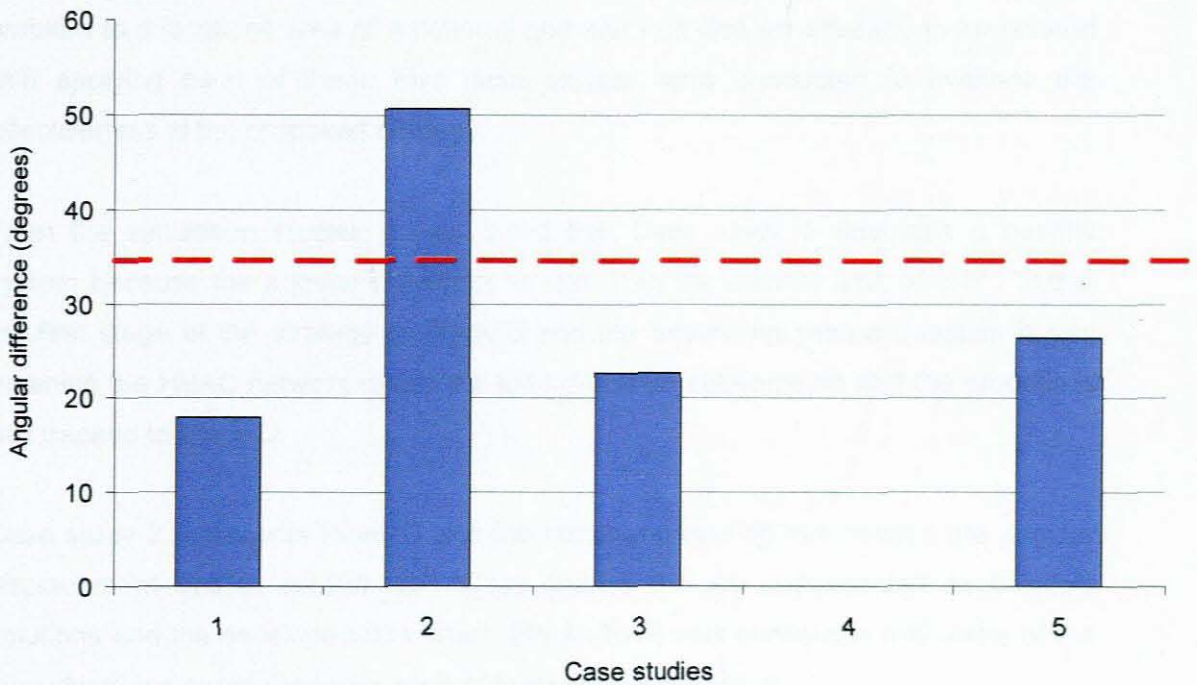
Figure 9.8: Angular difference across the transmission line

The red line indicates the maximum limit (-35°) that is allowed for the angular difference between the sending- and receiving-end voltages. It is clear that Case study 2, that demonstrates the problem, is above the maximum allowable angular difference. In Figure 9.8 the angular difference for Case study 4 is 0°. This proves that the power transmitted in a HVDC system is not a function of the angular difference. From Figure 9.8 it can be deduced that all three solutions (Case studies 3-5) are within the allowable angular displacement limit of -35 ° and because the load demand is met it is found that they all increase the power delivered to the localized area.

This proves that all three possible solutions are capable of increasing the power delivery to a localized area of a national grid.

CHAPTER TEN
CONCLUSIONS

In this research project a strategy was developed in the form of a flow chart that states a problem and proposes three possible solutions to alleviate a power delivery problem to a localized area of a national grid and includes considerations associated with applying each of them. Five case studies were conducted to evaluate the effectiveness of the proposed strategy.

From the simulation studies it was found that Case study 1 illustrates a healthy system because the angular difference is less than the stability limit of -35°. This is the first stage of the strategy at Block B and the answering yes/no question is yes meaning the HVAC network meets the load demand requirements and the process is fast tracked to Block U.

Case study 2 represents Block C and the increased loading has caused the angular displacement limit to exceed -35°. Case studies 3-5 are implemented as possible solutions and the developed flow chart (Blocks E-G) was successful and some of the considerations associated with each of them were highlighted.

In Case study 3 (parallel HVAC configuration) the load demand was met and stability limit was decreased back below -35° to -22.67°. With Case study 3 another transmission line was constructed which means the amount of land used (ROW) will be at least doubled and greatly influence the cost. This configuration needed no reactive compensation and actually supplied reactive power to the network. This line also has the advantage of contingency, due to the fact that some of the load demand can still be met if a problem occurs on one of the lines.

With Case study 4 the proposed solution in Block F (replacing the HVAC line with a HVDC transmission system) was examined. The load demand was met with almost half the power to spare, allowing for further load growth in the future. With the HVDC system the tower constructions are smaller and thus uses less land ROW than that of the HVAC system. If no new land is available, it is found that HVDC will increase the load delivery and optimize the already owned ROW. From literature HVDC has less line losses to that of HVAC systems for the same amount of power being transferred. Throughout the different case studies conducted no lines transferred the same amount of power, thus making them not comparable. With HVDC systems reactive compensation is necessary for converter operation. This problem can be solved by installing capacitors to supply this reactive power.

The main draw back of this system is the lack of contingency, if there is a line fault or loss of generation in the localized area then the HVDC transmission line can't supply any power to the load as it is a line commutated converter system.

Block G (Figure 6.1) implements the solution of an integrated HVAC/HVDC system. This system is the recommended choice because it combines the power delivery from HVAC and HVDC systems. It also provides for contingency analysis that is achieved with parallel HVAC operation if one line is lost, the remaining line can still supply some of the power required by the load. This means a total power outage is avoided. This system however will need more ROW and is not an option if no new land is available. With this configuration some of the reactive power needs of the converter station are supplied from the HVAC line.

It is found that the two industrial grade software packages that are utilized to perform the simulation studies are effective as their results give similar results to hand calculations taken as a benchmark. PSCAD is a time domain software tool and tools from its toolbox had to be implemented in a certain manner so that steady-state results can be generated. This innovation was found and confirms that PSCAD can be applied successfully for steady-state load-flow studies. It was also found that PSCAD can be applied for power flow studies, on integrated HVAC/HVDC systems. From this it was found that when a time domain package is used to perform steady-state analysis, time constants should be taken into account. Integrating elements are incorporated to integrate the time domain waveforms obtained from the measuring device to display steady-state results. It was found that when a Grid supply is modelled in PSCAD a standard voltage model should be used and by incorporating a feedback loop the voltage source will respond as a Grid supply supplied in the DIgSILENT frequency domain packages. It is found that despite PSCAD being a time domain package requiring complex modelling it is very effective in its method of displaying results.

DIgSILENT was used to verify the HVAC models used in all the studies. It was found that DIgSILENT has a Grid supply model in its library and that it is possible to model both a PV and Slack bus with the same grid element supplied in the DIgSILENT toolbox. It was found that power flow results can be displayed on the one- line-diagram. DIgSILENT was only used for HVAC systems.

From the hand calculations conducted it was found that when Newton-Raphson load-flow method is applied to the HVAC network having four buses, two specified and two unspecified, that the formulas only hold true for the specified buses.

The current conjugate power calculation method was selected and used to find the power flows at the unspecified buses, because the voltage results obtained after applying the Newton-Raphson load-flow method were similar to the software results. The results obtained from the current conjugate power calculation method were the same as that of the software results thus proving its effectiveness.

The developed strategy is found to be effective and functional as it moves through various stages in a sequence from investigating a healthy HVAC network to an unhealthy network in terms of angular displacement limit exceeded onto possible solutions that can be implemented to improve stability but at the same time meet the increased load demand of the localized area of a national grid. The flow chart also makes the researcher aware of all the factors (Block M-S) that need to be taken into account before deciding on a solution to be implemented. It is thus recommended that the developed flow chart should be used as a guideline when considering power delivery problems to a localized area of the national grid. All the considerations (Cost, ROW, Line losses, Reactive power support, harmonic impact, HVDC configurations and contingency analysis) should be taken into account when deciding on a solution.

For future work, DIgSILENT EMT (electro magnetic transient) package should be evaluated and compared to the integrated HVAC/HVDC results obtained with PSCAD. It is also necessary to research line losses for overhead lines that supply the same amount of power to the load area. Continuing on this, different HVDC configurations should be evaluated and simulated to illustrate the advantages and disadvantages of the HVDC configurations as well as evaluate the software when it comes to extremely complex HVDC systems.

In this thesis all the formulas and simulation processes were proven and illustrated, and the work contained herein, will save engineers and researchers time when entering the exciting field of HVDC systems and therefore its use is highly recommended.

REFERENCES

Arrillaga, J & Smith, B. 1998. *AC-DC Power System Analysis*. United Kingdom: The Institution of Electrical Engineers.

Arrillaga, J, Smith, B, Watson R. H & Alan, A. R. 1997. *Power System Harmonic Analysis*. Chichester: John Wiley & sons.

Arrillaga, J. & Arnold, C.P. 1990. *Computer Analysis of Power Systems*. Chichester: John Wiley & sons.

Arrillaga, J. 1988. *High Voltage Direct Current Transmission*. London: Peter Peregrinus.

Bathurst, G.N., Watson, N.R. & Arrillaga, J. 2000. Modelling of Bipolar HVDC Links in the Harmonic Domain. *IEEE Transactions on Power Delivery,* 15(3):1034-1038.

Del Toro, V. 1992. *Electric Power Systems*. New Jersey: Prentice Hall, Englewood Cliffs.

Dialynas, E.N. & Koskolos, N.C. 1994. Reliability Modelling and Evaluation of HVDC Power Transmission Systems. *IEEE Transactions on Power Delivery,* 9(2):872-878.

DIgSILENT GmbH. 2007. *PowerFactory Manual Version 13*. Gomaringen Germany April.

Doke, D.J. & Banerjee, S.K. 1986. A Simplified and Generalized Dynamic Simulation of Multi-Terminal HVDC Transmission System. *Pergamon Journals Computer. & Electrical. Engineering.* 13(2):69-82.

Fisher, J. M.1991. *Power Electronics*. Boston: PWS-Kent.

Glover. J.D & Sarma, M.S. 2002. *Power Systems Analysis and Design 3rd ed.* Pacific Grove: Brooks/Cole.

Grady, M. 2007. Fundamentals of Electric Power Systems, University of Texas at Austin, www.ece.utexas.edu/~grady June.

Katancevic, A.R. 2002. Challenging Opportunities for Incoming Engineers in HVDC Transmission Technology. *Paper presented at the 2002 IEEE Power Engineering Society Winter Meeting,* New York, 27-3. January.

Kimbark, E.D. 1971. *Direct Current Transmission Volume1*. New York: John Wiley & sons.

Koshcheev, L.A. 2003. Environmental Characteristics of HVDC Overhead Transmission. *Paper presented at the 3rd Work Shop on Power Grid Interconnection in Northeast Asia,* Vladivostok, Russia, 30 September – 3 October.

Larruskain, D.M., Zamora, I., Abarrategui, O., Iraolagoitia, A., Gutierrez, M.D., Lorono, E. & de la Bodega, F 2006. Power Transmission Capacity Upgrade of Overhead Lines. *Department of Electrical Engineering. University of the Basque Country.* Campus of Bizkaia Spain.

Laughton, M. A & Warne, D. J, 2003, *Electrical Engineer's Reference Book 17th ed.* Oxford: George Newness Ltd.

Manitoba HVDC Research Centre. 2005. *PSCAD User's Guide v.4.21.* Winnipeg Canada.

MathCAD Manual, Vol.1, version 14.0.0.163 [build 701291152]. 2007. Needham: Parametric Technology Corporation.

Operation Technology INC.2000. User Guide Powerstation 3.0. Nuclear Release 3.0N *American National Standard C57.12.10.*

Padiyar, K.R. 1990. *HVDC Power Transmission Systems Technology and System Interactions.* New York: John Wiley & sons.

Power Engineering Society. 1993. *IEEE Recommended Practices and Requirements for Harmonic Control in Electrical Power Systems (IEEE Std 519-1992).* New York: Institute of Electrical and Electronics Engineers Inc.

Power, PB. 2005. Analysis and Planning of a 1400 km HVDC Link. *Energize* August.

Reeve, J., Fahmy, G. & Scott, B. 1977. Versatile Load Flow Method for Multi-Terminal HVDC Systems. *IEEE Transactions. Power Apparatus and Systems,* 96(3):925-933.

Smith, J, Stemmet W.C & Atkinson-Hope, G. 2008. Modelling and Simulation of Integrated HVAC and HVAC Lines in a Power System. *17th South-African University Power Engineering Conference,* Durban, South-Africa. 24-25 January.

Sood. V.K., 2004. *HVDC and FACTS Controllers: Application of Static Converters in Power Systems.* United States of America: Lower Academic Publishers.

Stevenson, W.D, 1982. *Elements of Power System Analysis 4th ed.* Auckland: McGraw-HILL Book Company.

Szechman M, Wess T & Thio C.V. 1991. First Benchmark Model for HVDC Control Studies. *CIGRE Work Group:* 14(2), 54-73.

Von Meier, A. 2006. *Electrical Power Systems a Conceptual Introduction,* IEEE press, John Wiley & Sons, Inc.

Weimers, L. 2003. Bulk Power Transmission at Extra High Voltages, a Comparison Between Transmission Lines for HVDC at Voltages Above 600 kV DC and 800 kV AC. *ABB Power Technologies.* Sweden.

Wildi. T. 2000. *Electrical Machines, Drives, and Power Systems.* New Jersey: Charles E. Stewart, Jr.

Woodford, D.A., 1998, *HVDC Transmission.* Winnipeg: Manitoba HVDC Research Centre.

Woodford, D.A., Gole, A.M. & Menzies, R.W. 1983. Digital Simulation of DC Links and AC Machines. *IEEE Transactions. Power Apparatus and Systems,* 102(6):1616-1623.

APPENDIX A

To confirm the accuracy of the results obtained from the two industrial grade software packages (PSCAD and DIgSILENT), a hand calculation was performed using MathCAD. The Newton-Raphson load flow technique together with the current conjugate method was used to obtain the results.

A.1. Equivalent-π transmission line parameters

$$j := \sqrt{-1}$$

$$L := 500 \quad km$$

$$Z_{line} := 0.01 + j \cdot 0.75$$

$$Y_{line} := j \cdot 1.634 \cdot 10^{-6}$$

$$Z_{linetotal} := Z_{line} \cdot L$$

$$Z_{linetotal} = 5 + 375i$$

$$Y_{linetotal} := Y_{line} \cdot L$$

$$Y_{linetotal} = 0.0008i$$

$$\frac{Y_{linetotal}}{2} = 0.0004i$$

$$\tau L := \left[\sqrt{\left(Z_{line} \cdot Y_{line}\right)}\right] \cdot L$$

$$\tau L = 0.0037 + 0.5535i$$

$$F_1 := \frac{\sinh(\tau L)}{\tau L}$$

$$F_1 = 0.9497 + 0.0007i$$

$$F_2 := \frac{\tanh\left(\left(\frac{\tau L}{2}\right)\right)}{\left(\frac{\tau L}{2}\right)}$$

$$F_2 = 1.0263 - 0.0004i$$

$$Z_d := \left(F_1 \cdot Z_{linetotal}\right)$$

$$Z_d = 4.501 + 356.146i$$

$$Y_d := \left(F_2\right) \frac{Y_{linetotal}}{2}$$

$$Y_d = 0 + 0.0004i$$

$$Z_{base} := \frac{\left[\left(500 \cdot 10^3\right)^2\right]}{\left(1500 \cdot 10^6\right)}$$

$$Z_{base} = 166.6667$$

$$Z_{linepu} := \frac{Z_d}{Z_{base}}$$

$$Z_{linepu} = 0.027 + 2.1369i$$

$$Y_{base} := \frac{1}{Z_{base}}$$

$$Y_{base} = 0.006$$

$$Y_{pu} := \frac{Y_d}{Y_{base}}$$

$$Y_{pu} = 0 + 0.0699i$$

A1.1 Impedances

$$Z_{12} := 0.002 + j \cdot 0.1$$

$$Z_{34} := 0.002 + j \cdot 0.1$$

$$Z_{23} := 0.027 + j \cdot 2.1369$$

$$B_2 := 0 + 1j \cdot 0.0699$$

$$B_3 := 0 + j \cdot 0.0699$$

A.2. Y bus construction

$$Y_{11} := \frac{1}{Z_{12}}$$
$$Y_{11} = 0.1999 - 9.996i \qquad |Y_{11}| = 9.998 \qquad \arg(Y_{11})\frac{180}{\pi} = -88.8542$$

$$Y_{12} := \frac{-1}{Z_{12}}$$
$$Y_{12} = -0.1999 + 9.996i \qquad |Y_{12}| = 9.998$$

$$Y_{13} := 0 + j \cdot 0 \qquad Y_{13} = 0 \qquad |Y_{13}| = 0$$

$$Y_{14} := 0 + j \cdot 0 \qquad Y_{14} = 0 \qquad |Y_{14}| = 0$$

$$Y_{21} := \frac{-1}{Z_{12}}$$
$$Y_{21} = -0.1999 + 9.996i \qquad |Y_{21}| = 9.998$$

$$Y_{22} := \frac{1}{Z_{12}} + \frac{1}{Z_{23}} + B_2$$

$$Y_{22} = 0.2058 - 10.394i \qquad |Y_{22}| = 10.396 \qquad \arg(Y_{22})\frac{180}{\pi} = -88.8655$$

$$Y_{23} := \frac{-1}{Z_{23}}$$
$$Y_{23} = -0.0059 + 0.4679i \qquad |Y_{23}| = 0.4679 \qquad \arg(Y_{23})\frac{180}{\pi} = 90.7239$$

$$Y_{24} := 0 + j \cdot 0 \qquad Y_{24} = 0 \qquad |Y_{24}| = 0$$

$$Y_{31} := 0 + j \cdot 0 \qquad Y_{31} = 0 \qquad |Y_{31}| = 0$$

$$Y_{32} := \frac{-1}{Z_{23}}$$
$$Y_{32} = -0.0059 + 0.4679i \qquad |Y_{32}| = 0.4679 \qquad \arg(Y_{32})\frac{180}{\pi} = 90.7239$$

$$Y_{33} := \frac{1}{Z_{34}} + \frac{1}{Z_{23}} + B_3$$

$$Y_{33} = 0.2058 - 10.394i \qquad |Y_{33}| = 10.396 \qquad \arg(Y_{33})\frac{180}{\pi} = -88.8655$$

$$Y_{34} := \frac{-1}{Z_{34}}$$
$$Y_{34} = -0.1999 + 9.996i \qquad |Y_{34}| = 9.998 \qquad \arg(Y_{34})\frac{180}{\pi} = 91.1458$$

117

$Y_{41} := 0 + j \cdot 0$ $\qquad$ $Y_{41} = 0$ $\qquad$ $\left| Y_{41} \right| = 0$

$Y_{42} := 0 + j \cdot 0$ $\qquad$ $Y_{42} = 0$ $\qquad$ $\left| Y_{42} \right| = 0$

$Y_{43} := \dfrac{-1}{Z_{34}}$ $\qquad$ $Y_{43} = -0.1999 + 9.996i$ $\qquad$ $\left| Y_{43} \right| = 9.998$ $\qquad$ $\arg\left(Y_{43}\right)\dfrac{180}{\pi} = 91.1458$

$Y_{44} := \dfrac{1}{Z_{34}}$ $\qquad$ $Y_{44} = 0.1999 - 9.996i$ $\qquad$ $\left| Y_{44} \right| = 9.998$ $\qquad$ $\arg\left(Y_{44}\right)\dfrac{180}{\pi} = -88.8542$

$\zeta_{11} := \arg\left(Y_{11}\right)$ $\qquad$ $\zeta_{11} = -1.5508$

$\zeta_{12} := \arg\left(Y_{12}\right)$ $\qquad$ $\zeta_{12} = 1.5908$

$\zeta_{13} := 0$

$\zeta_{14} := 0$

$\zeta_{21} := \arg\left(Y_{21}\right)$ $\qquad$ $\zeta_{21} = 1.5908$

$\zeta_{22} := \arg\left(Y_{22}\right)$ $\qquad$ $\zeta_{22} = -1.551$

$\zeta_{23} := \arg\left(Y_{23}\right)$ $\qquad$ $\zeta_{23} = 1.5834$

$\zeta_{24} := 0$

$\zeta_{31} := 0$

$\zeta_{32} := \arg\left(Y_{23}\right)$ $\qquad$ $\zeta_{32} = 1.5834$

$\zeta_{33} := \arg\left(Y_{22}\right)$ $\qquad$ $\zeta_{33} = -1.551$

$\zeta_{34} := \arg\left(Y_{34}\right)$ $\qquad$ $\zeta_{34} = 1.5908$

$\zeta_{41} := 0$ $\qquad$ $\zeta_{42} := 0$

$\zeta_{43} := \arg\left(Y_{43}\right)$ $\qquad$ $\zeta_{43} = 1.5908$

$\zeta_{44} := \arg\left(Y_{44}\right)$ $\qquad$ $\zeta_{44} = -1.5508$

A.3. Initial voltages

$$V_{1.1} := 1 + j \cdot 0 \qquad |V_{1.1}| = 1 \qquad \arg(V_{1.1}) \frac{180}{\pi} = 0$$

$$V_{2.1} := 1 + j \cdot 0 \qquad |V_{2.1}| = 1 \qquad \arg(V_{2.1}) \frac{180}{\pi} = 0$$

$$V_{3.1} := 1 + j \cdot 0 \qquad |V_{3.1}| = 1 \qquad \arg(V_{3.1}) \frac{180}{\pi} = 0$$

$$V_{4.1} := 1 + j \cdot 0 \qquad |V_{4.1}| = 1 \qquad \arg(V_{4.1}) \frac{180}{\pi} = 0$$

$$V_1 := |V_{1.1}| \qquad \delta_1 := \arg(V_{1.1})$$

$$V_2 := |V_{2.1}| \qquad \delta_2 := \arg(V_{2.1})$$

$$V_3 := |V_{3.1}| \qquad \delta_3 := \arg(V_{3.1})$$

$$V_4 := |V_{4.1}| \qquad \delta_4 := \arg(V_{4.1})$$

$$V_{4MAG} := V_4$$

A.4. Initial conditions

A.4.1. Specified powers

$$P_{2S} := 0 \qquad\qquad P_{3S} := 0$$

$$Q_{2S} := 0 \qquad\qquad Q_{3S} := 0 \qquad\qquad P_{4S} := -0.133333$$

119

A.4.2 Calculated powers

$$P_{2C} := V_1 \cdot V_2 \cdot |Y_{21}| \cdot \cos(\delta_2 - \zeta_{21}) + V_2^2 \cdot |Y_{22}| \cdot \cos(-\zeta_{22}) + V_2 \cdot V_3 \cdot |Y_{23}| \cdot \cos(\delta_2 - \delta_3 - \zeta_{23}) + V_2 \cdot V_4 \cdot |Y_{24}| \cdot \cos(\delta_2 - \delta_4 - \zeta_{24})$$

$$P_{2C} = 0$$

$$Q_{2C} := V_1 \cdot V_2 \cdot |Y_{21}| \cdot \sin(\delta_2 - \zeta_{21}) + V_2^2 \cdot |Y_{22}| \cdot \sin(-\zeta_{22}) + V_2 \cdot V_3 \cdot |Y_{23}| \cdot \sin(\delta_2 - \delta_3 - \zeta_{23}) + V_2 \cdot V_4 \cdot |Y_{24}| \cdot \sin(\delta_2 - \delta_4 - \zeta_{24})$$

$$Q_{2C} = -0.0699$$

$$P_{3C} := V_1 \cdot V_3 \cdot |Y_{31}| \cdot \cos(\delta_3 - \zeta_{31}) + V_2 \cdot V_3 \cdot |Y_{32}| \cdot \cos(\delta_3 - \delta_2 - \zeta_{32}) + V_3^2 \cdot |Y_{33}| \cdot \cos(-\zeta_{33}) + V_4 \cdot V_3 \cdot |Y_{34}| \cdot \cos(\delta_3 - \delta_4 - \zeta_{34})$$

$$P_{3C} = 0$$

$$Q_{3C} := V_1 \cdot V_3 \cdot |Y_{31}| \cdot \sin(\delta_3 - \zeta_{31}) + V_2 \cdot V_3 \cdot |Y_{32}| \cdot \sin(\delta_3 - \delta_2 - \zeta_{32}) + V_3^2 \cdot |Y_{33}| \cdot \sin(-\zeta_{33}) + V_4 \cdot V_3 \cdot |Y_{34}| \cdot \sin(\delta_3 - \delta_4 - \zeta_{34})$$

$$Q_{3C} = -0.0699$$

$$P_{4C} := V_1 \cdot V_4 \cdot |Y_{41}| \cdot \cos(\delta_4 - \zeta_{41}) + V_2 \cdot V_4 \cdot |Y_{42}| \cdot \cos(\delta_4 - \delta_2 - \zeta_{42}) + V_3 \cdot V_4 \cdot |Y_{43}| \cdot \cos(\delta_4 - \delta_3 - \zeta_{43}) + V_4^2 \cdot |Y_{44}| \cdot \cos(-\zeta_{44})$$

$$P_{4C} = 0$$

$$\Delta P_2 := P_{2S} - P_{2C} \qquad \Delta Q_2 := Q_{2S} - Q_{2C} \qquad\qquad \Delta P_3 := P_{3S} - P_{3C}$$

$$\Delta P_2 = -0 \qquad\qquad \Delta Q_2 = 0.0699 \qquad\qquad \Delta P_3 = -0$$

$$\Delta P_4 := P_{4S} - P_{4C} \qquad \Delta Q_3 := Q_{3S} - Q_{3C}$$

$$\Delta P_4 = -0.1333 \qquad\qquad \Delta Q_3 = 0.0699$$

A.4.3 Jacobian Matrix

$$P_{2C} := V_1 \cdot V_2 \cdot |Y_{21}| \cdot \cos(\delta_2 - \zeta_{21}) + V_2^2 \cdot |Y_{22}| \cdot \cos(-\zeta_{22}) + V_2 \cdot V_3 \cdot |Y_{23}| \cdot \cos(\delta_2 - \delta_3 - \zeta_{23}) + V_2 \cdot V_4 \cdot |Y_{24}| \cdot \cos(\delta_2 - \delta_4 - \zeta_{24})$$

$$J_{11} := \frac{\partial}{\partial \delta_2}\left(V_1 \cdot V_2 \cdot |Y_{21}| \cdot \cos(\delta_2 - \zeta_{21}) + V_2^2 \cdot |Y_{22}| \cdot \cos(-\zeta_{22}) + V_2 \cdot V_3 \cdot |Y_{23}| \cdot \cos(\delta_2 - \delta_3 - \zeta_{23}) + V_2 \cdot V_4 \cdot |Y_{24}| \cdot \cos(\delta_2 - \delta_4 - \zeta_{24})\right)$$

$$J_{11} = 10.4639$$

$$P_{2C} := V_1 \cdot V_2 \cdot |Y_{21}| \cdot \cos(\delta_2 - \zeta_{21}) + V_2^2 \cdot |Y_{22}| \cdot \cos(-\zeta_{22}) + V_2 \cdot V_3 \cdot |Y_{23}| \cdot \cos(\delta_2 - \delta_3 - \zeta_{23}) + V_2 \cdot V_4 \cdot |Y_{24}| \cdot \cos(\delta_2 - \delta_4 - \zeta_{24})$$

$$J_{12} := \frac{\partial}{\partial \delta_3}\left(V_1 \cdot V_2 \cdot |Y_{21}| \cdot \cos(\delta_2 - \zeta_{21}) + V_2^2 \cdot |Y_{22}| \cdot \cos(-\zeta_{22}) + V_2 \cdot V_3 \cdot |Y_{23}| \cdot \cos(\delta_2 - \delta_3 - \zeta_{23}) + V_2 \cdot V_4 \cdot |Y_{24}| \cdot \cos(\delta_2 - \delta_4 - \zeta_{24})\right)$$

$$J_{12} = -0.4679$$

$$P_{2C} := V_1 \cdot V_2 \cdot |Y_{21}| \cdot \cos(\delta_2 - \zeta_{21}) + V_2^2 \cdot |Y_{22}| \cdot \cos(-\zeta_{22}) + V_2 \cdot V_3 \cdot |Y_{23}| \cdot \cos(\delta_2 - \delta_3 - \zeta_{23}) + V_2 \cdot V_4 \cdot |Y_{24}| \cdot \cos(\delta_2 - \delta_4 - \zeta_{24})$$

$$J_{13} := \frac{\partial}{\partial \delta_4}\left(V_1 \cdot V_2 \cdot |Y_{21}| \cdot \cos(\delta_2 - \zeta_{21}) + V_2^2 \cdot |Y_{22}| \cdot \cos(-\zeta_{22}) + V_2 \cdot V_3 \cdot |Y_{23}| \cdot \cos(\delta_2 - \delta_3 - \zeta_{23}) + V_2 \cdot V_4 \cdot |Y_{24}| \cdot \cos(\delta_2 - \delta_4 - \zeta_{24})\right)$$

$$J_{13} = 0$$

$$P_{2C} := V_1 \cdot V_2 \cdot |Y_{21}| \cdot \cos(\delta_2 - \zeta_{21}) + V_2^2 \cdot |Y_{22}| \cdot \cos(-\zeta_{22}) + V_2 \cdot V_3 \cdot |Y_{23}| \cdot \cos(\delta_2 - \delta_3 - \zeta_{23}) + V_2 \cdot V_4 \cdot |Y_{24}| \cdot \cos(\delta_2 - \delta_4 - \zeta_{24})$$

$$J_{14} := \frac{\partial}{\partial V_2}\left(V_1 \cdot V_2 \cdot |Y_{21}| \cdot \cos(\delta_2 - \zeta_{21}) + V_2^2 \cdot |Y_{22}| \cdot \cos(-\zeta_{22}) + V_2 \cdot V_3 \cdot |Y_{23}| \cdot \cos(\delta_2 - \delta_3 - \zeta_{23}) + V_2 \cdot V_4 \cdot |Y_{24}| \cdot \cos(\delta_2 - \delta_4 - \zeta_{24})\right)$$

$$J_{14} = 0.2058$$

$$P_{2C} := V_1 \cdot V_2 \cdot |Y_{21}| \cdot \cos(\delta_2 - \zeta_{21}) + V_2^2 \cdot |Y_{22}| \cdot \cos(-\zeta_{22}) + V_2 \cdot V_3 \cdot |Y_{23}| \cdot \cos(\delta_2 - \delta_3 - \zeta_{23}) + V_2 \cdot V_4 \cdot |Y_{24}| \cdot \cos(\delta_2 - \delta_4 - \zeta_{24})$$

$$J_{15} := \frac{\partial}{\partial V_3}\left(V_1 \cdot V_2 \cdot |Y_{21}| \cdot \cos(\delta_2 - \zeta_{21}) + V_2^2 \cdot |Y_{22}| \cdot \cos(-\zeta_{22}) + V_2 \cdot V_3 \cdot |Y_{23}| \cdot \cos(\delta_2 - \delta_3 - \zeta_{23}) + V_2 \cdot V_4 \cdot |Y_{24}| \cdot \cos(\delta_2 - \delta_4 - \zeta_{24})\right)$$

$$J_{15} = -0.0059$$

$$P_{3C} := V_1 \cdot V_3 \cdot |Y_{31}| \cdot \cos(\delta_3 - \zeta_{31}) + V_2 \cdot V_3 \cdot |Y_{32}| \cdot \cos(\delta_3 - \delta_2 - \zeta_{32}) + V_3^2 \cdot |Y_{33}| \cdot \cos(-\zeta_{33}) + V_4 \cdot V_3 \cdot |Y_{34}| \cdot \cos(\delta_3 - \delta_4 - \zeta_{34})$$

$$J_{21} := \frac{\partial}{\partial \delta_2}\left(V_1 \cdot V_3 \cdot |Y_{31}| \cdot \cos(\delta_3 - \zeta_{31}) + V_2 \cdot V_3 \cdot |Y_{32}| \cdot \cos(\delta_3 - \delta_2 - \zeta_{32}) + V_3^2 \cdot |Y_{33}| \cdot \cos(-\zeta_{33}) + V_4 \cdot V_3 \cdot |Y_{34}| \cdot \cos(\delta_3 - \delta_4 - \zeta_{34})\right)$$

$$J_{21} = -0.4679$$

$$P_{3C} := V_1 \cdot V_3 \cdot \left| Y_{31} \right| \cos(\delta_3 - \zeta_{31}) + V_2 \cdot V_3 \cdot \left| Y_{32} \right| \cdot \cos(\delta_3 - \delta_2 - \zeta_{32}) + V_3^2 \cdot \left| Y_{33} \right| \cdot \cos(-\zeta_{33}) + V_4 \cdot V_3 \cdot \left| Y_{34} \right| \cdot \cos(\delta_3 - \delta_4 - \zeta_{34})$$

$$J_{22} := \frac{\partial}{\partial \delta_3}\left(V_1 \cdot V_3 \cdot \left| Y_{31} \right| \cos(\delta_3 - \zeta_{31}) + V_2 \cdot V_3 \cdot \left| Y_{32} \right| \cdot \cos(\delta_3 - \delta_2 - \zeta_{32}) + V_3^2 \cdot \left| Y_{33} \right| \cdot \cos(-\zeta_{33}) + V_4 \cdot V_3 \cdot \left| Y_{34} \right| \cdot \cos(\delta_3 - \delta_4 - \zeta_{34})\right)$$

$$J_{22} = 10.4639$$

$$P_{3C} := V_1 \cdot V_3 \cdot \left| Y_{31} \right| \cos(\delta_3 - \zeta_{31}) + V_2 \cdot V_3 \cdot \left| Y_{32} \right| \cdot \cos(\delta_3 - \delta_2 - \zeta_{32}) + V_3^2 \cdot \left| Y_{33} \right| \cdot \cos(-\zeta_{33}) + V_4 \cdot V_3 \cdot \left| Y_{34} \right| \cdot \cos(\delta_3 - \delta_4 - \zeta_{34})$$

$$J_{23} := \frac{\partial}{\partial \delta_4}\left(V_1 \cdot V_3 \cdot \left| Y_{31} \right| \cos(\delta_3 - \zeta_{31}) + V_2 \cdot V_3 \cdot \left| Y_{32} \right| \cdot \cos(\delta_3 - \delta_2 - \zeta_{32}) + V_3^2 \cdot \left| Y_{33} \right| \cdot \cos(-\zeta_{33}) + V_4 \cdot V_3 \cdot \left| Y_{34} \right| \cdot \cos(\delta_3 - \delta_4 - \zeta_{34})\right)$$

$$J_{23} = -9.996$$

$$P_{3C} := V_1 \cdot V_3 \cdot \left| Y_{31} \right| \cos(\delta_3 - \zeta_{31}) + V_2 \cdot V_3 \cdot \left| Y_{32} \right| \cdot \cos(\delta_3 - \delta_2 - \zeta_{32}) + V_3^2 \cdot \left| Y_{33} \right| \cdot \cos(-\zeta_{33}) + V_4 \cdot V_3 \cdot \left| Y_{34} \right| \cdot \cos(\delta_3 - \delta_4 - \zeta_{34})$$

$$J_{24} := \frac{\partial}{\partial V_2}\left(V_1 \cdot V_3 \cdot \left| Y_{31} \right| \cos(\delta_3 - \zeta_{31}) + V_2 \cdot V_3 \cdot \left| Y_{32} \right| \cdot \cos(\delta_3 - \delta_2 - \zeta_{32}) + V_3^2 \cdot \left| Y_{33} \right| \cdot \cos(-\zeta_{33}) + V_4 \cdot V_3 \cdot \left| Y_{34} \right| \cdot \cos(\delta_3 - \delta_4 - \zeta_{34})\right)$$

$$J_{24} = -0.0059$$

$$P_{3C} := V_1 \cdot V_3 \cdot \left| Y_{31} \right| \cos(\delta_3 - \zeta_{31}) + V_2 \cdot V_3 \cdot \left| Y_{32} \right| \cdot \cos(\delta_3 - \delta_2 - \zeta_{32}) + V_3^2 \cdot \left| Y_{33} \right| \cdot \cos(-\zeta_{33}) + V_4 \cdot V_3 \cdot \left| Y_{34} \right| \cdot \cos(\delta_3 - \delta_4 - \zeta_{34})$$

$$J_{25} := \frac{\partial}{\partial V_3}\left(V_1 \cdot V_3 \cdot \left| Y_{31} \right| \cos(\delta_3 - \zeta_{31}) + V_2 \cdot V_3 \cdot \left| Y_{32} \right| \cdot \cos(\delta_3 - \delta_2 - \zeta_{32}) + V_3^2 \cdot \left| Y_{33} \right| \cdot \cos(-\zeta_{33}) + V_4 \cdot V_3 \cdot \left| Y_{34} \right| \cdot \cos(\delta_3 - \delta_4 - \zeta_{34})\right)$$

$$J_{25} = 0.2058$$

$$P_{4C} := V_1 \cdot V_4 \cdot \left| Y_{41} \right| \cdot \cos(\delta_4 - \zeta_{41}) + V_2 \cdot V_4 \cdot \left| Y_{42} \right| \cdot \cos(\delta_4 - \delta_2 - \zeta_{42}) + V_3 \cdot V_4 \cdot \left| Y_{43} \right| \cdot \cos(\delta_4 - \delta_3 - \zeta_{43}) + V_4^2 \cdot \left| Y_{44} \right| \cdot \cos(-\zeta_{44})$$

$$J_{31} := \frac{\partial}{\partial \delta_2}\left(V_1 \cdot V_4 \cdot \left| Y_{41} \right| \cdot \cos(\delta_4 - \zeta_{41}) + V_2 \cdot V_4 \cdot \left| Y_{42} \right| \cdot \cos(\delta_4 - \delta_2 - \zeta_{42}) + V_3 \cdot V_4 \cdot \left| Y_{43} \right| \cdot \cos(\delta_4 - \delta_3 - \zeta_{43}) + V_4^2 \cdot \left| Y_{44} \right| \cdot \cos(-\zeta_{44})\right)$$

$$J_{31} = 0$$

$$P_{4C} := V_1 \cdot V_4 \cdot \left| Y_{41} \right| \cdot \cos(\delta_4 - \zeta_{41}) + V_2 \cdot V_4 \cdot \left| Y_{42} \right| \cdot \cos(\delta_4 - \delta_2 - \zeta_{42}) + V_3 \cdot V_4 \cdot \left| Y_{43} \right| \cdot \cos(\delta_4 - \delta_3 - \zeta_{43}) + V_4^2 \cdot \left| Y_{44} \right| \cdot \cos(-\zeta_{44})$$

$$J_{32} := \frac{\partial}{\partial \delta_3}\left(V_1 \cdot V_4 \cdot \left| Y_{41} \right| \cdot \cos(\delta_4 - \zeta_{41}) + V_2 \cdot V_4 \cdot \left| Y_{42} \right| \cdot \cos(\delta_4 - \delta_2 - \zeta_{42}) + V_3 \cdot V_4 \cdot \left| Y_{43} \right| \cdot \cos(\delta_4 - \delta_3 - \zeta_{43}) + V_4^2 \cdot \left| Y_{44} \right| \cdot \cos(-\zeta_{44})\right)$$

$$J_{32} = -9.996$$

$$P_{4C} := V_1 \cdot V_4 \cdot \left| Y_{41} \right| \cdot \cos(\delta_4 - \zeta_{41}) + V_2 \cdot V_4 \cdot \left| Y_{42} \right| \cdot \cos(\delta_4 - \delta_2 - \zeta_{42}) + V_3 \cdot V_4 \cdot \left| Y_{43} \right| \cdot \cos(\delta_4 - \delta_3 - \zeta_{43}) + V_4^2 \cdot \left| Y_{44} \right| \cdot \cos(-\zeta_{44})$$

$$J_{33} := \frac{\partial}{\partial \delta_4}\left(V_1 \cdot V_4 \cdot |Y_{41}| \cdot \cos(\delta_4 - \zeta_{41}) + V_2 \cdot V_4 \cdot |Y_{42}| \cdot \cos(\delta_4 - \delta_2 - \zeta_{42}) + V_3 \cdot V_4 \cdot |Y_{43}| \cdot \cos(\delta_4 - \delta_3 - \zeta_{43}) + V_4^2 \cdot |Y_{44}| \cdot \cos(-\zeta_{44})\right)$$

$J_{33} = 9.996$

$$P_{4C} := V_1 \cdot V_4 \cdot |Y_{41}| \cdot \cos(\delta_4 - \zeta_{41}) + V_2 \cdot V_4 \cdot |Y_{42}| \cdot \cos(\delta_4 - \delta_2 - \zeta_{42}) + V_3 \cdot V_4 \cdot |Y_{43}| \cdot \cos(\delta_4 - \delta_3 - \zeta_{43}) + V_4^2 \cdot |Y_{44}| \cdot \cos(-\zeta_{44})$$

$$J_{34} := \frac{\partial}{\partial V_2}\left(V_1 \cdot V_4 \cdot |Y_{41}| \cdot \cos(\delta_4 - \zeta_{41}) + V_2 \cdot V_4 \cdot |Y_{42}| \cdot \cos(\delta_4 - \delta_2 - \zeta_{42}) + V_3 \cdot V_4 \cdot |Y_{43}| \cdot \cos(\delta_4 - \delta_3 - \zeta_{43}) + V_4^2 \cdot |Y_{44}| \cdot \cos(-\zeta_{44})\right)$$

$J_{34} = 0$

$$P_{4C} := V_1 \cdot V_4 \cdot |Y_{41}| \cdot \cos(\delta_4 - \zeta_{41}) + V_2 \cdot V_4 \cdot |Y_{42}| \cdot \cos(\delta_4 - \delta_2 - \zeta_{42}) + V_3 \cdot V_4 \cdot |Y_{43}| \cdot \cos(\delta_4 - \delta_3 - \zeta_{43}) + V_4^2 \cdot |Y_{44}| \cdot \cos(-\zeta_{44})$$

$$J_{35} := \frac{\partial}{\partial V_3}\left(V_1 \cdot V_4 \cdot |Y_{41}| \cdot \cos(\delta_4 - \zeta_{41}) + V_2 \cdot V_4 \cdot |Y_{42}| \cdot \cos(\delta_4 - \delta_2 - \zeta_{42}) + V_3 \cdot V_4 \cdot |Y_{43}| \cdot \cos(\delta_4 - \delta_3 - \zeta_{43}) + V_4^2 \cdot |Y_{44}| \cdot \cos(-\zeta_{44})\right)$$

$J_{35} = -0.1999$

$$Q_{2C} := V_1 \cdot V_2 \cdot |Y_{21}| \cdot \sin(\delta_2 - \zeta_{21}) + V_2^2 \cdot |Y_{22}| \cdot \sin(-\zeta_{22}) + V_2 \cdot V_3 \cdot |Y_{23}| \cdot \sin(\delta_2 - \delta_3 - \zeta_{23}) + V_2 \cdot V_4 \cdot |Y_{24}| \cdot \sin(\delta_2 - \delta_4 - \zeta_{24})$$

$$J_{41} := \frac{\partial}{\partial \delta_2}\left(V_1 \cdot V_2 \cdot |Y_{21}| \cdot \sin(\delta_2 - \zeta_{21}) + V_2^2 \cdot |Y_{22}| \cdot \sin(-\zeta_{22}) + V_2 \cdot V_3 \cdot |Y_{23}| \cdot \sin(\delta_2 - \delta_3 - \zeta_{23}) + V_2 \cdot V_4 \cdot |Y_{24}| \cdot \sin(\delta_2 - \delta_4 - \zeta_{24})\right)$$

$J_{41} = -0.2058$

$$Q_{2C} := V_1 \cdot V_2 \cdot |Y_{21}| \cdot \sin(\delta_2 - \zeta_{21}) + V_2^2 \cdot |Y_{22}| \cdot \sin(-\zeta_{22}) + V_2 \cdot V_3 \cdot |Y_{23}| \cdot \sin(\delta_2 - \delta_3 - \zeta_{23}) + V_2 \cdot V_4 \cdot |Y_{24}| \cdot \sin(\delta_2 - \delta_4 - \zeta_{24})$$

$$J_{42} := \frac{\partial}{\partial \delta_3}\left(V_1 \cdot V_2 \cdot |Y_{21}| \cdot \sin(\delta_2 - \zeta_{21}) + V_2^2 \cdot |Y_{22}| \cdot \sin(-\zeta_{22}) + V_2 \cdot V_3 \cdot |Y_{23}| \cdot \sin(\delta_2 - \delta_3 - \zeta_{23}) + V_2 \cdot V_4 \cdot |Y_{24}| \cdot \sin(\delta_2 - \delta_4 - \zeta_{24})\right)$$

$J_{42} = 0.0059$

$$Q_{2C} := V_1 \cdot V_2 \cdot |Y_{21}| \cdot \sin(\delta_2 - \zeta_{21}) + V_2^2 \cdot |Y_{22}| \cdot \sin(-\zeta_{22}) + V_2 \cdot V_3 \cdot |Y_{23}| \cdot \sin(\delta_2 - \delta_3 - \zeta_{23}) + V_2 \cdot V_4 \cdot |Y_{24}| \cdot \sin(\delta_2 - \delta_4 - \zeta_{24})$$

$$J_{43} := \frac{\partial}{\partial \delta_4}\left(V_1 \cdot V_2 \cdot |Y_{21}| \cdot \sin(\delta_2 - \zeta_{21}) + V_2^2 \cdot |Y_{22}| \cdot \sin(-\zeta_{22}) + V_2 \cdot V_3 \cdot |Y_{23}| \cdot \sin(\delta_2 - \delta_3 - \zeta_{23}) + V_2 \cdot V_4 \cdot |Y_{24}| \cdot \sin(\delta_2 - \delta_4 - \zeta_{24})\right)$$

$J_{43} = 0$

$$Q_{2C} := V_1 \cdot V_2 \cdot |Y_{21}| \cdot \sin(\delta_2 - \zeta_{21}) + V_2^2 \cdot |Y_{22}| \cdot \sin(-\zeta_{22}) + V_2 \cdot V_3 \cdot |Y_{23}| \cdot \sin(\delta_2 - \delta_3 - \zeta_{23}) + V_2 \cdot V_4 \cdot |Y_{24}| \cdot \sin(\delta_2 - \delta_4 - \zeta_{24})$$

$$J_{44} := \frac{\partial}{\partial V_2}\left(V_1 \cdot V_2 \cdot |Y_{21}| \cdot \sin(\delta_2 - \zeta_{21}) + V_2^2 \cdot |Y_{22}| \cdot \sin(-\zeta_{22}) + V_2 \cdot V_3 \cdot |Y_{23}| \cdot \sin(\delta_2 - \delta_3 - \zeta_{23}) + V_2 \cdot V_4 \cdot |Y_{24}| \cdot \sin(\delta_2 - \delta_4 - \zeta_{24})\right)$$

$J_{44} = 10.3241$

$$Q_{2C} := V_1 \cdot V_2 \cdot |Y_{21}| \cdot \sin(\delta_2 - \zeta_{21}) + V_2^2 \cdot |Y_{22}| \cdot \sin(-\zeta_{22}) + V_2 \cdot V_3 \cdot |Y_{23}| \cdot \sin(\delta_2 - \delta_3 - \zeta_{23}) + V_2 \cdot V_4 \cdot |Y_{24}| \cdot \sin(\delta_2 - \delta_4 - \zeta_{24})$$

$$J_{45} := \frac{\partial}{\partial V_3}\left(V_1 \cdot V_2 \cdot |Y_{21}| \cdot \sin(\delta_2 - \zeta_{21}) + V_2^2 \cdot |Y_{22}| \cdot \sin(-\zeta_{22}) + V_2 \cdot V_3 \cdot |Y_{23}| \cdot \sin(\delta_2 - \delta_3 - \zeta_{23}) + V_2 \cdot V_4 \cdot |Y_{24}| \cdot \sin(\delta_2 - \delta_4 - \zeta_{24}) \right)$$

$$J_{45} = -0.4679$$

$$Q_{3C} := V_1 \cdot V_3 \cdot |Y_{31}| \cdot \sin(\delta_3 - \zeta_{31}) + V_2 \cdot V_3 \cdot |Y_{32}| \cdot \sin(\delta_3 - \delta_2 - \zeta_{23}) + V_3^2 \cdot |Y_{33}| \cdot \sin(-\zeta_{33}) + V_3 \cdot V_4 \cdot |Y_{34}| \cdot \sin(\delta_3 - \delta_4 - \zeta_{34})$$

$$J_{51} := \frac{\partial}{\partial \delta_2}\left(V_1 \cdot V_3 \cdot |Y_{31}| \cdot \sin(\delta_3 - \zeta_{31}) + V_2 \cdot V_3 \cdot |Y_{32}| \cdot \sin(\delta_3 - \delta_2 - \zeta_{23}) + V_3^2 \cdot |Y_{33}| \cdot \sin(-\zeta_{33}) + V_3 \cdot V_4 \cdot |Y_{34}| \cdot \sin(\delta_3 - \delta_4 - \zeta_{34}) \right)$$

$$J_{51} = 0.0059$$

$$Q_{3C} := V_1 \cdot V_3 \cdot |Y_{31}| \cdot \sin(\delta_3 - \zeta_{31}) + V_2 \cdot V_3 \cdot |Y_{32}| \cdot \sin(\delta_3 - \delta_2 - \zeta_{23}) + V_3^2 \cdot |Y_{33}| \cdot \sin(-\zeta_{33}) + V_3 \cdot V_4 \cdot |Y_{34}| \cdot \sin(\delta_3 - \delta_4 - \zeta_{34})$$

$$J_{52} := \frac{\partial}{\partial \delta_3}\left(V_1 \cdot V_3 \cdot |Y_{31}| \cdot \sin(\delta_3 - \zeta_{31}) + V_2 \cdot V_3 \cdot |Y_{32}| \cdot \sin(\delta_3 - \delta_2 - \zeta_{23}) + V_3^2 \cdot |Y_{33}| \cdot \sin(-\zeta_{33}) + V_3 \cdot V_4 \cdot |Y_{34}| \cdot \sin(\delta_3 - \delta_4 - \zeta_{34}) \right)$$

$$J_{52} = -0.2058$$

$$Q_{3C} := V_1 \cdot V_3 \cdot |Y_{31}| \cdot \sin(\delta_3 - \zeta_{31}) + V_2 \cdot V_3 \cdot |Y_{32}| \cdot \sin(\delta_3 - \delta_2 - \zeta_{23}) + V_3^2 \cdot |Y_{33}| \cdot \sin(-\zeta_{33}) + V_3 \cdot V_4 \cdot |Y_{34}| \cdot \sin(\delta_3 - \delta_4 - \zeta_{34})$$

$$J_{53} := \frac{\partial}{\partial \delta_4}\left(V_1 \cdot V_3 \cdot |Y_{31}| \cdot \sin(\delta_3 - \zeta_{31}) + V_2 \cdot V_3 \cdot |Y_{32}| \cdot \sin(\delta_3 - \delta_2 - \zeta_{23}) + V_3^2 \cdot |Y_{33}| \cdot \sin(-\zeta_{33}) + V_3 \cdot V_4 \cdot |Y_{34}| \cdot \sin(\delta_3 - \delta_4 - \zeta_{34}) \right)$$

$$J_{53} = 0.1999$$

$$Q_{3C} := V_1 \cdot V_3 \cdot |Y_{31}| \cdot \sin(\delta_3 - \zeta_{31}) + V_2 \cdot V_3 \cdot |Y_{32}| \cdot \sin(\delta_3 - \delta_2 - \zeta_{23}) + V_3^2 \cdot |Y_{33}| \cdot \sin(-\zeta_{33}) + V_3 \cdot V_4 \cdot |Y_{34}| \cdot \sin(\delta_3 - \delta_4 - \zeta_{34})$$

$$J_{54} := \frac{\partial}{\partial V_2}\left(V_1 \cdot V_3 \cdot |Y_{31}| \cdot \sin(\delta_3 - \zeta_{31}) + V_2 \cdot V_3 \cdot |Y_{32}| \cdot \sin(\delta_3 - \delta_2 - \zeta_{23}) + V_3^2 \cdot |Y_{33}| \cdot \sin(-\zeta_{33}) + V_3 \cdot V_4 \cdot |Y_{34}| \cdot \sin(\delta_3 - \delta_4 - \zeta_{34}) \right)$$

$$J_{54} = -0.4679$$

$$Q_{3C} := V_1 \cdot V_3 \cdot |Y_{31}| \cdot \sin(\delta_3 - \zeta_{31}) + V_2 \cdot V_3 \cdot |Y_{32}| \cdot \sin(\delta_3 - \delta_2 - \zeta_{23}) + V_3^2 \cdot |Y_{33}| \cdot \sin(-\zeta_{33}) + V_3 \cdot V_4 \cdot |Y_{34}| \cdot \sin(\delta_3 - \delta_4 - \zeta_{34})$$

$$J_{55} := \frac{\partial}{\partial V_3}\left(V_1 \cdot V_3 \cdot |Y_{31}| \cdot \sin(\delta_3 - \zeta_{31}) + V_2 \cdot V_3 \cdot |Y_{32}| \cdot \sin(\delta_3 - \delta_2 - \zeta_{23}) + V_3^2 \cdot |Y_{33}| \cdot \sin(-\zeta_{33}) + V_3 \cdot V_4 \cdot |Y_{34}| \cdot \sin(\delta_3 - \delta_4 - \zeta_{34}) \right)$$

$$J_{55} = 10.3241$$

$$\text{Jacobian} := \begin{pmatrix} J_{11} & J_{12} & J_{13} & J_{14} & J_{15} \\ J_{21} & J_{22} & J_{23} & J_{24} & J_{25} \\ J_{31} & J_{32} & J_{33} & J_{34} & J_{35} \\ J_{41} & J_{42} & J_{43} & J_{44} & J_{45} \\ J_{51} & J_{52} & J_{53} & J_{54} & J_{55} \end{pmatrix}$$

$$\text{Jacobian} = \begin{pmatrix} 10.4639 & -0.4679 & 0 & 0.2058 & -0.0059 \\ -0.4679 & 10.4639 & -9.996 & -0.0059 & 0.2058 \\ 0 & -9.996 & 9.996 & 0 & -0.1999 \\ -0.2058 & 0.0059 & 0 & 10.3241 & -0.4679 \\ 0.0059 & -0.2058 & 0.1999 & -0.4679 & 10.3241 \end{pmatrix}$$

$$\text{IJacobian} := \begin{pmatrix} J_{11} & J_{12} & J_{13} & J_{14} & J_{15} \\ J_{21} & J_{22} & J_{23} & J_{24} & J_{25} \\ J_{31} & J_{32} & J_{33} & J_{34} & J_{35} \\ J_{41} & J_{42} & J_{43} & J_{44} & J_{45} \\ J_{51} & J_{52} & J_{53} & J_{54} & J_{55} \end{pmatrix}^{-1}$$

$$\text{IJacobian} = \begin{pmatrix} 0.1 & 0.1 & 0.1 & -0.0019 & -0.0001 \\ 0.1 & 2.2373 & 2.2373 & -0.0008 & -0.0013 \\ 0.1 & 2.2373 & 2.3373 & -0.0007 & 0.0007 \\ 0.0019 & 0.0008 & 0.0007 & 0.097 & 0.0044 \\ 0.0001 & 0.0013 & -0.0007 & 0.0044 & 0.097 \end{pmatrix}$$

$$\begin{pmatrix} \Delta\delta_2 \\ \Delta\delta_3 \\ \Delta\delta_4 \\ \Delta V_2 \\ \Delta V_3 \end{pmatrix} := \begin{pmatrix} J_{11} & J_{12} & J_{13} & J_{14} & J_{15} \\ J_{21} & J_{22} & J_{23} & J_{24} & J_{25} \\ J_{31} & J_{32} & J_{33} & J_{34} & J_{35} \\ J_{41} & J_{42} & J_{43} & J_{44} & J_{45} \\ J_{51} & J_{52} & J_{53} & J_{54} & J_{55} \end{pmatrix}^{-1} \cdot \begin{pmatrix} \Delta P_2 \\ \Delta P_3 \\ \Delta P_4 \\ \Delta Q_2 \\ \Delta Q_3 \end{pmatrix}$$

$$\begin{pmatrix} \Delta\delta_2 \\ \Delta\delta_3 \\ \Delta\delta_4 \\ \Delta V_2 \\ \Delta V_3 \end{pmatrix} = \begin{pmatrix} -0.0135 \\ -0.2984 \\ -0.3116 \\ 0.007 \\ 0.0072 \end{pmatrix}$$

125

$$V_{2MAG} := |V_{2.1}| + \Delta V_2$$

$$V_{3MAG} := |V_{3.1}| + \Delta V_3$$

$$V_{2MAG} = 1.007$$

$$V_{3MAG} = 1.0072$$

$$\delta_{2ANG} := \arg(V_{2.1}) + \Delta\delta_2$$

$$\delta_{3ANG} := \arg(V_{3.1}) + \Delta\delta_3$$

$$\delta_{2ANG} = -0.0135$$

$$\delta_{3ANG} = -0.2984$$

$$\delta_{4ANG} := \arg(V_{4.1}) + \Delta\delta_4$$

$$\delta_{4ANG} = -0.3116$$

$$V_{2.2} := V_{2MAG} \cdot (\cos(\delta_{2ANG}) + j \cdot \sin(\delta_{2ANG}))$$

$$V_{2.2} = 1.0069 - 0.0136i \qquad |V_{2.2}| = 1.007 \qquad \arg(V_{2.2}) = -0.0135$$

$$V_{3.2} := V_{3MAG} \cdot (\cos(\delta_{3ANG}) + j \cdot \sin(\delta_{3ANG}))$$

$$V_{3.2} = 0.9627 - 0.2961i$$

$$|V_{3.2}| = 1.0072 \qquad \arg(V_{3.2}) = -0.2984$$

$$V_{4.2} := V_{4MAG} \cdot (\cos(\delta_{4ANG}) + j \cdot \sin(\delta_{4ANG}))$$

$$V_{4.2} = 0.9518 - 0.3066i$$

$$|V_{4.2}| = 1 \qquad \arg(V_{4.2}) = -0.3116$$

$$V_2 := |V_{2.2}| \qquad \delta_2 := \arg(V_{2.2})$$

$$V_3 := |V_{3.2}| \qquad \delta_3 := \arg(V_{3.2})$$

$$V_4 := |V_{4.2}| \qquad \delta_4 := \arg(V_{4.2})$$

A.5 FIRST ITERATION

A.5.1 Specified powers

$P_{2S} := 0$ $\qquad P_{3S} := 0$

$Q_{2S} := 0$ $\qquad Q_{3S} := 0$ $\qquad P_{4S} := -0.133333$

A.5.2 Calculated powers

$$P_{2C} := V_1 \cdot V_2 \cdot |Y_{21}| \cdot \cos(\delta_2 - \zeta_{21}) + V_2^2 \cdot |Y_{22}| \cdot \cos(-\zeta_{22}) + V_2 \cdot V_3 \cdot |Y_{23}| \cdot \cos(\delta_2 - \delta_3 - \zeta_{23}) + V_2 \cdot V_4 \cdot |Y_{24}| \cdot \cos(\delta_2 - \delta_4 - \zeta_{24})$$

$P_{2C} = -0.0006$

$$Q_{2C} := V_1 \cdot V_2 \cdot |Y_{21}| \cdot \sin(\delta_2 - \zeta_{21}) + V_2^2 \cdot |Y_{22}| \cdot \sin(-\zeta_{22}) + V_2 \cdot V_3 \cdot |Y_{23}| \cdot \sin(\delta_2 - \delta_3 - \zeta_{23}) + V_2 \cdot V_4 \cdot |Y_{24}| \cdot \sin(\delta_2 - \delta_4 - \zeta_{24})$$

$Q_{2C} = 0.0206$

$$P_{3C} := V_1 \cdot V_3 \cdot |Y_{31}| \cdot \cos(\delta_3 - \zeta_{31}) + V_2 \cdot V_3 \cdot |Y_{32}| \cdot \cos(\delta_3 - \delta_2 - \zeta_{32}) + V_3^2 \cdot |Y_{33}| \cdot \cos(-\zeta_{33}) + V_4 \cdot V_3 \cdot |Y_{34}| \cdot \cos(\delta_3 - \delta_4 - \zeta_{34})$$

$P_{3C} = 0.0011$

$$Q_{3C} := V_1 \cdot V_3 \cdot |Y_{31}| \cdot \sin(\delta_3 - \zeta_{31}) + V_2 \cdot V_3 \cdot |Y_{32}| \cdot \sin(\delta_3 - \delta_2 - \zeta_{32}) + V_3^2 \cdot |Y_{33}| \cdot \sin(-\zeta_{33}) + V_4 \cdot V_3 \cdot |Y_{34}| \cdot \sin(\delta_3 - \delta_4 - \zeta_{34})$$

$Q_{3C} = 0.0205$

$$P_{4C} := V_1 \cdot V_4 \cdot |Y_{41}| \cdot \cos(\delta_4 - \zeta_{41}) + V_2 \cdot V_4 \cdot |Y_{42}| \cdot \cos(\delta_4 - \delta_2 - \zeta_{42}) + V_3 \cdot V_4 \cdot |Y_{43}| \cdot \cos(\delta_4 - \delta_3 - \zeta_{43}) + V_4^2 \cdot |Y_{44}| \cdot \cos(-\zeta_{44})$$

$P_{4C} = -0.1343$

$\Delta P_2 := P_{2S} - P_{2C}$ $\qquad \Delta Q_2 := Q_{2S} - Q_{2C}$ $\qquad \Delta P_3 := P_{3S} - P_{3C}$

$\Delta P_2 = 0.0006$ $\qquad \Delta Q_2 = -0.0206$ $\qquad \Delta P_3 = -0.0011$

$\Delta P_4 := P_{4S} - P_{4C}$ $\qquad \Delta Q_3 := Q_{3S} - Q_{3C}$

$\Delta P_4 = 0.0009$ $\qquad \Delta Q_3 = -0.0205$

A.5.3 Jacobian Matrix

$$P_{2C} := V_1 \cdot V_2 \cdot |Y_{21}| \cdot \cos(\delta_2 - \zeta_{21}) + V_2^2 \cdot |Y_{22}| \cdot \cos(-\zeta_{22}) + V_2 \cdot V_3 \cdot |Y_{23}| \cdot \cos(\delta_2 - \delta_3 - \zeta_{23}) + V_2 \cdot V_4 \cdot |Y_{24}| \cdot \cos(\delta_2 - \delta_4 - \zeta_{24})$$

$$J_{11} := \frac{\partial}{\partial \delta_2} \left(V_1 \cdot V_2 \cdot |Y_{21}| \cdot \cos(\delta_2 - \zeta_{21}) + V_2^2 \cdot |Y_{22}| \cdot \cos(-\zeta_{22}) + V_2 \cdot V_3 \cdot |Y_{23}| \cdot \cos(\delta_2 - \delta_3 - \zeta_{23}) + V_2 \cdot V_4 \cdot |Y_{24}| \cdot \cos(\delta_2 - \delta_4 - \zeta_{24}) \right)$$

$$J_{11} = 10.5194$$

$$P_{2C} := V_1 \cdot V_2 \cdot |Y_{21}| \cdot \cos(\delta_2 - \zeta_{21}) + V_2^2 \cdot |Y_{22}| \cdot \cos(-\zeta_{22}) + V_2 \cdot V_3 \cdot |Y_{23}| \cdot \cos(\delta_2 - \delta_3 - \zeta_{23}) + V_2 \cdot V_4 \cdot |Y_{24}| \cdot \cos(\delta_2 - \delta_4 - \zeta_{24})$$

$$J_{12} := \frac{\partial}{\partial \delta_3} \left(V_1 \cdot V_2 \cdot |Y_{21}| \cdot \cos(\delta_2 - \zeta_{21}) + V_2^2 \cdot |Y_{22}| \cdot \cos(-\zeta_{22}) + V_2 \cdot V_3 \cdot |Y_{23}| \cdot \cos(\delta_2 - \delta_3 - \zeta_{23}) + V_2 \cdot V_4 \cdot |Y_{24}| \cdot \cos(\delta_2 - \delta_4 - \zeta_{24}) \right)$$

$$J_{12} = -0.4571$$

$$P_{2C} := V_1 \cdot V_2 \cdot |Y_{21}| \cdot \cos(\delta_2 - \zeta_{21}) + V_2^2 \cdot |Y_{22}| \cdot \cos(-\zeta_{22}) + V_2 \cdot V_3 \cdot |Y_{23}| \cdot \cos(\delta_2 - \delta_3 - \zeta_{23}) + V_2 \cdot V_4 \cdot |Y_{24}| \cdot \cos(\delta_2 - \delta_4 - \zeta_{24})$$

$$J_{13} := \frac{\partial}{\partial \delta_4} \left(V_1 \cdot V_2 \cdot |Y_{21}| \cdot \cos(\delta_2 - \zeta_{21}) + V_2^2 \cdot |Y_{22}| \cdot \cos(-\zeta_{22}) + V_2 \cdot V_3 \cdot |Y_{23}| \cdot \cos(\delta_2 - \delta_3 - \zeta_{23}) + V_2 \cdot V_4 \cdot |Y_{24}| \cdot \cos(\delta_2 - \delta_4 - \zeta_{24}) \right)$$

$$J_{13} = 0$$

$$P_{2C} := V_1 \cdot V_2 \cdot |Y_{21}| \cdot \cos(\delta_2 - \zeta_{21}) + V_2^2 \cdot |Y_{22}| \cdot \cos(-\zeta_{22}) + V_2 \cdot V_3 \cdot |Y_{23}| \cdot \cos(\delta_2 - \delta_3 - \zeta_{23}) + V_2 \cdot V_4 \cdot |Y_{24}| \cdot \cos(\delta_2 - \delta_4 - \zeta_{24})$$

$$J_{14} := \frac{\partial}{\partial V_2} \left(V_1 \cdot V_2 \cdot |Y_{21}| \cdot \cos(\delta_2 - \zeta_{21}) + V_2^2 \cdot |Y_{22}| \cdot \cos(-\zeta_{22}) + V_2 \cdot V_3 \cdot |Y_{23}| \cdot \cos(\delta_2 - \delta_3 - \zeta_{23}) + V_2 \cdot V_4 \cdot |Y_{24}| \cdot \cos(\delta_2 - \delta_4 - \zeta_{24}) \right)$$

$$J_{14} = 0.2067$$

$$P_{2C} := V_1 \cdot V_2 \cdot |Y_{21}| \cdot \cos(\delta_2 - \zeta_{21}) + V_2^2 \cdot |Y_{22}| \cdot \cos(-\zeta_{22}) + V_2 \cdot V_3 \cdot |Y_{23}| \cdot \cos(\delta_2 - \delta_3 - \zeta_{23}) + V_2 \cdot V_4 \cdot |Y_{24}| \cdot \cos(\delta_2 - \delta_4 - \zeta_{24})$$

$$J_{15} := \frac{\partial}{\partial V_3} \left(V_1 \cdot V_2 \cdot |Y_{21}| \cdot \cos(\delta_2 - \zeta_{21}) + V_2^2 \cdot |Y_{22}| \cdot \cos(-\zeta_{22}) + V_2 \cdot V_3 \cdot |Y_{23}| \cdot \cos(\delta_2 - \delta_3 - \zeta_{23}) + V_2 \cdot V_4 \cdot |Y_{24}| \cdot \cos(\delta_2 - \delta_4 - \zeta_{24}) \right)$$

$$J_{15} = 0.1267$$

$$P_{3C} := V_1 \cdot V_3 \cdot |Y_{31}| \cdot \cos(\delta_3 - \zeta_{31}) + V_2 \cdot V_3 \cdot |Y_{32}| \cdot \cos(\delta_3 - \delta_2 - \zeta_{32}) + V_3^2 \cdot |Y_{33}| \cdot \cos(-\zeta_{33}) + V_4 \cdot V_3 \cdot |Y_{34}| \cdot \cos(\delta_3 - \delta_4 - \zeta_{34})$$

$$J_{21} := \frac{\partial}{\partial \delta_2} \left(V_1 \cdot V_3 \cdot |Y_{31}| \cdot \cos(\delta_3 - \zeta_{31}) + V_2 \cdot V_3 \cdot |Y_{32}| \cdot \cos(\delta_3 - \delta_2 - \zeta_{32}) + V_3^2 \cdot |Y_{33}| \cdot \cos(-\zeta_{33}) + V_4 \cdot V_3 \cdot |Y_{34}| \cdot \cos(\delta_3 - \delta_4 - \zeta_{34}) \right)$$

$$J_{21} = -0.4537$$

$$P_{3C} := V_1 \cdot V_3 \cdot |Y_{31}| \cdot \cos(\delta_3 - \zeta_{31}) + V_2 \cdot V_3 \cdot |Y_{32}| \cdot \cos(\delta_3 - \delta_2 - \zeta_{32}) + V_3^2 \cdot |Y_{33}| \cdot \cos(-\zeta_{33}) + V_4 \cdot V_3 \cdot |Y_{34}| \cdot \cos(\delta_3 - \delta_4 - \zeta_{34})$$

$$J_{22} := \frac{\partial}{\partial \delta_3}\left(V_1 \cdot V_3 \cdot |Y_{31}| \cdot \cos(\delta_3 - \zeta_{31}) + V_2 \cdot V_3 \cdot |Y_{32}| \cdot \cos(\delta_3 - \delta_2 - \zeta_{32}) + V_3^2 \cdot |Y_{33}| \cdot \cos(-\zeta_{33}) + V_4 \cdot V_3 \cdot |Y_{34}| \cdot \cos(\delta_3 - \delta_4 - \zeta_{34})\right)$$

$$J_{22} = 10.5233$$

$$P_{3C} := V_1 \cdot V_3 \cdot |Y_{31}| \cdot \cos(\delta_3 - \zeta_{31}) + V_2 \cdot V_3 \cdot |Y_{32}| \cdot \cos(\delta_3 - \delta_2 - \zeta_{32}) + V_3^2 \cdot |Y_{33}| \cdot \cos(-\zeta_{33}) + V_4 \cdot V_3 \cdot |Y_{34}| \cdot \cos(\delta_3 - \delta_4 - \zeta_{34})$$

$$J_{23} := \frac{\partial}{\partial \delta_4}\left(V_1 \cdot V_3 \cdot |Y_{31}| \cdot \cos(\delta_3 - \zeta_{31}) + V_2 \cdot V_3 \cdot |Y_{32}| \cdot \cos(\delta_3 - \delta_2 - \zeta_{32}) + V_3^2 \cdot |Y_{33}| \cdot \cos(-\zeta_{33}) + V_4 \cdot V_3 \cdot |Y_{34}| \cdot \cos(\delta_3 - \delta_4 - \zeta_{34})\right)$$

$$J_{23} = -10.0696$$

$$P_{3C} := V_1 \cdot V_3 \cdot |Y_{31}| \cdot \cos(\delta_3 - \zeta_{31}) + V_2 \cdot V_3 \cdot |Y_{32}| \cdot \cos(\delta_3 - \delta_2 - \zeta_{32}) + V_3^2 \cdot |Y_{33}| \cdot \cos(-\zeta_{33}) + V_4 \cdot V_3 \cdot |Y_{34}| \cdot \cos(\delta_3 - \delta_4 - \zeta_{34})$$

$$J_{24} := \frac{\partial}{\partial V_2}\left(V_1 \cdot V_3 \cdot |Y_{31}| \cdot \cos(\delta_3 - \zeta_{31}) + V_2 \cdot V_3 \cdot |Y_{32}| \cdot \cos(\delta_3 - \delta_2 - \zeta_{32}) + V_3^2 \cdot |Y_{33}| \cdot \cos(-\zeta_{33}) + V_4 \cdot V_3 \cdot |Y_{34}| \cdot \cos(\delta_3 - \delta_4 - \zeta_{34})\right)$$

$$J_{24} = -0.1382$$

$$P_{3C} := V_1 \cdot V_3 \cdot |Y_{31}| \cdot \cos(\delta_3 - \zeta_{31}) + V_2 \cdot V_3 \cdot |Y_{32}| \cdot \cos(\delta_3 - \delta_2 - \zeta_{32}) + V_3^2 \cdot |Y_{33}| \cdot \cos(-\zeta_{33}) + V_4 \cdot V_3 \cdot |Y_{34}| \cdot \cos(\delta_3 - \delta_4 - \zeta_{34})$$

$$J_{25} := \frac{\partial}{\partial V_3}\left(V_1 \cdot V_3 \cdot |Y_{31}| \cdot \cos(\delta_3 - \zeta_{31}) + V_2 \cdot V_3 \cdot |Y_{32}| \cdot \cos(\delta_3 - \delta_2 - \zeta_{32}) + V_3^2 \cdot |Y_{33}| \cdot \cos(-\zeta_{33}) + V_4 \cdot V_3 \cdot |Y_{34}| \cdot \cos(\delta_3 - \delta_4 - \zeta_{34})\right)$$

$$J_{25} = 0.2084$$

$$P_{4C} := V_1 \cdot V_4 \cdot |Y_{41}| \cdot \cos(\delta_4 - \zeta_{41}) + V_2 \cdot V_4 \cdot |Y_{42}| \cdot \cos(\delta_4 - \delta_2 - \zeta_{42}) + V_3 \cdot V_4 \cdot |Y_{43}| \cdot \cos(\delta_4 - \delta_3 - \zeta_{43}) + V_4^2 \cdot |Y_{44}| \cdot \cos(-\zeta_{44})$$

$$J_{31} := \frac{\partial}{\partial \delta_2}\left(V_1 \cdot V_4 \cdot |Y_{41}| \cdot \cos(\delta_4 - \zeta_{41}) + V_2 \cdot V_4 \cdot |Y_{42}| \cdot \cos(\delta_4 - \delta_2 - \zeta_{42}) + V_3 \cdot V_4 \cdot |Y_{43}| \cdot \cos(\delta_4 - \delta_3 - \zeta_{43}) + V_4^2 \cdot |Y_{44}| \cdot \cos(-\zeta_{44})\right)$$

$$J_{31} = 0$$

$$P_{4C} := V_1 \cdot V_4 \cdot |Y_{41}| \cdot \cos(\delta_4 - \zeta_{41}) + V_2 \cdot V_4 \cdot |Y_{42}| \cdot \cos(\delta_4 - \delta_2 - \zeta_{42}) + V_3 \cdot V_4 \cdot |Y_{43}| \cdot \cos(\delta_4 - \delta_3 - \zeta_{43}) + V_4^2 \cdot |Y_{44}| \cdot \cos(-\zeta_{44})$$

$$J_{32} := \frac{\partial}{\partial \delta_3}\left(V_1 \cdot V_4 \cdot |Y_{41}| \cdot \cos(\delta_4 - \zeta_{41}) + V_2 \cdot V_4 \cdot |Y_{42}| \cdot \cos(\delta_4 - \delta_2 - \zeta_{42}) + V_3 \cdot V_4 \cdot |Y_{43}| \cdot \cos(\delta_4 - \delta_3 - \zeta_{43}) + V_4^2 \cdot |Y_{44}| \cdot \cos(-\zeta_{44})\right)$$

$$J_{32} = -10.0642$$

$$P_{4C} := V_1 \cdot V_4 \cdot |Y_{41}| \cdot \cos(\delta_4 - \zeta_{41}) + V_2 \cdot V_4 \cdot |Y_{42}| \cdot \cos(\delta_4 - \delta_2 - \zeta_{42}) + V_3 \cdot V_4 \cdot |Y_{43}| \cdot \cos(\delta_4 - \delta_3 - \zeta_{43}) + V_4^2 \cdot |Y_{44}| \cdot \cos(-\zeta_{44})$$

$$J_{33} := \frac{\partial}{\partial \delta_4}\left(V_1 \cdot V_4 \cdot |Y_{41}| \cdot \cos(\delta_4 - \zeta_{41}) + V_2 \cdot V_4 \cdot |Y_{42}| \cdot \cos(\delta_4 - \delta_2 - \zeta_{42}) + V_3 \cdot V_4 \cdot |Y_{43}| \cdot \cos(\delta_4 - \delta_3 - \zeta_{43}) + V_4^2 \cdot |Y_{44}| \cdot \cos(-\zeta_{44})\right)$$

$$J_{33} = 10.0642$$

$$P_{4C} := V_1 \cdot V_4 \cdot |Y_{41}| \cdot \cos(\delta_4 - \zeta_{41}) + V_2 \cdot V_4 \cdot |Y_{42}| \cdot \cos(\delta_4 - \delta_2 - \zeta_{42}) + V_3 \cdot V_4 \cdot |Y_{43}| \cdot \cos(\delta_4 - \delta_3 - \zeta_{43}) + V_4{}^2 \cdot |Y_{44}| \cdot \cos(-\zeta_{44})$$

$$J_{34} := \frac{\partial}{\partial V_2}\left(V_1 \cdot V_4 \cdot |Y_{41}| \cdot \cos(\delta_4 - \zeta_{41}) + V_2 \cdot V_4 \cdot |Y_{42}| \cdot \cos(\delta_4 - \delta_2 - \zeta_{42}) + V_3 \cdot V_4 \cdot |Y_{43}| \cdot \cos(\delta_4 - \delta_3 - \zeta_{43}) + V_4{}^2 \cdot |Y_{44}| \cdot \cos(-\zeta_{44})\right)$$

$$J_{34} = 0$$

$$P_{4C} := V_1 \cdot V_4 \cdot |Y_{41}| \cdot \cos(\delta_4 - \zeta_{41}) + V_2 \cdot V_4 \cdot |Y_{42}| \cdot \cos(\delta_4 - \delta_2 - \zeta_{42}) + V_3 \cdot V_4 \cdot |Y_{43}| \cdot \cos(\delta_4 - \delta_3 - \zeta_{43}) + V_4{}^2 \cdot |Y_{44}| \cdot \cos(-\zeta_{44})$$

$$J_{35} := \frac{\partial}{\partial V_3}\left(V_1 \cdot V_4 \cdot |Y_{41}| \cdot \cos(\delta_4 - \zeta_{41}) + V_2 \cdot V_4 \cdot |Y_{42}| \cdot \cos(\delta_4 - \delta_2 - \zeta_{42}) + V_3 \cdot V_4 \cdot |Y_{43}| \cdot \cos(\delta_4 - \delta_3 - \zeta_{43}) + V_4{}^2 \cdot |Y_{44}| \cdot \cos(-\zeta_{44})\right)$$

$$J_{35} = -0.3318$$

$$Q_{2C} := V_1 \cdot V_2 \cdot |Y_{21}| \cdot \sin(\delta_2 - \zeta_{21}) + V_2{}^2 \cdot |Y_{22}| \cdot \sin(-\zeta_{22}) + V_2 \cdot V_3 \cdot |Y_{23}| \cdot \sin(\delta_2 - \delta_3 - \zeta_{23}) + V_2 \cdot V_4 \cdot |Y_{24}| \cdot \sin(\delta_2 - \delta_4 - \zeta_{24})$$

$$J_{41} := \frac{\partial}{\partial \delta_2}\left(V_1 \cdot V_2 \cdot |Y_{21}| \cdot \sin(\delta_2 - \zeta_{21}) + V_2{}^2 \cdot |Y_{22}| \cdot \sin(-\zeta_{22}) + V_2 \cdot V_3 \cdot |Y_{23}| \cdot \sin(\delta_2 - \delta_3 - \zeta_{23}) + V_2 \cdot V_4 \cdot |Y_{24}| \cdot \sin(\delta_2 - \delta_4 - \zeta_{24})\right)$$

$$J_{41} = -0.2093$$

$$Q_{2C} := V_1 \cdot V_2 \cdot |Y_{21}| \cdot \sin(\delta_2 - \zeta_{21}) + V_2{}^2 \cdot |Y_{22}| \cdot \sin(-\zeta_{22}) + V_2 \cdot V_3 \cdot |Y_{23}| \cdot \sin(\delta_2 - \delta_3 - \zeta_{23}) + V_2 \cdot V_4 \cdot |Y_{24}| \cdot \sin(\delta_2 - \delta_4 - \zeta_{24})$$

$$J_{42} := \frac{\partial}{\partial \delta_3}\left(V_1 \cdot V_2 \cdot |Y_{21}| \cdot \sin(\delta_2 - \zeta_{21}) + V_2{}^2 \cdot |Y_{22}| \cdot \sin(-\zeta_{22}) + V_2 \cdot V_3 \cdot |Y_{23}| \cdot \sin(\delta_2 - \delta_3 - \zeta_{23}) + V_2 \cdot V_4 \cdot |Y_{24}| \cdot \sin(\delta_2 - \delta_4 - \zeta_{24})\right)$$

$$J_{42} = -0.1277$$

$$Q_{2C} := V_1 \cdot V_2 \cdot |Y_{21}| \cdot \sin(\delta_2 - \zeta_{21}) + V_2{}^2 \cdot |Y_{22}| \cdot \sin(-\zeta_{22}) + V_2 \cdot V_3 \cdot |Y_{23}| \cdot \sin(\delta_2 - \delta_3 - \zeta_{23}) + V_2 \cdot V_4 \cdot |Y_{24}| \cdot \sin(\delta_2 - \delta_4 - \zeta_{24})$$

$$J_{43} := \frac{\partial}{\partial \delta_4}\left(V_1 \cdot V_2 \cdot |Y_{21}| \cdot \sin(\delta_2 - \zeta_{21}) + V_2{}^2 \cdot |Y_{22}| \cdot \sin(-\zeta_{22}) + V_2 \cdot V_3 \cdot |Y_{23}| \cdot \sin(\delta_2 - \delta_3 - \zeta_{23}) + V_2 \cdot V_4 \cdot |Y_{24}| \cdot \sin(\delta_2 - \delta_4 - \zeta_{24})\right)$$

$$J_{43} = 0$$

$$Q_{2C} := V_1 \cdot V_2 \cdot |Y_{21}| \cdot \sin(\delta_2 - \zeta_{21}) + V_2{}^2 \cdot |Y_{22}| \cdot \sin(-\zeta_{22}) + V_2 \cdot V_3 \cdot |Y_{23}| \cdot \sin(\delta_2 - \delta_3 - \zeta_{23}) + V_2 \cdot V_4 \cdot |Y_{24}| \cdot \sin(\delta_2 - \delta_4 - \zeta_{24})$$

$$J_{44} := \frac{\partial}{\partial V_2}\left(V_1 \cdot V_2 \cdot |Y_{21}| \cdot \sin(\delta_2 - \zeta_{21}) + V_2{}^2 \cdot |Y_{22}| \cdot \sin(-\zeta_{22}) + V_2 \cdot V_3 \cdot |Y_{23}| \cdot \sin(\delta_2 - \delta_3 - \zeta_{23}) + V_2 \cdot V_4 \cdot |Y_{24}| \cdot \sin(\delta_2 - \delta_4 - \zeta_{24})\right)$$

$$J_{44} = 10.4871$$

$$Q_{2C} := V_1 \cdot V_2 \cdot \left|Y_{21}\right| \cdot \sin(\delta_2 - \zeta_{21}) + V_2^2 \cdot \left|Y_{22}\right| \cdot \sin(-\zeta_{22}) + V_2 \cdot V_3 \cdot \left|Y_{23}\right| \cdot \sin(\delta_2 - \delta_3 - \zeta_{23}) + V_2 \cdot V_4 \cdot \left|Y_{24}\right| \cdot \sin(\delta_2 - \delta_4 - \zeta_{24})$$

$$J_{45} := \frac{\partial}{\partial V_3}\left(V_1 \cdot V_2 \cdot \left|Y_{21}\right| \cdot \sin(\delta_2 - \zeta_{21}) + V_2^2 \cdot \left|Y_{22}\right| \cdot \sin(-\zeta_{22}) + V_2 \cdot V_3 \cdot \left|Y_{23}\right| \cdot \sin(\delta_2 - \delta_3 - \zeta_{23}) + V_2 \cdot V_4 \cdot \left|Y_{24}\right| \cdot \sin(\delta_2 - \delta_4 - \zeta_{24})\right)$$

$$J_{45} = -0.4538$$

$$Q_{3C} := V_1 \cdot V_3 \cdot \left|Y_{31}\right| \cdot \sin(\delta_3 - \zeta_{31}) + V_2 \cdot V_3 \cdot \left|Y_{32}\right| \cdot \sin(\delta_3 - \delta_2 - \zeta_{23}) + V_3^2 \cdot \left|Y_{33}\right| \cdot \sin(-\zeta_{33}) + V_3 \cdot V_4 \cdot \left|Y_{34}\right| \cdot \sin(\delta_3 - \delta_4 - \zeta_{34})$$

$$J_{51} := \frac{\partial}{\partial \delta_2}\left(V_1 \cdot V_3 \cdot \left|Y_{31}\right| \cdot \sin(\delta_3 - \zeta_{31}) + V_2 \cdot V_3 \cdot \left|Y_{32}\right| \cdot \sin(\delta_3 - \delta_2 - \zeta_{23}) + V_3^2 \cdot \left|Y_{33}\right| \cdot \sin(-\zeta_{33}) + V_3 \cdot V_4 \cdot \left|Y_{34}\right| \cdot \sin(\delta_3 - \delta_4 - \zeta_{34})\right)$$

$$J_{51} = 0.1392$$

$$Q_{3C} := V_1 \cdot V_3 \cdot \left|Y_{31}\right| \cdot \sin(\delta_3 - \zeta_{31}) + V_2 \cdot V_3 \cdot \left|Y_{32}\right| \cdot \sin(\delta_3 - \delta_2 - \zeta_{23}) + V_3^2 \cdot \left|Y_{33}\right| \cdot \sin(-\zeta_{33}) + V_3 \cdot V_4 \cdot \left|Y_{34}\right| \cdot \sin(\delta_3 - \delta_4 - \zeta_{34})$$

$$J_{52} := \frac{\partial}{\partial \delta_3}\left(V_1 \cdot V_3 \cdot \left|Y_{31}\right| \cdot \sin(\delta_3 - \zeta_{31}) + V_2 \cdot V_3 \cdot \left|Y_{32}\right| \cdot \sin(\delta_3 - \delta_2 - \zeta_{23}) + V_3^2 \cdot \left|Y_{33}\right| \cdot \sin(-\zeta_{33}) + V_3 \cdot V_4 \cdot \left|Y_{34}\right| \cdot \sin(\delta_3 - \delta_4 - \zeta_{34})\right)$$

$$J_{52} = -0.2077$$

$$Q_{3C} := V_1 \cdot V_3 \cdot \left|Y_{31}\right| \cdot \sin(\delta_3 - \zeta_{31}) + V_2 \cdot V_3 \cdot \left|Y_{32}\right| \cdot \sin(\delta_3 - \delta_2 - \zeta_{23}) + V_3^2 \cdot \left|Y_{33}\right| \cdot \sin(-\zeta_{33}) + V_3 \cdot V_4 \cdot \left|Y_{34}\right| \cdot \sin(\delta_3 - \delta_4 - \zeta_{34})$$

$$J_{53} := \frac{\partial}{\partial \delta_4}\left(V_1 \cdot V_3 \cdot \left|Y_{31}\right| \cdot \sin(\delta_3 - \zeta_{31}) + V_2 \cdot V_3 \cdot \left|Y_{32}\right| \cdot \sin(\delta_3 - \delta_2 - \zeta_{23}) + V_3^2 \cdot \left|Y_{33}\right| \cdot \sin(-\zeta_{33}) + V_3 \cdot V_4 \cdot \left|Y_{34}\right| \cdot \sin(\delta_3 - \delta_4 - \zeta_{34})\right)$$

$$J_{53} = 0.0685$$

$$Q_{3C} := V_1 \cdot V_3 \cdot \left|Y_{31}\right| \cdot \sin(\delta_3 - \zeta_{31}) + V_2 \cdot V_3 \cdot \left|Y_{32}\right| \cdot \sin(\delta_3 - \delta_2 - \zeta_{23}) + V_3^2 \cdot \left|Y_{33}\right| \cdot \sin(-\zeta_{33}) + V_3 \cdot V_4 \cdot \left|Y_{34}\right| \cdot \sin(\delta_3 - \delta_4 - \zeta_{34})$$

$$J_{54} := \frac{\partial}{\partial V_2}\left(V_1 \cdot V_3 \cdot \left|Y_{31}\right| \cdot \sin(\delta_3 - \zeta_{31}) + V_2 \cdot V_3 \cdot \left|Y_{32}\right| \cdot \sin(\delta_3 - \delta_2 - \zeta_{23}) + V_3^2 \cdot \left|Y_{33}\right| \cdot \sin(-\zeta_{33}) + V_3 \cdot V_4 \cdot \left|Y_{34}\right| \cdot \sin(\delta_3 - \delta_4 - \zeta_{34})\right)$$

$$J_{54} = -0.4506$$

$$Q_{3C} := V_1 \cdot V_3 \cdot \left|Y_{31}\right| \cdot \sin(\delta_3 - \zeta_{31}) + V_2 \cdot V_3 \cdot \left|Y_{32}\right| \cdot \sin(\delta_3 - \delta_2 - \zeta_{23}) + V_3^2 \cdot \left|Y_{33}\right| \cdot \sin(-\zeta_{33}) + V_3 \cdot V_4 \cdot \left|Y_{34}\right| \cdot \sin(\delta_3 - \delta_4 - \zeta_{34})$$

$$J_{55} := \frac{\partial}{\partial V_3}\left(V_1 \cdot V_3 \cdot \left|Y_{31}\right| \cdot \sin(\delta_3 - \zeta_{31}) + V_2 \cdot V_3 \cdot \left|Y_{32}\right| \cdot \sin(\delta_3 - \delta_2 - \zeta_{23}) + V_3^2 \cdot \left|Y_{33}\right| \cdot \sin(-\zeta_{33}) + V_3 \cdot V_4 \cdot \left|Y_{34}\right| \cdot \sin(\delta_3 - \delta_4 - \zeta_{34})\right)$$

$$J_{55} = 10.489$$

$$\text{Jacobian} := \begin{pmatrix} J_{11} & J_{12} & J_{13} & J_{14} & J_{15} \\ J_{21} & J_{22} & J_{23} & J_{24} & J_{25} \\ J_{31} & J_{32} & J_{33} & J_{34} & J_{35} \\ J_{41} & J_{42} & J_{43} & J_{44} & J_{45} \\ J_{51} & J_{52} & J_{53} & J_{54} & J_{55} \end{pmatrix}$$

$$\text{Jacobian} = \begin{pmatrix} 10.5194 & -0.4571 & 0 & 0.2067 & 0.1267 \\ -0.4537 & 10.5233 & -10.0696 & -0.1382 & 0.2084 \\ 0 & -10.0642 & 10.0642 & 0 & -0.3318 \\ -0.2093 & -0.1277 & 0 & 10.4871 & -0.4538 \\ 0.1392 & -0.2077 & 0.0685 & -0.4506 & 10.489 \end{pmatrix}$$

$$\text{IJacobian} := \begin{pmatrix} J_{11} & J_{12} & J_{13} & J_{14} & J_{15} \\ J_{21} & J_{22} & J_{23} & J_{24} & J_{25} \\ J_{31} & J_{32} & J_{33} & J_{34} & J_{35} \\ J_{41} & J_{42} & J_{43} & J_{44} & J_{45} \\ J_{51} & J_{52} & J_{53} & J_{54} & J_{55} \end{pmatrix}^{-1}$$

$$\text{IJacobian} = \begin{pmatrix} 0.0994 & 0.0999 & 0.1 & -0.0006 & -0.0001 \\ 0.1004 & 2.3219 & 2.3229 & 0.0298 & 0.0274 \\ 0.1004 & 2.3229 & 2.4233 & 0.0299 & 0.0306 \\ 0.0032 & 0.0316 & 0.0316 & 0.0959 & 0.0045 \\ 0.0002 & 0.0308 & 0.0302 & 0.0045 & 0.0959 \end{pmatrix}$$

$$\begin{pmatrix} \Delta\delta_2 \\ \Delta\delta_3 \\ \Delta\delta_4 \\ \Delta V_2 \\ \Delta V_3 \end{pmatrix} := \begin{pmatrix} J_{11} & J_{12} & J_{13} & J_{14} & J_{15} \\ J_{21} & J_{22} & J_{23} & J_{24} & J_{25} \\ J_{31} & J_{32} & J_{33} & J_{34} & J_{35} \\ J_{41} & J_{42} & J_{43} & J_{44} & J_{45} \\ J_{51} & J_{52} & J_{53} & J_{54} & J_{55} \end{pmatrix}^{-1} \begin{pmatrix} \Delta P_2 \\ \Delta P_3 \\ \Delta P_4 \\ \Delta Q_2 \\ \Delta Q_3 \end{pmatrix}$$

$$\begin{pmatrix} \Delta\delta_2 \\ \Delta\delta_3 \\ \Delta\delta_4 \\ \Delta V_2 \\ \Delta V_3 \end{pmatrix} = \begin{pmatrix} 0.0001 \\ -0.0016 \\ -0.0016 \\ -0.0021 \\ -0.0021 \end{pmatrix}$$

132

$V_{2MAG} := |V_{2.2}| + \Delta V_2$

$V_{3MAG} := |V_{3.2}| + \Delta V_3$

$V_{2MAG} = 1.0049$

$V_{3MAG} = 1.0051$

$\delta_{2ANG} := \arg(V_{2.2}) + \Delta\delta_2$

$\delta_{3ANG} := \arg(V_{3.2}) + \Delta\delta_3$

$\delta_{2ANG} = -0.0134$

$\delta_{3ANG} = -0.3001$

$\delta_{4ANG} := \arg(V_{4.2}) + \Delta\delta_4$

$\delta_{4ANG} = -0.3132$

$V_{2.3} := V_{2MAG}(\cos(\delta_{2ANG}) + j \cdot \sin(\delta_{2ANG}))$

$V_{2.3} = 1.0048 - 0.0135i$ $\qquad |V_{2.3}| = 1.0049$ $\qquad \arg(V_{2.3}) = -0.0134$

$V_{3.3} := V_{3MAG}(\cos(\delta_{3ANG}) + j \cdot \sin(\delta_{3ANG}))$

$V_{3.3} = 0.9602 - 0.2971i$

$\qquad\qquad |V_{3.3}| = 1.0051$ $\qquad \arg(V_{3.3}) = -0.3001$

$V_{4.3} := V_{4MAG}(\cos(\delta_{4ANG}) + j \cdot \sin(\delta_{4ANG}))$

$V_{4.3} = 0.9513 - 0.3081i$

$\qquad\qquad |V_{4.3}| = 1$ $\qquad \arg(V_{4.3}) = -0.3132$

$V_2 := |V_{2.3}|$ $\qquad\qquad \delta_2 := \arg(V_{2.3})$

$V_3 := |V_{3.3}|$ $\qquad\qquad \delta_3 := \arg(V_{3.3})$

$V_4 := |V_{4.3}|$ $\qquad\qquad \delta_4 := \arg(V_{4.3})$

A.6. SECOND ITERATION

A.6.1 Specified powers

$$P_{2S} := 0 \qquad P_{3S} := 0$$

$$Q_{2S} := 0 \qquad Q_{3S} := 0 \qquad P_{4S} := -0.133333$$

A.6.2 Calculated powers

$$P_{2C} := V_1 \cdot V_2 \cdot |Y_{21}| \cdot \cos(\delta_2 - \zeta_{21}) + V_2^2 \cdot |Y_{22}| \cdot \cos(-\zeta_{22}) + V_2 \cdot V_3 \cdot |Y_{23}| \cdot \cos(\delta_2 - \delta_3 - \zeta_{23}) + V_2 \cdot V_4 \cdot |Y_{24}| \cdot \cos(\delta_2 - \delta_4 - \zeta_{24})$$

$$P_{2C} = -0$$

$$Q_{2C} := V_1 \cdot V_2 \cdot |Y_{21}| \cdot \sin(\delta_2 - \zeta_{21}) + V_2^2 \cdot |Y_{22}| \cdot \sin(-\zeta_{22}) + V_2 \cdot V_3 \cdot |Y_{23}| \cdot \sin(\delta_2 - \delta_3 - \zeta_{23}) + V_2 \cdot V_4 \cdot |Y_{24}| \cdot \sin(\delta_2 - \delta_4 - \zeta_{24})$$

$$Q_{2C} = 0$$

$$P_{3C} := V_1 \cdot V_3 \cdot |Y_{31}| \cdot \cos(\delta_3 - \zeta_{31}) + V_2 \cdot V_3 \cdot |Y_{32}| \cdot \cos(\delta_3 - \delta_2 - \zeta_{32}) + V_3^2 \cdot |Y_{33}| \cdot \cos(-\zeta_{33}) + V_4 \cdot V_3 \cdot |Y_{34}| \cdot \cos(\delta_3 - \delta_4 - \zeta_{34})$$

$$P_{3C} = 0$$

$$Q_{3C} := V_1 \cdot V_3 \cdot |Y_{31}| \cdot \sin(\delta_3 - \zeta_{31}) + V_2 \cdot V_3 \cdot |Y_{32}| \cdot \sin(\delta_3 - \delta_2 - \zeta_{32}) + V_3^2 \cdot |Y_{33}| \cdot \sin(-\zeta_{33}) + V_4 \cdot V_3 \cdot |Y_{34}| \cdot \sin(\delta_3 - \delta_4 - \zeta_{34})$$

$$Q_{3C} = 0$$

$$P_{4C} := V_1 \cdot V_4 \cdot |Y_{41}| \cdot \cos(\delta_4 - \zeta_{41}) + V_2 \cdot V_4 \cdot |Y_{42}| \cdot \cos(\delta_4 - \delta_2 - \zeta_{42}) + V_3 \cdot V_4 \cdot |Y_{43}| \cdot \cos(\delta_4 - \delta_3 - \zeta_{43}) + V_4^2 \cdot |Y_{44}| \cdot \cos(-\zeta_{44})$$

$$P_{4C} = -0.1333$$

$$\Delta P_2 := P_{2S} - P_{2C} \qquad \Delta Q_2 := Q_{2S} - Q_{2C} \qquad \Delta P_3 := P_{3S} - P_{3C}$$

$$\Delta P_2 = 0 \qquad \Delta Q_2 = -0 \qquad \Delta P_3 = -0$$

$$\Delta P_4 := P_{4S} - P_{4C} \qquad \Delta Q_3 := Q_{3S} - Q_{3C}$$

$$\Delta P_4 = 0 \qquad \Delta Q_3 = -0$$

A.6.3 Jacobian Matrix

$$P_{2C} := V_1 \cdot V_2 \cdot |Y_{21}| \cdot \cos(\delta_2 - \zeta_{21}) + V_2^2 \cdot |Y_{22}| \cdot \cos(-\zeta_{22}) + V_2 \cdot V_3 \cdot |Y_{23}| \cdot \cos(\delta_2 - \delta_3 - \zeta_{23}) + V_2 \cdot V_4 \cdot |Y_{24}| \cdot \cos(\delta_2 - \delta_4 - \zeta_{24})$$

$$J_{11} := \frac{\partial}{\partial \delta_2} \left(V_1 \cdot V_2 \cdot |Y_{21}| \cdot \cos(\delta_2 - \zeta_{21}) + V_2^2 \cdot |Y_{22}| \cdot \cos(-\zeta_{22}) + V_2 \cdot V_3 \cdot |Y_{23}| \cdot \cos(\delta_2 - \delta_3 - \zeta_{23}) + V_2 \cdot V_4 \cdot |Y_{24}| \cdot \cos(\delta_2 - \delta_4 - \zeta_{24}) \right)$$

$$J_{11} = 10.4967$$

$$P_{2C} := V_1 \cdot V_2 \cdot |Y_{21}| \cdot \cos(\delta_2 - \zeta_{21}) + V_2^2 \cdot |Y_{22}| \cdot \cos(-\zeta_{22}) + V_2 \cdot V_3 \cdot |Y_{23}| \cdot \cos(\delta_2 - \delta_3 - \zeta_{23}) + V_2 \cdot V_4 \cdot |Y_{24}| \cdot \cos(\delta_2 - \delta_4 - \zeta_{24})$$

$$J_{12} := \frac{\partial}{\partial \delta_3} \left(V_1 \cdot V_2 \cdot |Y_{21}| \cdot \cos(\delta_2 - \zeta_{21}) + V_2^2 \cdot |Y_{22}| \cdot \cos(-\zeta_{22}) + V_2 \cdot V_3 \cdot |Y_{23}| \cdot \cos(\delta_2 - \delta_3 - \zeta_{23}) + V_2 \cdot V_4 \cdot |Y_{24}| \cdot \cos(\delta_2 - \delta_4 - \zeta_{24}) \right)$$

$$J_{12} = -0.455$$

$$P_{2C} := V_1 \cdot V_2 \cdot |Y_{21}| \cdot \cos(\delta_2 - \zeta_{21}) + V_2^2 \cdot |Y_{22}| \cdot \cos(-\zeta_{22}) + V_2 \cdot V_3 \cdot |Y_{23}| \cdot \cos(\delta_2 - \delta_3 - \zeta_{23}) + V_2 \cdot V_4 \cdot |Y_{24}| \cdot \cos(\delta_2 - \delta_4 - \zeta_{24})$$

$$J_{13} := \frac{\partial}{\partial \delta_4} \left(V_1 \cdot V_2 \cdot |Y_{21}| \cdot \cos(\delta_2 - \zeta_{21}) + V_2^2 \cdot |Y_{22}| \cdot \cos(-\zeta_{22}) + V_2 \cdot V_3 \cdot |Y_{23}| \cdot \cos(\delta_2 - \delta_3 - \zeta_{23}) + V_2 \cdot V_4 \cdot |Y_{24}| \cdot \cos(\delta_2 - \delta_4 - \zeta_{24}) \right)$$

$$J_{13} = 0$$

$$P_{2C} := V_1 \cdot V_2 \cdot |Y_{21}| \cdot \cos(\delta_2 - \zeta_{21}) + V_2^2 \cdot |Y_{22}| \cdot \cos(-\zeta_{22}) + V_2 \cdot V_3 \cdot |Y_{23}| \cdot \cos(\delta_2 - \delta_3 - \zeta_{23}) + V_2 \cdot V_4 \cdot |Y_{24}| \cdot \cos(\delta_2 - \delta_4 - \zeta_{24})$$

$$J_{14} := \frac{\partial}{\partial V_2} \left(V_1 \cdot V_2 \cdot |Y_{21}| \cdot \cos(\delta_2 - \zeta_{21}) + V_2^2 \cdot |Y_{22}| \cdot \cos(-\zeta_{22}) + V_2 \cdot V_3 \cdot |Y_{23}| \cdot \cos(\delta_2 - \delta_3 - \zeta_{23}) + V_2 \cdot V_4 \cdot |Y_{24}| \cdot \cos(\delta_2 - \delta_4 - \zeta_{24}) \right)$$

$$J_{14} = 0.2068$$

$$P_{2C} := V_1 \cdot V_2 \cdot |Y_{21}| \cdot \cos(\delta_2 - \zeta_{21}) + V_2^2 \cdot |Y_{22}| \cdot \cos(-\zeta_{22}) + V_2 \cdot V_3 \cdot |Y_{23}| \cdot \cos(\delta_2 - \delta_3 - \zeta_{23}) + V_2 \cdot V_4 \cdot |Y_{24}| \cdot \cos(\delta_2 - \delta_4 - \zeta_{24})$$

$$J_{15} := \frac{\partial}{\partial V_3} \left(V_1 \cdot V_2 \cdot |Y_{21}| \cdot \cos(\delta_2 - \zeta_{21}) + V_2^2 \cdot |Y_{22}| \cdot \cos(-\zeta_{22}) + V_2 \cdot V_3 \cdot |Y_{23}| \cdot \cos(\delta_2 - \delta_3 - \zeta_{23}) + V_2 \cdot V_4 \cdot |Y_{24}| \cdot \cos(\delta_2 - \delta_4 - \zeta_{24}) \right)$$

$$J_{15} = 0.1272$$

$$P_{3C} := V_1 \cdot V_3 \cdot |Y_{31}| \cdot \cos(\delta_3 - \zeta_{31}) + V_2 \cdot V_3 \cdot |Y_{32}| \cdot \cos(\delta_3 - \delta_2 - \zeta_{32}) + V_3^2 \cdot |Y_{33}| \cdot \cos(-\zeta_{33}) + V_4 \cdot V_3 \cdot |Y_{34}| \cdot \cos(\delta_3 - \delta_4 - \zeta_{34})$$

$$J_{21} := \frac{\partial}{\partial \delta_2} \left(V_1 \cdot V_3 \cdot |Y_{31}| \cdot \cos(\delta_3 - \zeta_{31}) + V_2 \cdot V_3 \cdot |Y_{32}| \cdot \cos(\delta_3 - \delta_2 - \zeta_{32}) + V_3^2 \cdot |Y_{33}| \cdot \cos(-\zeta_{33}) + V_4 \cdot V_3 \cdot |Y_{34}| \cdot \cos(\delta_3 - \delta_4 - \zeta_{34}) \right)$$

$$J_{21} = -0.4516$$

$$P_{3C} := V_1 \cdot V_3 \cdot |Y_{31}| \cos(\delta_3 - \zeta_{31}) + V_2 \cdot V_3 \cdot |Y_{32}| \cdot \cos(\delta_3 - \delta_2 - \zeta_{32}) + V_3^2 \cdot |Y_{33}| \cdot \cos(-\zeta_{33}) + V_4 \cdot V_3 \cdot |Y_{34}| \cdot \cos(\delta_3 - \delta_4 - \zeta_{34})$$

$$J_{22} := \frac{\partial}{\partial \delta_3} \left(V_1 \cdot V_3 \cdot |Y_{31}| \cos(\delta_3 - \zeta_{31}) + V_2 \cdot V_3 \cdot |Y_{32}| \cdot \cos(\delta_3 - \delta_2 - \zeta_{32}) + V_3^2 \cdot |Y_{33}| \cdot \cos(-\zeta_{33}) + V_4 \cdot V_3 \cdot |Y_{34}| \cdot \cos(\delta_3 - \delta_4 - \zeta_{34}) \right)$$

$$J_{22} = 10.5005$$

$$P_{3C} := V_1 \cdot V_3 \cdot |Y_{31}| \cos(\delta_3 - \zeta_{31}) + V_2 \cdot V_3 \cdot |Y_{32}| \cdot \cos(\delta_3 - \delta_2 - \zeta_{32}) + V_3^2 \cdot |Y_{33}| \cdot \cos(-\zeta_{33}) + V_4 \cdot V_3 \cdot |Y_{34}| \cdot \cos(\delta_3 - \delta_4 - \zeta_{34})$$

$$J_{23} := \frac{\partial}{\partial \delta_4} \left(V_1 \cdot V_3 \cdot |Y_{31}| \cos(\delta_3 - \zeta_{31}) + V_2 \cdot V_3 \cdot |Y_{32}| \cdot \cos(\delta_3 - \delta_2 - \zeta_{32}) + V_3^2 \cdot |Y_{33}| \cdot \cos(-\zeta_{33}) + V_4 \cdot V_3 \cdot |Y_{34}| \cdot \cos(\delta_3 - \delta_4 - \zeta_{34}) \right)$$

$$J_{23} = -10.0489$$

$$P_{3C} := V_1 \cdot V_3 \cdot |Y_{31}| \cos(\delta_3 - \zeta_{31}) + V_2 \cdot V_3 \cdot |Y_{32}| \cdot \cos(\delta_3 - \delta_2 - \zeta_{32}) + V_3^2 \cdot |Y_{33}| \cdot \cos(-\zeta_{33}) + V_4 \cdot V_3 \cdot |Y_{34}| \cdot \cos(\delta_3 - \delta_4 - \zeta_{34})$$

$$J_{24} := \frac{\partial}{\partial V_2} \left(V_1 \cdot V_3 \cdot |Y_{31}| \cos(\delta_3 - \zeta_{31}) + V_2 \cdot V_3 \cdot |Y_{32}| \cdot \cos(\delta_3 - \delta_2 - \zeta_{32}) + V_3^2 \cdot |Y_{33}| \cdot \cos(-\zeta_{33}) + V_4 \cdot V_3 \cdot |Y_{34}| \cdot \cos(\delta_3 - \delta_4 - \zeta_{34}) \right)$$

$$J_{24} = -0.1387$$

$$P_{3C} := V_1 \cdot V_3 \cdot |Y_{31}| \cos(\delta_3 - \zeta_{31}) + V_2 \cdot V_3 \cdot |Y_{32}| \cdot \cos(\delta_3 - \delta_2 - \zeta_{32}) + V_3^2 \cdot |Y_{33}| \cdot \cos(-\zeta_{33}) + V_4 \cdot V_3 \cdot |Y_{34}| \cdot \cos(\delta_3 - \delta_4 - \zeta_{34})$$

$$J_{25} := \frac{\partial}{\partial V_3} \left(V_1 \cdot V_3 \cdot |Y_{31}| \cos(\delta_3 - \zeta_{31}) + V_2 \cdot V_3 \cdot |Y_{32}| \cdot \cos(\delta_3 - \delta_2 - \zeta_{32}) + V_3^2 \cdot |Y_{33}| \cdot \cos(-\zeta_{33}) + V_4 \cdot V_3 \cdot |Y_{34}| \cdot \cos(\delta_3 - \delta_4 - \zeta_{34}) \right)$$

$$J_{25} = 0.2069$$

$$P_{4C} := V_1 \cdot V_4 \cdot |Y_{41}| \cdot \cos(\delta_4 - \zeta_{41}) + V_2 \cdot V_4 \cdot |Y_{42}| \cdot \cos(\delta_4 - \delta_2 - \zeta_{42}) + V_3 \cdot V_4 \cdot |Y_{43}| \cdot \cos(\delta_4 - \delta_3 - \zeta_{43}) + V_4^2 \cdot |Y_{44}| \cdot \cos(-\zeta_{44})$$

$$J_{31} := \frac{\partial}{\partial \delta_2} \left(V_1 \cdot V_4 \cdot |Y_{41}| \cdot \cos(\delta_4 - \zeta_{41}) + V_2 \cdot V_4 \cdot |Y_{42}| \cdot \cos(\delta_4 - \delta_2 - \zeta_{42}) + V_3 \cdot V_4 \cdot |Y_{43}| \cdot \cos(\delta_4 - \delta_3 - \zeta_{43}) + V_4^2 \cdot |Y_{44}| \cdot \cos(-\zeta_{44}) \right)$$

$$J_{31} = 0$$

$$P_{4C} := V_1 \cdot V_4 \cdot |Y_{41}| \cdot \cos(\delta_4 - \zeta_{41}) + V_2 \cdot V_4 \cdot |Y_{42}| \cdot \cos(\delta_4 - \delta_2 - \zeta_{42}) + V_3 \cdot V_4 \cdot |Y_{43}| \cdot \cos(\delta_4 - \delta_3 - \zeta_{43}) + V_4^2 \cdot |Y_{44}| \cdot \cos(-\zeta_{44})$$

$$J_{32} := \frac{\partial}{\partial \delta_3} \left(V_1 \cdot V_4 \cdot |Y_{41}| \cdot \cos(\delta_4 - \zeta_{41}) + V_2 \cdot V_4 \cdot |Y_{42}| \cdot \cos(\delta_4 - \delta_2 - \zeta_{42}) + V_3 \cdot V_4 \cdot |Y_{43}| \cdot \cos(\delta_4 - \delta_3 - \zeta_{43}) + V_4^2 \cdot |Y_{44}| \cdot \cos(-\zeta_{44}) \right)$$

$$J_{32} = -10.0436$$

$$P_{4C} := V_1 \cdot V_4 \cdot |Y_{41}| \cdot \cos(\delta_4 - \zeta_{41}) + V_2 \cdot V_4 \cdot |Y_{42}| \cdot \cos(\delta_4 - \delta_2 - \zeta_{42}) + V_3 \cdot V_4 \cdot |Y_{43}| \cdot \cos(\delta_4 - \delta_3 - \zeta_{43}) + V_4^2 \cdot |Y_{44}| \cdot \cos(-\zeta_{44})$$

$$J_{33} := \frac{\partial}{\partial \delta_4}\left(V_1 \cdot V_4 \cdot |Y_{41}| \cdot \cos(\delta_4 - \zeta_{41}) + V_2 \cdot V_4 \cdot |Y_{42}| \cdot \cos(\delta_4 - \delta_2 - \zeta_{42}) + V_3 \cdot V_4 \cdot |Y_{43}| \cdot \cos(\delta_4 - \delta_3 - \zeta_{43}) + V_4^2 \cdot |Y_{44}| \cdot \cos(-\zeta_{44})\right)$$

$$J_{33} = 10.0436$$

$$P_{4C} := V_1 \cdot V_4 \cdot |Y_{41}| \cdot \cos(\delta_4 - \zeta_{41}) + V_2 \cdot V_4 \cdot |Y_{42}| \cdot \cos(\delta_4 - \delta_2 - \zeta_{42}) + V_3 \cdot V_4 \cdot |Y_{43}| \cdot \cos(\delta_4 - \delta_3 - \zeta_{43}) + V_4^2 \cdot |Y_{44}| \cdot \cos(-\zeta_{44})$$

$$J_{34} := \frac{\partial}{\partial V_2}\left(V_1 \cdot V_4 \cdot |Y_{41}| \cdot \cos(\delta_4 - \zeta_{41}) + V_2 \cdot V_4 \cdot |Y_{42}| \cdot \cos(\delta_4 - \delta_2 - \zeta_{42}) + V_3 \cdot V_4 \cdot |Y_{43}| \cdot \cos(\delta_4 - \delta_3 - \zeta_{43}) + V_4^2 \cdot |Y_{44}| \cdot \cos(-\zeta_{44})\right)$$

$$J_{34} = 0$$

$$P_{4C} := V_1 \cdot V_4 \cdot |Y_{41}| \cdot \cos(\delta_4 - \zeta_{41}) + V_2 \cdot V_4 \cdot |Y_{42}| \cdot \cos(\delta_4 - \delta_2 - \zeta_{42}) + V_3 \cdot V_4 \cdot |Y_{43}| \cdot \cos(\delta_4 - \delta_3 - \zeta_{43}) + V_4^2 \cdot |Y_{44}| \cdot \cos(-\zeta_{44})$$

$$J_{35} := \frac{\partial}{\partial V_3}\left(V_1 \cdot V_4 \cdot |Y_{41}| \cdot \cos(\delta_4 - \zeta_{41}) + V_2 \cdot V_4 \cdot |Y_{42}| \cdot \cos(\delta_4 - \delta_2 - \zeta_{42}) + V_3 \cdot V_4 \cdot |Y_{43}| \cdot \cos(\delta_4 - \delta_3 - \zeta_{43}) + V_4^2 \cdot |Y_{44}| \cdot \cos(-\zeta_{44})\right)$$

$$J_{35} = -0.3316$$

$$Q_{2C} := V_1 \cdot V_2 \cdot |Y_{21}| \cdot \sin(\delta_2 - \zeta_{21}) + V_2^2 \cdot |Y_{22}| \cdot \sin(-\zeta_{22}) + V_2 \cdot V_3 \cdot |Y_{23}| \cdot \sin(\delta_2 - \delta_3 - \zeta_{23}) + V_2 \cdot V_4 \cdot |Y_{24}| \cdot \sin(\delta_2 - \delta_4 - \zeta_{24})$$

$$J_{41} := \frac{\partial}{\partial \delta_2}\left(V_1 \cdot V_2 \cdot |Y_{21}| \cdot \sin(\delta_2 - \zeta_{21}) + V_2^2 \cdot |Y_{22}| \cdot \sin(-\zeta_{22}) + V_2 \cdot V_3 \cdot |Y_{23}| \cdot \sin(\delta_2 - \delta_3 - \zeta_{23}) + V_2 \cdot V_4 \cdot |Y_{24}| \cdot \sin(\delta_2 - \delta_4 - \zeta_{24})\right)$$

$$J_{41} = -0.2079$$

$$Q_{2C} := V_1 \cdot V_2 \cdot |Y_{21}| \cdot \sin(\delta_2 - \zeta_{21}) + V_2^2 \cdot |Y_{22}| \cdot \sin(-\zeta_{22}) + V_2 \cdot V_3 \cdot |Y_{23}| \cdot \sin(\delta_2 - \delta_3 - \zeta_{23}) + V_2 \cdot V_4 \cdot |Y_{24}| \cdot \sin(\delta_2 - \delta_4 - \zeta_{24})$$

$$J_{42} := \frac{\partial}{\partial \delta_3}\left(V_1 \cdot V_2 \cdot |Y_{21}| \cdot \sin(\delta_2 - \zeta_{21}) + V_2^2 \cdot |Y_{22}| \cdot \sin(-\zeta_{22}) + V_2 \cdot V_3 \cdot |Y_{23}| \cdot \sin(\delta_2 - \delta_3 - \zeta_{23}) + V_2 \cdot V_4 \cdot |Y_{24}| \cdot \sin(\delta_2 - \delta_4 - \zeta_{24})\right)$$

$$J_{42} = -0.1279$$

$$Q_{2C} := V_1 \cdot V_2 \cdot |Y_{21}| \cdot \sin(\delta_2 - \zeta_{21}) + V_2^2 \cdot |Y_{22}| \cdot \sin(-\zeta_{22}) + V_2 \cdot V_3 \cdot |Y_{23}| \cdot \sin(\delta_2 - \delta_3 - \zeta_{23}) + V_2 \cdot V_4 \cdot |Y_{24}| \cdot \sin(\delta_2 - \delta_4 - \zeta_{24})$$

$$J_{43} := \frac{\partial}{\partial \delta_4}\left(V_1 \cdot V_2 \cdot |Y_{21}| \cdot \sin(\delta_2 - \zeta_{21}) + V_2^2 \cdot |Y_{22}| \cdot \sin(-\zeta_{22}) + V_2 \cdot V_3 \cdot |Y_{23}| \cdot \sin(\delta_2 - \delta_3 - \zeta_{23}) + V_2 \cdot V_4 \cdot |Y_{24}| \cdot \sin(\delta_2 - \delta_4 - \zeta_{24})\right)$$

$$J_{43} = 0$$

$$Q_{2C} := V_1 \cdot V_2 \cdot |Y_{21}| \cdot \sin(\delta_2 - \zeta_{21}) + V_2^2 \cdot |Y_{22}| \cdot \sin(-\zeta_{22}) + V_2 \cdot V_3 \cdot |Y_{23}| \cdot \sin(\delta_2 - \delta_3 - \zeta_{23}) + V_2 \cdot V_4 \cdot |Y_{24}| \cdot \sin(\delta_2 - \delta_4 - \zeta_{24})$$

$$J_{44} := \frac{\partial}{\partial V_2}\left(V_1 \cdot V_2 \cdot |Y_{21}| \cdot \sin(\delta_2 - \zeta_{21}) + V_2^2 \cdot |Y_{22}| \cdot \sin(-\zeta_{22}) + V_2 \cdot V_3 \cdot |Y_{23}| \cdot \sin(\delta_2 - \delta_3 - \zeta_{23}) + V_2 \cdot V_4 \cdot |Y_{24}| \cdot \sin(\delta_2 - \delta_4 - \zeta_{24})\right)$$

$$J_{44} = 10.4453$$

$$Q_{2C} := V_1 \cdot V_2 \cdot \left| Y_{21} \right| \cdot \sin\left(\delta_2 - \zeta_{21} \right) + V_2{}^2 \cdot \left| Y_{22} \right| \cdot \sin\left(-\zeta_{22} \right) + V_2 \cdot V_3 \cdot \left| Y_{23} \right| \cdot \sin\left(\delta_2 - \delta_3 - \zeta_{23} \right) + V_2 \cdot V_4 \cdot \left| Y_{24} \right| \cdot \sin\left(\delta_2 - \delta_4 - \zeta_{24} \right)$$

$$J_{45} := \frac{\partial}{\partial V_3} \left(V_1 \cdot V_2 \cdot \left| Y_{21} \right| \cdot \sin\left(\delta_2 - \zeta_{21} \right) + V_2{}^2 \cdot \left| Y_{22} \right| \cdot \sin\left(-\zeta_{22} \right) + V_2 \cdot V_3 \cdot \left| Y_{23} \right| \cdot \sin\left(\delta_2 - \delta_3 - \zeta_{23} \right) + V_2 \cdot V_4 \cdot \left| Y_{24} \right| \cdot \sin\left(\delta_2 - \delta_4 - \zeta_{24} \right) \right)$$

$$J_{45} = -0.4527$$

$$Q_{3C} := V_1 \cdot V_3 \cdot \left| Y_{31} \right| \cdot \sin\left(\delta_3 - \zeta_{31} \right) + V_2 \cdot V_3 \cdot \left| Y_{32} \right| \cdot \sin\left(\delta_3 - \delta_2 - \zeta_{23} \right) + V_3{}^2 \cdot \left| Y_{33} \right| \cdot \sin\left(-\zeta_{33} \right) + V_3 \cdot V_4 \cdot \left| Y_{34} \right| \cdot \sin\left(\delta_3 - \delta_4 - \zeta_{34} \right)$$

$$J_{51} := \frac{\partial}{\partial \delta_2} \left(V_1 \cdot V_3 \cdot \left| Y_{31} \right| \cdot \sin\left(\delta_3 - \zeta_{31} \right) + V_2 \cdot V_3 \cdot \left| Y_{32} \right| \cdot \sin\left(\delta_3 - \delta_2 - \zeta_{23} \right) + V_3{}^2 \cdot \left| Y_{33} \right| \cdot \sin\left(-\zeta_{33} \right) + V_3 \cdot V_4 \cdot \left| Y_{34} \right| \cdot \sin\left(\delta_3 - \delta_4 - \zeta_{34} \right) \right)$$

$$J_{51} = 0.1393$$

$$Q_{3C} := V_1 \cdot V_3 \cdot \left| Y_{31} \right| \cdot \sin\left(\delta_3 - \zeta_{31} \right) + V_2 \cdot V_3 \cdot \left| Y_{32} \right| \cdot \sin\left(\delta_3 - \delta_2 - \zeta_{23} \right) + V_3{}^2 \cdot \left| Y_{33} \right| \cdot \sin\left(-\zeta_{33} \right) + V_3 \cdot V_4 \cdot \left| Y_{34} \right| \cdot \sin\left(\delta_3 - \delta_4 - \zeta_{34} \right)$$

$$J_{52} := \frac{\partial}{\partial \delta_3} \left(V_1 \cdot V_3 \cdot \left| Y_{31} \right| \cdot \sin\left(\delta_3 - \zeta_{31} \right) + V_2 \cdot V_3 \cdot \left| Y_{32} \right| \cdot \sin\left(\delta_3 - \delta_2 - \zeta_{23} \right) + V_3{}^2 \cdot \left| Y_{33} \right| \cdot \sin\left(-\zeta_{33} \right) + V_3 \cdot V_4 \cdot \left| Y_{34} \right| \cdot \sin\left(\delta_3 - \delta_4 - \zeta_{34} \right) \right)$$

$$J_{52} = -0.2079$$

$$Q_{3C} := V_1 \cdot V_3 \cdot \left| Y_{31} \right| \cdot \sin\left(\delta_3 - \zeta_{31} \right) + V_2 \cdot V_3 \cdot \left| Y_{32} \right| \cdot \sin\left(\delta_3 - \delta_2 - \zeta_{23} \right) + V_3{}^2 \cdot \left| Y_{33} \right| \cdot \sin\left(-\zeta_{33} \right) + V_3 \cdot V_4 \cdot \left| Y_{34} \right| \cdot \sin\left(\delta_3 - \delta_4 - \zeta_{34} \right)$$

$$J_{53} := \frac{\partial}{\partial \delta_4} \left(V_1 \cdot V_3 \cdot \left| Y_{31} \right| \cdot \sin\left(\delta_3 - \zeta_{31} \right) + V_2 \cdot V_3 \cdot \left| Y_{32} \right| \cdot \sin\left(\delta_3 - \delta_2 - \zeta_{23} \right) + V_3{}^2 \cdot \left| Y_{33} \right| \cdot \sin\left(-\zeta_{33} \right) + V_3 \cdot V_4 \cdot \left| Y_{34} \right| \cdot \sin\left(\delta_3 - \delta_4 - \zeta_{34} \right) \right)$$

$$J_{53} = 0.0686$$

$$Q_{3C} := V_1 \cdot V_3 \cdot \left| Y_{31} \right| \cdot \sin\left(\delta_3 - \zeta_{31} \right) + V_2 \cdot V_3 \cdot \left| Y_{32} \right| \cdot \sin\left(\delta_3 - \delta_2 - \zeta_{23} \right) + V_3{}^2 \cdot \left| Y_{33} \right| \cdot \sin\left(-\zeta_{33} \right) + V_3 \cdot V_4 \cdot \left| Y_{34} \right| \cdot \sin\left(\delta_3 - \delta_4 - \zeta_{34} \right)$$

$$J_{54} := \frac{\partial}{\partial V_2} \left(V_1 \cdot V_3 \cdot \left| Y_{31} \right| \cdot \sin\left(\delta_3 - \zeta_{31} \right) + V_2 \cdot V_3 \cdot \left| Y_{32} \right| \cdot \sin\left(\delta_3 - \delta_2 - \zeta_{23} \right) + V_3{}^2 \cdot \left| Y_{33} \right| \cdot \sin\left(-\zeta_{33} \right) + V_3 \cdot V_4 \cdot \left| Y_{34} \right| \cdot \sin\left(\delta_3 - \delta_4 - \zeta_{34} \right) \right)$$

$$J_{54} = -0.4494$$

$$Q_{3C} := V_1 \cdot V_3 \cdot \left| Y_{31} \right| \cdot \sin\left(\delta_3 - \zeta_{31} \right) + V_2 \cdot V_3 \cdot \left| Y_{32} \right| \cdot \sin\left(\delta_3 - \delta_2 - \zeta_{23} \right) + V_3{}^2 \cdot \left| Y_{33} \right| \cdot \sin\left(-\zeta_{33} \right) + V_3 \cdot V_4 \cdot \left| Y_{34} \right| \cdot \sin\left(\delta_3 - \delta_4 - \zeta_{34} \right)$$

$$J_{55} := \frac{\partial}{\partial V_3} \left(V_1 \cdot V_3 \cdot \left| Y_{31} \right| \cdot \sin\left(\delta_3 - \zeta_{31} \right) + V_2 \cdot V_3 \cdot \left| Y_{32} \right| \cdot \sin\left(\delta_3 - \delta_2 - \zeta_{23} \right) + V_3{}^2 \cdot \left| Y_{33} \right| \cdot \sin\left(-\zeta_{33} \right) + V_3 \cdot V_4 \cdot \left| Y_{34} \right| \cdot \sin\left(\delta_3 - \delta_4 - \zeta_{34} \right) \right)$$

$$J_{55} = 10.4472$$

138

$$\text{Jacobian} := \begin{pmatrix} J_{11} & J_{12} & J_{13} & J_{14} & J_{15} \\ J_{21} & J_{22} & J_{23} & J_{24} & J_{25} \\ J_{31} & J_{32} & J_{33} & J_{34} & J_{35} \\ J_{41} & J_{42} & J_{43} & J_{44} & J_{45} \\ J_{51} & J_{52} & J_{53} & J_{54} & J_{55} \end{pmatrix}$$

$$\text{Jacobian} = \begin{pmatrix} 10.4967 & -0.455 & 0 & 0.2068 & 0.1272 \\ -0.4516 & 10.5005 & -10.0489 & -0.1387 & 0.2069 \\ 0 & -10.0436 & 10.0436 & 0 & -0.3316 \\ -0.2079 & -0.1279 & 0 & 10.4453 & -0.4527 \\ 0.1393 & -0.2079 & 0.0686 & -0.4494 & 10.4472 \end{pmatrix}$$

$$\text{IJacobian} := \begin{pmatrix} J_{11} & J_{12} & J_{13} & J_{14} & J_{15} \\ J_{21} & J_{22} & J_{23} & J_{24} & J_{25} \\ J_{31} & J_{32} & J_{33} & J_{34} & J_{35} \\ J_{41} & J_{42} & J_{43} & J_{44} & J_{45} \\ J_{51} & J_{52} & J_{53} & J_{54} & J_{55} \end{pmatrix}^{-1}$$

$$\text{IJacobian} = \begin{pmatrix} 0.0996 & 0.1001 & 0.1002 & -0.0006 & -0 \\ 0.1006 & 2.3327 & 2.3337 & 0.0302 & 0.028 \\ 0.1006 & 2.3337 & 2.4343 & 0.0303 & 0.0311 \\ 0.0032 & 0.0319 & 0.0319 & 0.0963 & 0.0045 \\ 0.0002 & 0.0311 & 0.0305 & 0.0046 & 0.0963 \end{pmatrix}$$

$$\begin{pmatrix} \Delta\delta_2 \\ \Delta\delta_3 \\ \Delta\delta_4 \\ \Delta V_2 \\ \Delta V_3 \end{pmatrix} := \begin{pmatrix} J_{11} & J_{12} & J_{13} & J_{14} & J_{15} \\ J_{21} & J_{22} & J_{23} & J_{24} & J_{25} \\ J_{31} & J_{32} & J_{33} & J_{34} & J_{35} \\ J_{41} & J_{42} & J_{43} & J_{44} & J_{45} \\ J_{51} & J_{52} & J_{53} & J_{54} & J_{55} \end{pmatrix}^{-1} \cdot \begin{pmatrix} \Delta P_2 \\ \Delta P_3 \\ \Delta P_4 \\ \Delta Q_2 \\ \Delta Q_3 \end{pmatrix}$$

$$\begin{pmatrix} \Delta\delta_2 \\ \Delta\delta_3 \\ \Delta\delta_4 \\ \Delta V_2 \\ \Delta V_3 \end{pmatrix} = \begin{pmatrix} -0 \\ -0 \\ -0 \\ -0 \\ -0 \end{pmatrix} \qquad \text{Tolerance is met}$$

139

$V_{2MAG} := |V_{2.3}| + \Delta V_2$

$V_{2MAG} = 1.0049$

$\delta_{2ANG} := \arg(V_{2.3}) + \Delta\delta_2$

$\delta_{2ANG} = -0.0134$

$\delta_{4ANG} := \arg(V_{4.3}) + \Delta\delta_4$

$\delta_{4ANG} = -0.3132$

$V_{3MAG} := |V_{3.3}| + \Delta V_3$

$V_{3MAG} = 1.0051$

$\delta_{3ANG} := \arg(V_{3.3}) + \Delta\delta_3$

$\delta_{3ANG} = -0.3001$

$V_{2.4} := V_{2MAG} \left(\cos(\delta_{2ANG}) + j\cdot\sin(\delta_{2ANG})\right)$

$V_{2.4} = 1.0048 - 0.0135i$ $\qquad |V_{2.4}| = 1.0049$ $\qquad \arg(V_{2.4}) = -0.0134$

$V_{3.4} := V_{3MAG} \left(\cos(\delta_{3ANG}) + j\cdot\sin(\delta_{3ANG})\right)$

$V_{3.4} = 0.9602 - 0.2971i$

$|V_{3.4}| = 1.0051$ $\qquad \arg(V_{3.4}) = -0.3001$

$V_{4.4} := V_{4MAG} \left(\cos(\delta_{4ANG}) + j\cdot\sin(\delta_{4ANG})\right)$

$V_{4.4} = 0.9513 - 0.3081i$

$|V_{4.4}| = 1$ $\qquad \arg(V_{4.4}) = -0.3132$

$V_2 := |V_{2.4}|$ $\qquad \delta_2 := \arg(V_{2.4})$

$V_3 := |V_{3.4}|$ $\qquad \delta_3 := \arg(V_{3.4})$

$V_4 := |V_{4.4}|$ $\qquad \delta_4 := \arg(V_{4.4})$

$V_1 = 1$ $\qquad$ $\delta_1 \dfrac{180}{\pi} = 0$

$V_2 = 1.0049$ $\qquad$ $\delta_2 \dfrac{180}{\pi} = -0.7693$

$V_3 = 1.0051$ $\qquad$ $\delta_3 \dfrac{180}{\pi} = -17.1924$

$V_4 = 1$ $\qquad$ $\delta_4 \dfrac{180}{\pi} = -17.9471$

A.7 Actual values

$V_{1act} := V_1 \cdot 345$

$V_{1act} = 345$

$V_{2act} := V_2 \cdot 500$

$V_{2act} = 502.4629$

$V_{3act} := V_3 \cdot 500$

$V_{3act} = 502.5547$

$V_{4act} := V_4 \cdot 230$

$V_{4act} = 230$

$\Delta\delta_{12} := \delta_1 - \delta_2$

$\Delta\delta_{23} := \delta_2 - \delta_3$

$\Delta\delta_{34} := \delta_3 - \delta_4$

A.7.1 BUS 1

$$P_{S12pu} := \frac{(|V_1|)^2}{|Z_{12}|} \cdot \cos(\arg(Z_{12})) - \frac{|V_1| \cdot |V_2|}{|Z_{12}|} \cdot \cos(\arg(Z_{12}) + \Delta\delta_{12})$$

$$P_{S12pu} = 0.1339$$

$$Q_{S12pu} := \frac{(|V_1|)^2}{|Z_{12}|} \cdot \sin(\arg(Z_{12})) - \frac{|V_1| \cdot |V_2|}{|Z_{12}|} \cdot \sin(\arg(Z_{12}) + \Delta\delta_{12})$$

$$Q_{S12pu} = -0.051$$

A.7.2 BUS 2

$$P_{S23pu} := \frac{(|V_2|)^2}{|Z_{23}|} \cdot \cos(\arg(Z_{23})) - \frac{|V_2| \cdot |V_3|}{|Z_{23}|} \cdot \cos(\arg(Z_{23}) + \Delta\delta_{23})$$

$$P_{S23pu} = 0.1339$$

$$Q_{S23pu} := \left[\frac{(|V_2|)^2}{|Z_{23}|} \cdot \sin(\arg(Z_{23})) - \frac{|V_2| \cdot |V_3|}{|Z_{23}|} \cdot \sin(\arg(Z_{23}) + \Delta\delta_{23}) \right]$$

$$Q_{S23pu} = 0.0175$$

$$Q_{CAP} := \left[\frac{(1.0049)^2}{\left(\frac{1}{0.0699} \right)} \right]$$

$$Q_{CAP} = -0.0706$$

$$Q_{Bus2total} := Q_{CAP} + Q_{S23pu}$$

$$Q_{Bus2total} = -0.0531$$

A.7.3 BUS 3

$$P_{S34pu} := \frac{\left(|V_3|\right)^2}{|Z_{34}|} \cdot \cos\left(\arg\left(Z_{34}\right)\right) - \frac{|V_3| \cdot |V_4|}{|Z_{34}|} \cdot \cos\left(\arg\left(Z_{34}\right) + \Delta\delta_{34}\right)$$

$$P_{S34pu} = 0.1334$$

$$Q_{S34pu} := \frac{\left(|V_3|\right)^2}{|Z_{34}|} \cdot \sin\left(\arg\left(Z_{34}\right)\right) - \frac{|V_3| \cdot |V_4|}{|Z_{34}|} \cdot \sin\left(\arg\left(Z_{34}\right) + \Delta\delta_{34}\right)$$

$$Q_{S34pu} = 0.0496$$

A.7.4 BUS 4

$$P_{R34pu} := \frac{|V_3| \cdot |V_4|}{|Z_{34}|} \cdot \cos\left(\arg\left(Z_{34}\right) - \Delta\delta_{34}\right) - \frac{\left(|V_4|\right)^2}{|Z_{34}|} \cdot \cos\left(\arg\left(Z_{34}\right)\right)$$

$$P_{R34pu} = 0.1333$$

$$Q_{R34pu} := \frac{|V_3| \cdot |V_4|}{|Z_{34}|} \cdot \sin\left(\arg\left(Z_{34}\right) - \Delta\delta_{34}\right) - \frac{\left(|V_4|\right)^2}{|Z_{34}|} \cdot \sin\left(\arg\left(Z_{34}\right)\right)$$

$$Q_{R34pu} = 0.0476$$

$P_{Bus1} := P_{S12pu} \cdot 1500$

$P_{Bus2} := P_{S23pu} \cdot 1500$

$P_{Bus1} = 200.8521$

$P_{Bus2} = 200.7905$

$Q_{Bus1} := Q_{S12pu} \cdot 1500$

$Q_{Bus2} := Q_{Bus2total} \cdot 1500$

$Q_{Bus1} = -76.5441$

$Q_{Bus2} = -79.6187$

$P_{Bus3} := P_{S34pu} \cdot 1500$

$P_{Bus4} := P_{R34pu} \cdot 1500$

$P_{Bus3} = 200.0596$

$P_{Bus4} = 199.9995$

$Q_{Bus3} := Q_{S34pu} \cdot 1500$

$Q_{Bus4} := Q_{R34pu} \cdot 1500$

$Q_{Bus3} = 74.3389$

$Q_{Bus4} = 71.333$

APPENDIX B

In Appendix B the same technique is used as that of Appendix A. The results obtained for the last iteration is shown from where the Jacobian matrix is constructed to the point where the final results are obtained.

B.1 Jacobian Matrix

$$\text{Jacobian} := \begin{pmatrix} J_{11} & J_{12} & J_{13} & J_{14} & J_{15} \\ J_{21} & J_{22} & J_{23} & J_{24} & J_{25} \\ J_{31} & J_{32} & J_{33} & J_{34} & J_{35} \\ J_{41} & J_{42} & J_{43} & J_{44} & J_{45} \\ J_{51} & J_{52} & J_{53} & J_{54} & J_{55} \end{pmatrix}$$

$$\text{Jacobian} = \begin{pmatrix} 10.2179 & -0.3193 & 0 & 0.2041 & 0.3341 \\ -0.3109 & 10.2275 & -9.9167 & -0.3423 & 0.2042 \\ 0 & -9.9033 & 9.9033 & 0 & -0.5376 \\ -0.2024 & -0.3314 & 0 & 10.3056 & -0.3219 \\ 0.3394 & -0.2025 & -0.1369 & -0.3135 & 10.3104 \end{pmatrix}$$

$$\text{IJacobian} := \begin{pmatrix} J_{11} & J_{12} & J_{13} & J_{14} & J_{15} \\ J_{21} & J_{22} & J_{23} & J_{24} & J_{25} \\ J_{31} & J_{32} & J_{33} & J_{34} & J_{35} \\ J_{41} & J_{42} & J_{43} & J_{44} & J_{45} \\ J_{51} & J_{52} & J_{53} & J_{54} & J_{55} \end{pmatrix}^{-1}$$

$$\text{IJacobian} := \begin{pmatrix} 0.1011 & 0.1057 & 0.1058 & 0.0015 & 0.0002 \\ 0.1075 & 3.583 & 3.5894 & 0.1204 & 0.1165 \\ 0.1075 & 3.5894 & 3.6969 & 0.1208 & 0.122 \\ 0.0055 & 0.121 & 0.1212 & 0.1012 & 0.0069 \\ 0.0004 & 0.1182 & 0.1198 & 0.007 & 0.1011 \end{pmatrix}$$

$$\begin{pmatrix} \Delta\delta_2 \\ \Delta\delta_3 \\ \Delta\delta_4 \\ \Delta V_2 \\ \Delta V_3 \end{pmatrix} := \begin{pmatrix} J_{11} & J_{12} & J_{13} & J_{14} & J_{15} \\ J_{21} & J_{22} & J_{23} & J_{24} & J_{25} \\ J_{31} & J_{32} & J_{33} & J_{34} & J_{35} \\ J_{41} & J_{42} & J_{43} & J_{44} & J_{45} \\ J_{51} & J_{52} & J_{53} & J_{54} & J_{55} \end{pmatrix}^{-1} \cdot \begin{pmatrix} \Delta P_2 \\ \Delta P_3 \\ \Delta P_4 \\ \Delta Q_2 \\ \Delta Q_3 \end{pmatrix}$$

$$\begin{pmatrix} \Delta\delta_2 \\ \Delta\delta_3 \\ \Delta\delta_4 \\ \Delta V_2 \\ \Delta V_3 \end{pmatrix} = \begin{pmatrix} -0 \\ -0.0001 \\ -0.0001 \\ -0 \\ -0 \end{pmatrix}$$

$V_{2MAG} := \left| V_{2.4} \right| + \Delta V_2$

$V_{2MAG} = 0.9915$

$\delta_{2ANG} := \arg\left(V_{2.4} \right) + \Delta\delta_2$

$\delta_{2ANG} = -0.0339$

$\delta_{4ANG} := \arg\left(V_{4.4} \right) + \Delta\delta_4$

$\delta_{4ANG} = -0.8843$

$V_{2.5} := V_{2MAG} \cdot \left(\cos\left(\delta_{2ANG} \right) + j \cdot \sin\left(\delta_{2ANG} \right) \right)$

$V_{2.5} = 0.9909 - 0.0336i \qquad \left| V_{2.5} \right| = 0.9915$

$V_{3.5} := V_{3MAG} \cdot \left(\cos\left(\delta_{3ANG} \right) + j \cdot \sin\left(\delta_{3ANG} \right) \right)$

$V_{3.5} = 0.6543 - 0.7456i \qquad \left| V_{3.5} \right| = 0.992 \qquad \arg\left(V_{3.5} \right) = -0.8505$

$V_{4.5} := V_{4MAG} \cdot \left(\cos\left(\delta_{4ANG} \right) + j \cdot \sin\left(\delta_{4ANG} \right) \right)$

$V_{4.5} = 0.6338 - 0.7735i \qquad \left| V_{4.5} \right| = 1 \qquad \arg\left(V_{4.5} \right) = -0.8843$

$V_2 := \left| V_{2.5} \right| \qquad \delta_2 := \arg\left(V_{2.5} \right)$

$V_3 := \left| V_{3.5} \right| \qquad \delta_3 := \arg\left(V_{3.5} \right)$

$V_4 := \left| V_{4.5} \right| \qquad \delta_4 := \arg\left(V_{4.5} \right)$

$V_{3MAG} := \left| V_{3.4} \right| + \Delta V_3$

$V_{3MAG} = 0.992$

$\delta_{3ANG} := \arg\left(V_{3.4} \right) + \Delta\delta_3$

$\delta_{3ANG} = -0.8505$

$\arg\left(V_{2.5} \right) = -0.0339$

$$V_1 = 1 \qquad\qquad \delta_1 \cdot \frac{180}{\pi} = 0$$

$$V_2 = 0.9915 \qquad \delta_2 \cdot \frac{180}{\pi} = -1.9409$$

$$V_3 = 0.992 \qquad\quad \delta_3 \cdot \frac{180}{\pi} = -48.7321$$

$$V_4 = 1 \qquad\qquad \delta_4 \cdot \frac{180}{\pi} = -50.6686$$

B.1.1   Actual voltage values

$$V_{1act} := V_1 \cdot 345$$

$$V_{1act} = 345$$

$$V_{2act} := V_2 \cdot 500$$

$$V_{2act} = 495.7449$$

$$V_{3act} := V_3 \cdot 500$$

$$V_{3act} = 495.9786$$

$$V_{4act} := V_4 \cdot 230$$

$$V_{4act} = 230$$

$$\Delta\delta_{12} := \delta_1 - \delta_2$$

$$\Delta\delta_{23} := \delta_2 - \delta_3$$

$$\Delta\delta_{34} := \delta_3 - \delta_4 \qquad \Delta\delta_{23} = 0.8167$$

B.2 Power values
B.2.1 Bus 1

$$P_{S12pu} := \frac{\left(|V_1|\right)^2}{|Z_{12}|} \cdot \cos\left(\arg\left(Z_{12}\right)\right) - \frac{|V_1| \cdot |V_2|}{|Z_{12}|} \cdot \cos\left(\arg\left(Z_{12}\right) + \Delta\delta_{12}\right)$$

$$P_{S12pu} = 0.3375$$

$$Q_{S12pu} := \frac{\left(|V_1|\right)^2}{|Z_{12}|} \cdot \sin\left(\arg\left(Z_{12}\right)\right) - \frac{|V_1| \cdot |V_2|}{|Z_{12}|} \cdot \sin\left(\arg\left(Z_{12}\right) + \Delta\delta_{12}\right)$$

$$Q_{S12pu} = 0.084$$

B.2.2 Bus 2

$$P_{S23pu} := \frac{\left(|V_2|\right)^2}{|Z_{23}|} \cdot \cos\left(\arg\left(Z_{23}\right)\right) - \frac{|V_2| \cdot |V_3|}{|Z_{23}|} \cdot \cos\left(\arg\left(Z_{23}\right) + \Delta\delta_{23}\right)$$

$$P_{S23pu} = 0.3372$$

$$Q_{S23pu} := \left[\frac{\left(|V_2|\right)^2}{|Z_{23}|} \cdot \sin\left(\arg\left(Z_{23}\right)\right) - \frac{|V_2| \cdot |V_3|}{|Z_{23}|} \cdot \sin\left(\arg\left(Z_{23}\right) + \Delta\delta_{23}\right)\right]$$

$$Q_{S23pu} = 0.1407$$

$$Q_{CAP} := -\left[\frac{(1.0049)^2}{\left(\frac{1}{0.0699}\right)}\right]$$

$$Q_{CAP} = -0.0706$$

$$Q_{Bus2total} := Q_{CAP} + Q_{S23pu}$$

$$Q_{Bus2total} = 0.0701$$

B.2.3 Bus 3

$$P_{S34pu} := \frac{\left(|V_3|\right)^2}{|Z_{34}|} \cdot \cos\left(\arg\left(Z_{34}\right)\right) - \frac{|V_3| \cdot |V_4|}{|Z_{34}|} \cdot \cos\left(\arg\left(Z_{34}\right) + \Delta\delta_{34}\right)$$

$$P_{S34pu} = 0.3336$$

$$Q_{S34pu} := \frac{\left(|V_3|\right)^2}{|Z_{34}|} \cdot \sin\left(\arg\left(Z_{34}\right)\right) - \frac{|V_3| \cdot |V_4|}{|Z_{34}|} \cdot \sin\left(\arg\left(Z_{34}\right) + \Delta\delta_{34}\right)$$

$$Q_{S34pu} = -0.0808$$

B.2.4 Bus 4

$$P_{R34pu} := \frac{|V_3| \cdot |V_4|}{|Z_{34}|} \cdot \cos\left(\arg\left(Z_{34}\right) - \Delta\delta_{34}\right) - \frac{\left(|V_4|\right)^2}{|Z_{34}|} \cdot \cos\left(\arg\left(Z_{34}\right)\right)$$

$$P_{R34pu} = 0.3333$$

$$Q_{R34pu} := \frac{|V_3| \cdot |V_4|}{|Z_{34}|} \cdot \sin\left(\arg\left(Z_{34}\right) - \Delta\delta_{34}\right) - \frac{\left(|V_4|\right)^2}{|Z_{34}|} \cdot \sin\left(\arg\left(Z_{34}\right)\right)$$

$$Q_{R34pu} = -0.0928$$

B.2.5 Actual power values

$$P_{Bus1} := P_{S12pu} \cdot 1500 \qquad\qquad P_{Bus2} := P_{S23pu} \cdot 1500$$

$$P_{Bus1} = 506.2221 \qquad\qquad P_{Bus2} = 505.8592$$

$$Q_{Bus1} := Q_{S12pu} \cdot 1500 \qquad\qquad Q_{Bus2} := Q_{Bus2total} \cdot 1500$$

$$Q_{Bus1} = 126.0593 \qquad\qquad Q_{Bus2} = 105.1089$$

$$P_{Bus3} := P_{S34pu} \cdot 1500 \qquad\qquad P_{Bus4} := P_{R34pu} \cdot 1500$$

$$P_{Bus3} = 500.3586 \qquad\qquad P_{Bus4} = 499.9995$$

$$Q_{Bus3} := Q_{S34pu} \cdot 1500 \qquad\qquad Q_{Bus4} := Q_{R34pu} \cdot 1500$$

$$Q_{Bus3} = -121.1829 \qquad\qquad Q_{Bus4} = -139.1402$$

APPENDIX C

In Appendix C all the calculations done in regard to Case study 4 are shown. It is assumed that the DC current that flows across the line is constant and known (due to control files situated inside the rectifier and inverter stations.

C.1   Rectifier side

$I_d := 2000$ A

$V_{Bus1ac} := 213455.7$ V

$\alpha_{rec} := 0.265$ Rac

$$Z_{base} := \frac{(213455.7)^2}{(603.73 \cdot 10^6)}$$

$Z_{base} = 75.47$

$X_{com} := 0.18$ pu

$X_{comact} := X_{com} \cdot Z_{base}$

$X_{comact} = 13.585$

$$V_{dBus26p} := \left(\frac{3\sqrt{2}}{\pi} \cdot V_{Bus1ac} \cdot \cos(\alpha_{rec})\right) - \left(\frac{3}{\pi} \cdot X_{comact} \cdot I_d\right)$$

$V_{dBus26p} = 252259.233$

$V_{dBus212p} := V_{dBus26p} \cdot 2$

$V_{dBus212p} = 504518.466\,V$

C.2 Inverter side

$$V_{Bus4ac} := 209228.\varepsilon \quad V$$

$$\beta_{inv} := 2.473 \quad Rac$$

$$Z_{baseinv} := \frac{\left(V_{Bus4ac}\right)^2}{\left(591.79 \cdot 10^6\right)}$$

$$Z_{baseinv} = 73.973$$

$$X_{cominv} := 0.18 \quad pu$$

$$X_{cominvact} := X_{com} \cdot Z_{base}$$

$$X_{cominvact} = 13.585$$

$$V_{dBus36p} := \left(\frac{3\sqrt{2}}{\pi} \cdot V_{Bus4ac} \cdot \cos\left(\beta_{inv}\right)\right) - \left(\frac{3}{\pi} \cdot X_{cominvact} \cdot I_d\right)$$

$$V_{dBus36p} = -247666.503$$

$$V_{dBus312p} := V_{dBus36p} \cdot 2$$

$$V_{dBus312p} = -495333.005 \quad V$$

C.3 Power at the sending end

$$P_s := I_d \cdot V_{dBus212p}$$

$$P_s = 1.009 \times 10^9$$

C.4 Power at the receiving end

$$P_r := I_d \cdot V_{dBus312p}$$

$$P_r = -990.666 \times 10^6$$

$$Rect := P_s$$

$$Rect = 1.009 \times 10^9 \ \text{W}$$

$$Line := P_r$$

$$Line = -990.666 \times 10^6$$

$$Bus2 := V_{dBus212p}$$

$$Bus2 = 504518.466 \ \text{V}$$

$$Bus3 := -495333.005 \ \text{V}$$